UNVERSITY OF CALIFORNIA
RIVERSIDE

Interactions of Lignin and Hemicellulose and Effects on Biomass Deconstruction

A Dissertation submitted in partial satisfaction
of the requirements for the degree of

Doctor of Philosophy

in

Chemical and Environmental Engineering

by

Hongjia Li

December 2012

Dissertation Committee:

Dr. Charles E. Wyman, Chairperson
Dr. Eugene A. Nothnagel
Dr. Joseph M. Norbeck

The Dissertation of Hongjia Li is approved:

_____

_____

_____

Committee Chairperson

University of California, Riverside

ACKNOWLEDGMENTS

This thesis was supported by the BioEnergy Science Center (BESC), a U.S. Department of Energy Bioenergy Research Center supported by the Office of Biological and Environmental Research in the DOE Office of Science. The BESC people, organization, and research collaborations provided me an incredible learning opportunity as well as valuable experience in my whole graduate study period. Gratitude is also extended to the supports from Ford Motor Company and the Center for Environmental Research and Technology of the Bourns College of Engineering at UCR.

I would like to give extraordinary thanks to my thesis advisor Professor Charles E. Wyman for his mentorship over the past four and half years. Your valuable guidance, encouragements, and kindly tolerance have made me not only a better researcher, but also a better man. I would like to thank Professor Eugene A. Nothnagel and Dr. Rajeev Kumar for valuable guidance and discussions in several studies within this thesis. I also want to thank my lab mates, especially Dr. Jaclyn DeMartini, Dr. Jian Shi, Dr. Qing Qing, Dr. Heather Trajano and Dr. Taiying Zhang for many helpful trainings, discussions and suggestions. This thesis cannot be done without contributions from my outstanding BESC collaborators, and their names are noted at the start of each chapter. There are several friends who helped me get through the new life in the U.S. and always be around.

At last, I can never be in this position without the love from my dear parents: Mr. Fu Li and Mrs. Jing Liu; my beloved wife: Xiadi Gao (who will be a doctor in 2013); and all other family members. Special gratitude and miss to my loving grandparents, they must be very proud of the first doctor in the family.

ABSTRACT OF THE DISSERTATION

Interactions of Lignin and Hemicellulose
and Effects on Biomass Deconstruction

by

Hongjia Li

Doctor of Philosophy, Graduate Program in Chemical and Environmental Engineering
University of California, Riverside, December 2012
Dr. Charles E. Wyman, Chairperson

Facing inexorable growth of global population and energy consumption, lignocellulosic biomass has taken a more central role in global energy strategy by providing sustainable sources for both liquid fuels and chemicals without competing with food and feed supplies. To establish a large scale, reliable, and economic lignocellulosic industry, biomass recalcitrance must be well understood and overcome. Currently cutting edge biological conversion research focuses mainly on three aspects: genetic modification of plant cell wall structure to reduce biomass recalcitrance, pretreatment of biomass as a critical prerequisite to achieve high sugar yields, and consolidated processing of enzymes and microorganisms to lower deconstruction costs. More

importantly, however, synergistic concert of these three approaches is critical to develop practical solutions for this challenge. Thus, interactions and impacts among cell wall structural characteristics, pretreatment, and biological deconstruction are vital to understand.

In light of this, six technical studies towards three main objectives were pursued in this thesis. First, an integrated chromatographic method for xylooligosaccharides determination and a high throughput system using dilute alkali conditions were developed as characterization tools to facilitate understanding how pretreatment affects cell wall polysaccharide deconstruction. Next, two fundamental studies on lignin deposition during pretreatment and reduced methylation of xylan side-chains, respectively, were employed to identify important recalcitrant aspects of lignin and hemicellulose on biomass digestion. Finally, systematic research was undertaken to develop Agave as a low recalcitrant, drought resistant biofuels feedstock for semi-arid lands. The findings of this thesis provide fundamental insights towards understanding interactions of lignin and hemicellulose, the two primary barriers to biological conversion, for more effective biomass deconstruction and better energy crops design.

Table of Contents

List of Figures

List of Tables

Chapter 1

Introduction

1.1 Overview

For several decades, petroleum has been used as the major source for the production of transportation fuels and chemicals. Particularly in the past twenty years, the global consumption of petroleum has increased alarmingly, while the accessibility and reliability of petroleum continues to dwindle, creating a critical need for alternative sources of fuels and chemicals (1). First generation bioethanol using corn starch and sugarcane sucrose is not suitable for a sustainable, large scale bioethanol industry because of the competition with cultivated lands, food and feed supply, as well as exposure to feedstock market risks (2-4). To date, lignocellulosic biomass has emerged as the only promising source for the production of both sustainable fuels and chemicals in a post-petroleum era.

A major challenge in lignocellulosic biomass conversion, however, is to effectively break down cell wall polysaccharides and achieve high sugar yields with low costs, low energy input and environmentally friendly techniques. To address these issues, breeding and genetic modification can be used to promote biomass productivity, increase carbohydrate content, and reduce cell wall recalcitrance; leading pretreatment technologies are applied to further reduce biomass recalcitrance for economically viable deconstruction; advanced enzymes and microorganisms are engineered for efficient polysaccharide hydrolysis and biofuels fermentation and synthesis. To effectively apply these three approaches in practical renewable solutions, understanding interactions and impacts among the three is needed to develop promising process combinations. Thus, fundamental investigation of important cell wall recalcitrant structures and mechanisms,

and their impacts on biomass deconstruction during pretreatment and enzymatic hydrolysis have become very important.

1.2 Liquid phase conversion of lignocellulosic biomass into ethanol

For a long time, research has been conducted towards developing promising sustainable energy resources to reduce dependence on petroleum. Lignocellulosic biomass is the only promising renewable resource that can be produced at large scale for transportation fuels (5, 6) and chemical manufacturing (6, 7). With its unique environmental, economic, and strategic benefits (3), lignocellulosic ethanol is particularly promising because it is derived from non-food, low cost and abundant feedstocks, can be produced *via* green processing techniques, and has been shown to have high octane and other desirable fuel properties (3-5).

As the second generation of bioethanol developed in the United States, lignocellulosic ethanol research seeks to utilize plentiful resources including agricultural residues such as corn stover and sugarcane bagasse, fast growing woody crops such as poplar, and perennial grasses such as switchgrass and miscanthus. Conversion of such lignocellulosic biomass feedstocks into ethanol *via* a biological approach include the major processing stages illustrated in Figure 1.1. Biomass pretreatment, enzyme production, and cellulose hydrolysis are the most costly steps in the conversion process but also the most susceptible to advancements that improve efficiency and economics. The goal of pretreatment is to disrupt that plant cell wall structure to make cellulose more accessible and digestible for enzymes; the way in which this is accomplished varies

significantly by pretreatment type. The following step is enzymatic hydrolysis, in which cellulose and hemicellulose remaining in the pretreated solid residue is hydrolyzed by enzymes into monomers such as glucose, xylose, and arabinose. After hydrolysis, the hexose and pentose sugars produced from pretreatment and enzymatic hydrolysis are fermented into ethanol a biological reaction by yeast or bacteria that feed on the sugars.

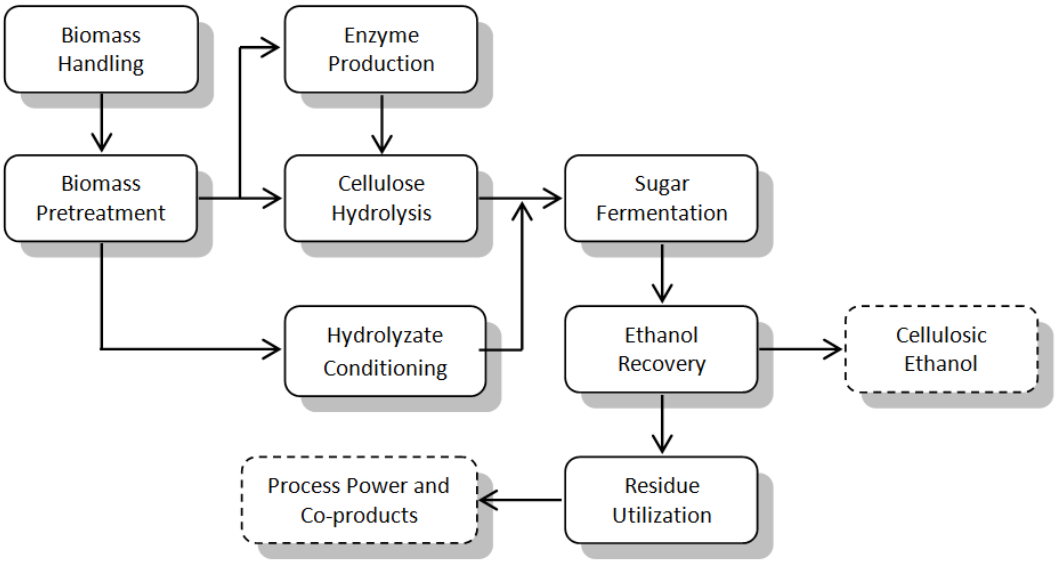

Figure 1.1. Schematic of an ethanol production from cellulosic biomass (adapted from process described by Wooley et al. (8)).

1.3 Biomass recalcitrance and cell wall structure

From the epidermis to crystalline cellulose, plants have evolved their own defensive lines to resist assault from physical, chemical, and biological factors; this collective resistance of plant cell wall structural polymers, including lignin, hemicellulose, and cellulose, to chemical or biological deconstruction, is defined as biomass recalcitrance (9, 10). Although little is known about what aspects cause recalcitrance to biomass conversion, a better understanding would greatly facilitate advanced processing

designs that will achieve more effective breakdown of such defenses with lower cost, as well as aid in the production of less recalcitrant plants using genetic tools.

Different biomass feedstocks have different cell wall compositions and structures. In general, cell walls represent an enormous storehouse of complex polysaccharides that can be broken down to form fermentable sugars for potential conversion to ethanol. The predominant polysaccharide in plant cell walls is cellulose, which contributes about 30-50% of the plant's dry weight. Cellulose is a highly ordered, water-excluding natural crystallite polymer of glucose molecules joined by β-(1-4)-glycosidic bonds with chains connected by many interchain hydrogen bonds. This crystal structure of cellulose is a significant obstacle to enzyme digestion. The cellulose is embedded in matrix polysaccharides, including hemicellulose, which is the second most abundant carbohydrates in plant cell walls. Hemicellulose represents several different polysaccharides that interlock cellulose microfibrils through hydrogen bonds, forming another defensive line for protecting cellulose (11). In secondary cell walls, polyphenolic lignin cross-links hemicellulose to form lignin-carbohydrate complexes (LCC) (9, 12). Lignin cannot be hydrolyzed by cellulase enzymes, but its hydrophobic structure not only limits accessibility of cellulase and water to the surface of carbohydrates but also non-productively binds enzymes (9, 13, 14). Lignin and hemicellulose represent about 15-25% and 15-30% of the plant's dry weight, respectively.

The content and composition of lignin and hemicellulose have been previously demonstrated to affect cell wall digestibility (15-19), while others have indicated that the interaction of lignin and hemicellulose is also important (20-22). Lignocellulosic

biomass must be pretreated to overcome the structural recalcitrance of the cell wall for high biomass digestibility (6, 23, 24). Thus, fundamental research is critical to understand how lignin, hemicellulose and their interactions affect cell wall deconstruction during pretreatment and enzymatic hydrolysis in order to develop effective strategies to reduce the recalcitrant nature of lignocellulosic biomass.

1.4 Thesis motivation and organization

Despite numerous studies that have shown significant negative impacts of lignin and hemicellulose on biomass pretreatment and enzymatic hydrolysis, a thorough understanding of the effects of lignin-hemicellulose interactions on cell wall synthesis and deconstruction is still very limited. Based on previous observations and findings, the overall goal of this thesis is to further elucidate important structural characteristics of plant cell walls that contribute to biomass recalcitrance, and in particular, seek to better understand how the interaction of lignin and hemicellulose affects sugar release in pretreatment and enzymatic hydrolysis.

Chapter 2 begins with a literature review of information mainly relevant to the role of hemicellulose during lignocellulosic biomass processing. As such, four main topics were covered starting with physical and chemical structure of xylans and xylooligosaccharides in plant cell walls. Then, important reactions and kinetics of xylooligosaccharides hydrolysis during pretreatment and enzymatic hydrolysis will be reviewed. Next, several methods and applications are introduced for xylooligosaccharides separation and preparation. Finally, a variety of analytical

technologies are discussed for xylooligosaccharides characterization, with particular attention paid to the quantification of xylooligosaccharides with different chain lengths.

Chapters 3 through 8 are then split into three main categories: 1) experimental methods development and verification of integrated chromatographic system for determining xylooligosaccharides of different degree of polymerization (DP), and dilute alkali high throughput pretreatment and enzymatic hydrolysis system (HTPH) for screening biomass recalcitrance by comparison of sugar release; 2) fundamental investigation of important changes of lignin and hemicellulose during hydrothermal pretreatment and how such changes affect cellulose enzymatic hydrolysis; 3) integrated study of a variety of important cell wall recalcitrant characteristics that affect biomass digestibility and development of Agave as a low recalcitrant, drought resistant biofuels feedstock for semi-arid lands.

As such, Chapter 3 reports on integrated gel permeation chromatography (GPC), high performance anion exchange chromatography with pulsed amperometric detection (HPAEC-PAD), and high performance liquid chromatography (HPLC) methods to successfully isolate and characterize 1,4-β-xylooligosaccharides with DP of 2-14. Response differences of xylooligosaccharides on PAD detector were determined and a series of response factors were developed, which allowed quantification of xylooligosaccharides of different lengths without corresponding sugar standards available in the market. Chapter 4 describes extending the application of HTPH system, an effective screening tool for biomass sugar release, to dilute alkali pretreatment conditions, without extra labor or time consumption. Using these powerful high throughput tools,

additional insight was provided to better understanding the role of lignin in biomass recalcitrance. Chapters 5-8 then delve into the main focus of this thesis. In Chapter 5, lignin from poplar wood was found to deposit on the surface of a cellulose surface (Avicel) during hydrothermal pretreatment, with characterization by wet chemistry methods, scanning electron microscope (SEM) and nuclear magnetic resonance (NMR). The inhibition pattern of deposited lignin droplets on enzymatic hydrolysis was studied and the physical surface blockage was determined as the primary mechanism for such inhibition. Chapter 6 moves away from lignin droplets to examine the effects of reduced methylation in glucuronoxylan side-chains of Arabidopsis on lignin and hemicellulose removal during hydrothermal pretreatment in flowthrough reactors. New insights into methyl groups and the interaction of lignin and hemicellulose synthesis and biomass deconstruction were discovered that can aid in improving future genetic modification of cell wall structure. Finally, in Chapters 7 and 8, detailed chemical and structural characterization of Agave cell walls was performed using various advanced analytical techniques for the first time. The cell wall differences of Agave, poplar and switchgrass were compared and used toward understanding the significantly lower recalcitrance and high biomass digestibility of agave cell walls. Finally, Chapter 9 summarizes the conclusions and key findings from this thesis.

1.5 References

1. Huber GW, Iborra S, Corma A. Synthesis of transportation fuels from biomass: Chemistry, catalysts, and engineering. Chem Rev. 2006 Sep 13;106(9):4044-98.
2. Wyman CE. Ethanol from lignocellulosic biomass - technology, economics, and opportunities. Bioresource Technol. 1994;50(1):3-16.

3. Wyman CE. Biomass ethanol: Technical progress, opportunities, and commercial challenges. Annu Rev Energ Env. 1999;24:189-226.
4. Wyman CE. Twenty years of trials, tribulations, and research progress in bioethanol technology - Selected key events along the way. Appl Biochem Biotech. 2001 Spr;91-3:5-21.
5. Wyman CE. What is (and is not) vital to advancing cellulosic ethanol. Trends in Biotechnology. 2007;25(4):153-7.
6. Wyman CE, Dale BE, Elander RT, Holtzapple M, Ladisch MR, Lee YY. Coordinated development of leading biomass pretreatment technologies. Bioresource Technol. 2005 Dec;96(18):1959-66.
7. Dodds DR, Gross RA. Chemicals from biomass. Science. 2007 Nov 23;318(5854):1250.
8. Wooley R, Ruth M, Glassner D, Sheehan J. Process design and costing of bioethanol technology: A tool for determining the status and direction of research and development. Biotechnol Progr. 1999 Sep-Oct;15(5):794-803.
9. Himmel ME. Biomass recalcitrance : deconstructing the plant cell wall for bioenergy. Oxford: Blackwell Pub.; 2008.
10. Lynd LR, Wyman CE, Gerngross TU. Biocommodity engineering. Biotechnol Prog. 1999 Oct 1;15(5):777-93.
11. Carpita NC, Gibeaut DM. Structural models of primary-cell walls in flowering plants - consistency of molecular-structure with the physical-properties of the walls during growth. Plant J. 1993 Jan;3(1):1-30.
12. Fengel D, Wegener G. Wood : chemistry, ultrastructure, reactions. Berlin ; New York: W. de Gruyter; 1984.
13. Kumar R, Wyman CE. Access of cellulase to cellulose and lignin for poplar solids produced by leading pretreatment technologies. Biotechnol Progr. 2009 May-Jun;25(3):807-19.
14. Pu YQ, Ziemer C, Ragauskas AJ. CP/MAS ^{13}C NMR analysis of cellulase treated bleached softwood kraft pulp. Carbohyd Res. 2006 Apr 10;341(5):591-7.
15. Studer MH, DeMartini JD, Davis MF, Sykes RW, Davison B, Keller M, et al. Lignin content in natural Populus variants affects sugar release. Proc. Natl Acad Sci USA. 2011 Apr 12;108(15):6300-5.
16. Chen F, Dixon RA. Lignin modification improves fermentable sugar yields for biofuel production. Nat Biotechnol. 2007 Jul;25(7):759-61.
17. Davison BH, Drescher SR, Tuskan GA, Davis MF, Nghiem NP. Variation of S/G ratio and lignin content in a Populus family influences the release of xylose by dilute acid hydrolysis. Appl Biochem Biotech. 2006 Mar;130(1-3):427-35.
18. Grabber JH. How do lignin composition, structure, and cross-linking affect degradability? A review of cell wall model studies. Crop Sci. 2005 May-Jun;45(3):820-31.
19. Lee CH, Teng Q, Huang WL, Zhong RQ, Ye ZH. Down-Regulation of PoGT47C Expression in Poplar Results in a Reduced Glucuronoxylan Content and an Increased Wood Digestibility by Cellulase. Plant Cell Physiol. 2009 Jun;50(6):1075-89.

20. DeMartini JD, Pattathil S, Avci U, Szekalski K, Mazumder K, Hahn MG, et al. Application of monoclonal antibodies to investigate plant cell wall deconstruction for biofuels production. Energy & Environmental Science. 2011 Oct;4(10):4332-9.
21. Chundawat SPS, Beckham GT, Himmel ME, Dale BE. Deconstruction of Lignocellulosic biomass to fuels and chemicals. Annu Rev Chem Biomol. 2011;2:121-45.
22. Chundawat SPS, Donohoe BS, Sousa LD, Elder T, Agarwal UP, Lu FC, et al. Multi-scale visualization and characterization of lignocellulosic plant cell wall deconstruction during thermochemical pretreatment. Energy & Environmental Science. 2011 Mar;4(3):973-84.
23. Mosier N, Wyman C, Dale B, Elander R, Lee YY, Holtzapple M, et al. Features of promising technologies for pretreatment of lignocellulosic biomass. Bioresource Technol. 2005 Apr;96(6):673-86.
24. Wyman CE, Dale BE, Elander RT, Holtzapple M, Ladisch MR, Lee YY. Comparative sugar recovery data from laboratory scale application of leading pretreatment technologies to corn stover. Bioresource Technol. 2005 Dec;96(18):2026-32.

Chapter 2

Xylooligosaccharides Production, Quantification, and Characterization in Context of Lignocellulosic Biomass Pretreatment*

*This whole chapter is reprinted from the book chapter under the following citation: Qing Q, Li H, Kumar R, Wyman CE. *Xylooligosaccharides Production, Quantification, and Characterization in Context of Lignocellulosic Biomass Pretreatment*, in *Aqueous Pretreatment of Plant Biomass for Biological and Chemical Convention to Fuels and Chemicals*, Wyman CE, Ed, (In Press), Wiley Blackwell, Oxford, UK. Please contact publishers for details

2.1 Abstract

Xylooligosaccharides (XOs) released during hydrothermal pretreatment, low severity dilute acid pretreatment, or enzymatic hydrolysis of lignocellulosic biomass can be fermented directly, further hydrolyzed into fermentable sugars for biofuels production, or used immediately as high value-added prebiotic feedstocks which can be incorporated into many food products. Quantification and detailed characterization of xylooligosaccharides are vital to understand reaction kinetics and sugar release mechanisms during pretreatment and enzymatic hydrolysis, clarify cell wall structural recalcitrance, and facilitate XOs as important prebiotic products. This chapter reviews chemical and enzymatic methods for production of xylooligosaccharide mixtures as well as separation and purification processes. In addition, characterization methods such as by high-pressure liquid chromatography (HPLC), high-performance anion exchange chromatography (HPAEC), mass spectrometry (MS), and nuclear magnetic resonance (NMR) are summarized for quantitative determination and structural characterization of xylooligosaccharides.

2.2 Introduction

2.2.1 Definition of oligosaccharides

Oligosaccharides, also often termed as sugar oligomers, refer to short chain polymers of monosaccharide units connected by α and/or β glycosidic bonds. In structure, oligosaccharides represent a class of carbohydrates between polysaccharides and monosaccharides, but the range of degree of polymerization (DP, chain length) spanned by oligosaccharides has not been consistently defined. For example, the MeSH® database of the U.S. National Library of Medicine defines oligosaccharides as carbohydrates consisting of 2 to 10 monosaccharide units, while in some literature, sugar polymers with DPs up to 30 to 40 have been included as oligosaccharides (1-3).

2.2.2 Types of oligosaccharides released during lignocellulosic biomass pretreatment

Oligosaccharides exist naturally in plant tissues, but their amounts are small comparing to cell wall structural polysaccharides, such as cellulose and hemicellulose (4). During pretreatment of lignocellulosic biomass, most of the insoluble hemicellulose is removed from the surface of cellulose microfibrils and broken into various soluble oligosaccharides. However, the amounts and structures vary with pretreatment types and severity. The majority of oligosaccharides released during lignocellulosic biomass pretreatment are hydrolysis products of hemicellulose, and the types of oligosaccharides (composition, DP, and substitution) depend on the structure and composition of the corresponding hemicellulose.

Hemicellulose refers to several amorphous polysaccharides found in the plant cell wall matrix that have β-(1-4)-linked backbones with an equatorial configuration (5), which are commonly categorized into several groups, such as xyloglucans, heteroxylans, (galacto) glucomannans, and arabinogalactans (6-8). For example, glucuronoarabinoxylan refers to one type of heteroxylans which have a backbone of β-(1-4)-xylosyl residues with a few short side chains that mainly contain arabinosyl residues and glucuronic acid residues, but could also contain other sugars or sugar acid residues (4). The number of side chains and the side chain residues composition vary with biomass and cell wall types and life stage of the same plant. Dominant forms of hemicellulose polysaccharides in major lignocellulosic biomass feedstocks, except softwoods, are xyloglucans and "heteroxylans," as enumerated in Table 2.1. In lignocellulosic biomass feedstocks, the mass fraction of secondary cell walls based on total plant dry weight is much greater than that of primary cell walls (4). Thus, xylooligosaccharides from heteroxylans hydrolysis are the predominant type of oligosaccharides released during pretreatment.

Table 2.1. Lignocellulosic feedstocks that have heteroxylans as dominant hemicellulose types

Plant group	Examples	Wall type	
		Primary cell wall	Secondary cell wall
Hardwood	Poplar	Xyloglucan	4-O-methyl-glucuronoxylan
Energy grasses	Switchgrass	Glucuronoarabinoxylan	Glucuronoarabinoxylan
Agricultural Residues	Corn stover	Glucuronoarabinoxylan	Glucuronoarabinoxylan

2.2.3 The importance of measuring xylooligosaccharides

2.2.3.1 Understand plant cell wall structure and its role in biomass recalcitrance

In general, plant cell walls represent an enormous source of complex polysaccharides that can be broken down to monosaccharides for potential conversion into biofuels and chemicals. The framework of plant cell walls is cellulose, a highly ordered, water-excluding natural crystalline polymer of glucose molecules joined by β-(1-4)-glycosidic bonds, with its chains connected by many intra/inter chain hydrogen bonds. Outside the framework, cellulose microfibrils and hemicellulose are intimately interlocked with one another and often with lignin, both covalently and non-covalently (5). The hydrophobic association of cell wall polysaccharides and lignin, termed as the lignin-carbohydrate complex (LCC), is an important part of plant cell wall defense and has been recognized as the main barrier for economic deconstruction of cell wall polysaccharides (5, 9-11). Such collective resistance, which plants and plant materials pose to deconstruction by microbes and enzymes, is defined as “biomass recalcitrance” (5, 12). Although the aspect/s most responsible for biomass recalcitrance to conversion are not clear, a better understanding of cell wall polysaccharides compositions and structures would greatly facilitate advanced process designs that achieve more effective breaking of such defenses with lower cost as well as aid in production of less recalcitrance plants using genetic tools. For example, through comparison of glucuronoxylan (GX) structures in poplar wood, Lee et al. found transgenic reduction of GX in secondary cell wall reduced recalcitrance of wood to cellulase digestion (13).

Unfortunately, direct characterization of cell wall polysaccharides is difficult because of the heterogeneous and complex nature of cell walls. Thus, using either enzymes or chemicals to breakdown cell wall polysaccharides followed by characterizing the corresponding oligosaccharides and monomers has been an effective way to study cell wall polysaccharides structures and their possible roles in biomass recalcitrance. Effective structural studies normally contain two parts. First, optimized enzymatic or chemical treatment methods are applied to extract certain types of polysaccharides from the insoluble cell wall in which they are held. For example, heteroxylans are typically extracted by 4% KOH whereas heteroglucans may require 24% KOH (5, 14). The isolated polysaccharides or fragments are then purified and broken down into oligosaccharides for detailed characterization. Important structural information about hemicellulose polysaccharides can be determined, such as the glycosyl residue composition, the glycosyl linkage composition, the sequence of glycosyl residues in both the backbone and side chains, and non-carbohydrate substituents through characterizing hemicellulose oligosaccharides (4).

2.2.3.2 Engineer reaction pathways for economic deconstruction of structural cell wall polysaccharides

Lignocellulosic biomass, as a feedstock for fuels and chemicals production, has many benefits such as not competing for food and feed supply, low production costs, and wide availability over a range of locations and climates (15, 16). Utilization of cell wall carbohydrates makes lignocellulosic biomass a promising renewable feedstock for large-

scale conversion into liquid fuels and organic chemicals. Different reaction pathways have been devised to breakdown cell wall polysaccharides in lignocellulosic biomass into monomeric sugars: thermal, chemical, biological, and/or their combination. In lignocellulosic ethanol production, for example, cellulase, which is a synergistic combination of several proteins, in combination with hemicellulases and other accessory enzymes degrade cellulose and residual hemicellulose into glucose and xylose. However, pretreatments have proven to be essential to open up the rigid biomass structure through removing or altering hemicellulose and lignin and loosening the structure of cellulose, to enhance access of enzymes to their respective substrates. Hemicellulose polysaccharide chains can be broken into oligosaccharides and then further hydrolyzed to monosaccharides, especially during low to neutral pH pretreatments, which in turn can react to degradation products as depicted below:

$$\text{Polysaccharides}_{(\text{solid})} \rightarrow \text{Hemicellulose Oligosaccarides}_{(\text{aq})} \rightarrow \text{Monosaccharides}_{(\text{aq})} \rightarrow \text{Degradation products}_{(\text{aq})}$$

Employing harsh pretreatment conditions can reduce macro barriers to enzymes reaching cellulose and improve micro accessibility of cellulose to enzymes through changes in its crystal structure and degree of polymerization and result in better conversion to sugars (17-19). But such conditions also degrade xylooligosaccharides and xylose into byproducts, such as furfural (20, 21), resulting in sugar losses and formation of inhibitors to enzymes and microbes for sugars fermentation (22, 23). Thus, pathway optimization is needed to achieve the highest sugar recovery for economical processing. For that reason, qualitative and quantitative measurements of xylooligosaccharides are

important because they are essential for detailed studies of hemicellulose hydrolysis kinetics and degradation mechanisms. Such studies can also play a key role in engineering effective pretreatment technologies to achieve high sugar recovery with good economics.

It is also important to note that xylooligosaccharides have recently been shown to have a strong negative effect on cellulase activity in decomposing cell wall polysaccharides into fermentable sugars (24, 25). Quantitative analysis and characterization of xylooligosaccharides, including improved purification and characterization techniques, facilitate understanding xylooligosaccharides inhibition mechanisms and developing strategies for reducing inhibition.

2.2.3.3 Oligosaccharides for high value-added products

Xylooligosaccharides have been shown to have important prebiotic properties and thus great potential for use in medicinal, food, and health products (26). Xylooligosaccharides for such uses are mainly derived from lignocellulosic biomass by enzymatic and/or chemical hydrolysis to remove hemicellulose polysaccharides (mainly heteroxylans in the case of cellulosic biomass) from the surface of cellulose and break them into water soluble xylooligosaccharides. Then separation technologies isolate and purify these xylooligosaccharides into desired DP ranges for prebiotic applications. This fast growing market for xylooligosaccharides creates great opportunities to process xylan-rich pretreatment hydrolyzates in cellulosic biorefineries into high value products which could improve conversion economics.

2.3 Xylooligosaccharides production

Xylooligosaccharides are usually produced from xylan rich lignocellulosic materials (LCM) by autohydrolysis from heating in water or steam, chemical treatments in dilute aqueous solutions of mineral acids (27, 28), direct enzymatic hydrolysis of susceptible lignocellulosic materials (29-31), or chemical fractionation of a suitable LCM to isolate (or solubilize) xylan with further enzymatic hydrolysis to XOs (32). Typical raw materials for XOs production are hardwoods (e.g., birchwood, beechwood), corn cobs, straws, bagasse, rice hulls, malt cakes, and bran (26). In recent years, the fast growing functional food market and the increasing number of other industrial applications are encouraging identification of renewable and cheap xylan sources instead of hardwood xylan for XOs production. As a result, agricultural residues such as cotton stalks, tobacco stalks, and wheat straw have also been intensively studied (27).

2.3.1 Thermochemical production of XOs

Thermochemical production of XOs is usually accomplished by steam, dilute mineral acids, or dilute alkaline solutions. The single step production of XOs by reaction with steam or water through hydronium-catalyzed degradation of xylan is known as autohydrolysis, hydrothermolysis, or water prehydrolysis (26). Autohydrolysis takes place at slightly acidic ($pH \leq 4$) conditions created by acetic acid released by partial cleavage of acetyl groups in plant cell wall. A considerable fraction of acetyl and uronic acid groups remain attached to the oligosaccharides, giving them distinctive characteristics like very high solubility in water (33). In autohydrolysis treatment, XOs

behave as typical reaction intermediates whose concentration depends mainly on the tradeoff between breakdown of polymeric hemicellulose in biomass to XOs and their further decomposition to monomeric xylose. Therefore, reaction severity (R_o) influences the concentrations of total XOs as well as of monomeric xylose that could be achieved in hydrolysate and is often represented by a single parameter that combines temperature, time, and reaction pH (34).

$$R_o = t \exp \{(T-100)/14.75\} - pH$$

Medium severity conditions are usually preferred to balance formation of oligosaccharides against their degradation and maximize XO concentration (35). However, the degree of polymerization DP (or molecular weight) distribution in XOs mixtures generally depends on not only the treatment severity but also on the substrate and its concentration during treatment (33). In a study by Nabarlatz et al., comparative assessment of six agricultural residues of different botanic origin showed that characteristics of the raw material played a major role in the yield and composition of XOs. However, their yield also depended on the initial content of acetyl groups, since their cleavage liberated acetic acid, which in turn catalyzed xylan depolymerization into XOs (33). In the initial stage of autohydrolysis, hydronium ions were generated through autoionization (dissociation) of water under high temperature or pressure. However, as the reaction proceeded, cleavage of acetyl groups from the xylan backbone formed acetic acid and was believed to contribute more hydronium ions. Although adding acids beyond that released naturally from biomass can facilitate xylan or hemicellulose degradation, XO yields will generally be reduced by generating more monomeric xylose than without

added acid. Controlling the temperature and reaction time can also influence XO characteristics such as the acetyl content and the molar mass distribution (36), although the nature of the raw material plays a significant role (33).

Autohydrolysis has the advantage of eliminating corrosive chemicals for extraction and hydrolysis of xylan but requires equipment that can be operated at as high or higher temperatures and pressures as acid or alkali treatments. In addition, besides xylan degradation, several concurrent processes occur including extractives removal, solubilization of acid-soluble lignin, and solubilization of ash, all of which contribute to undesired non-saccharide compounds in liquors from autohydrolysis processing. The molecular weight distribution of XOs produced by autohydrolysis after solvent extraction contains a large proportion of high DP compounds (MW 1000-3000 g/mol) and a much smaller fraction of low DP compounds (MW<300 g/mol) (33). In addition, autohydrolysis at mild temperatures does not modify cellulose and lignin substantially, allowing their recovery for further processing and utilization.

XOs can also be produced by hydrolytic processes either in basic or dilute acidic media. Dilute sulfuric acid (0.1M-0.5M) is most commonly used for acid production of XOs. The DP distribution of the XOs depends on acid concentration, temperature, and reaction time, but the yield of monosaccharides also depends on the structure and composition of xylan (27). A major disadvantage of acid hydrolysis is low yields of oligomers compared to monomers in addition to production of furfural and other degradation products. However, this disadvantage could be controlled by shortening the reaction time, reducing acid concentration, or removing these by-products by adsorption

chromatography and membrane separation. A major advantage of acid hydrolysis is simple, rapid kinetics; for example, dilute acid hydrolysis requires much less reaction time compared to enzymatic hydrolysis to achieve the same xylan to XOs conversion (a few minutes compared to several hours) (27).

Figure 2.1 summarizes the xylan reaction pathway. The depolymerization of xylan has been described as combined reactions of fast-reacting and slow-reacting fractions, which are first decomposed into high molecular weight XOs (28). As the hydrolytic degradation reaction proceeds, high molecular weight XOs are converted into lower molecular weight XOs, which are further depolymerized to xylose; and xylose is degraded to furfural and many unidentified degradation products. In some cases, low molecular weight XOs can be directly degraded to furfural or other degradation products (21, 28). First-order kinetics with Arrhenius-type dependence on temperature are usually adequate to describe reaction rates profiles, with the weight fraction of fast-reacting xylan, the pre-exponential factors of the kinetic coefficients involved in the reaction, and the corresponding activation energies determined by fitting the data to the kinetic model. In the study by Kumar and Wyman with purified xylooligosaccharides degradation at different pH values, they showed that all the XOs disappeared at higher rates compared to monomeric xylose, and the ratio of XOs disappearance rate constants to xylose degradation rate constant increased with decreasing pH. In addition, the direct degradation of low DP XOs, mainly DP 2 and 3, to undesired products was significant for hydrothermal reactions but could be minimized by adding acid (21).

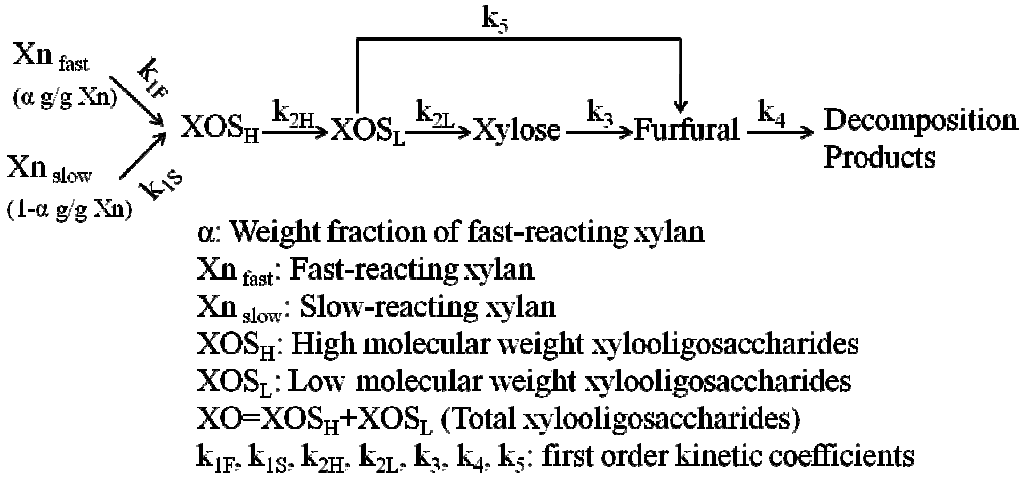

Figure 2.1. Xylan reaction pathway in autohydrolysis to oligomers, xylose, furfural, and degradation products, adapted from Parajo et al., 2004 (28) with permission of Elsevier.

Alternatively, depolymerized hemicellulose may be extracted from lignocellulosic materials by strong alkali solutions (for example, a solution of KOH, NaOH, $Ca(OH)_2$, ammonia, or a mixture of these compounds). However, the extractability of depolymerized hemicellulose varies with the alkali type and isolation conditions used for different plants. In general, alkaline treatment disrupts the cell wall of lignocellulosic materials by dissolving hemicelluloses and lignin, hydrolyzing uronic and acetic esters, swelling the cellulose, decreasing cellulose crystallinity, and cleaving the α-ether linkages between lignin and hemicelluloses as well as the ester bonds between lignin and/or hemicelluloses and hydroxycinnamic acids, such as *p*-coumaric and ferulic acids. Therefore, the depolymerized xylan loses acetyl groups and uronic acids by saponification during extraction and has very limited solubility in neutral aqueous solutions (37). Alkali processing of xylan-containing materials is favored by the pH stability of this polymer, and solubilized xylan and xylan degradation products can be

recovered by precipitation with organic compounds (including acids, alcohols or ketones) (26). However, xylan or soluble XOs obtained from alkali extraction require dilute acid or enzymatic treatment to break them down further to lower DP XOs (26).

2.3.2 Production of XOs by enzymatic hydrolysis

XOs can also be produced by enzymatic hydrolysis of xylan containing materials. However, because the xylan-lignin complex is naturally resistant to enzyme attack, current commercial processes are usually carried out in a two stage sequence: alkaline extraction followed by enzymatic hydrolysis. Xylan, in most plant materials, is a heteropolymer with homopolymeric backbone composed of β-1, 4-linked xylose units and various branching units including D-glucose, L-arabinose, D-galactose, D-mannose, D-glucuronic acid, 4-O-methyl glucuronic acid, D-galacturonic acid, ferulic acid, coumaric, and acetic acid residues, and to a lesser extent L-rhamnose, L-fucose, and various O-methylated neutral sugars (38). Consequently, synergistic action of different enzymes is needed to completely hydrolyze these complex xylan structures. Generally, endo-β-1, 4 xylanases degrade xylan by attacking the β-1, 4 bonds between xylose units to produce XOs, and β-xylosidase converts lower DP XOs into monomeric xylose. In order to maximize production of XOs and minimize xylose production, enzyme mixtures with low exo-xylanase and/or β-xylosidase activity are desirable. Debranching enzymes such as α-L-arabinofuranosidase, α-glucuronidase, and several esterases are needed to cleave xylan side groups (39, 40) and can be dissolved in the reaction media or immobilized. They can also be produced in situ by microorganisms such as fungi and

bacteria that make multiple endoxylanase isoenzymes, reflecting the need for xylanases with specificities that are capable of acting on different substrates (41).

In contrast to autohydrolysis and chemical treatment methods, enzymatic hydrolysis avoids production of undesirable byproducts or high amounts of monosaccharides, or require high pressure or high temperature equipment. However, enzymatic methods usually require much longer reaction times than acid hydrolysis or autohydrolysis. In addition, xylanase with different substrate specificities produces different hydrolysis end-products, and control of production of XOs with a desired DP range can be more difficult. On the other hand, acid hydrolysis of xylan randomly hydrolyzes glycosidic bonds between adjacent xylose units. Thus, acid hydrolysis is more practical for production of XOs in the DP range of two to fifteen (42). A study of the hydrolysis patterns of purified endo-xylanase on birchwood, beechwood, and oat spelt xylans indicated that xylotriose (X3) is the shortest XOs released by xylanase (41). Xylotriose and xylotetraose (X4) fragments are believed to be inaccessible to xylanase enzymes, probably due to substitution with arabinosyl residues. Commercial xylanase preparations are often low in β-xylosidase activity, resulting in xylobiose accumulation (X_2) (43). Similarly, commercial cellulase preparations are usually low in β-xylosidase activity, and that deficiency coupled with the high inhibition of cellulase by xylooligosaccharides has recently been shown to be an important contributor to reduced hydrolysis of xylooligosaccharides to xylose (43) as well as cellulose to glucose (25).

2.4 Xylooligosaccharides separation and purification

XOs from thermochemical or enzymatic treatment usually contain a wide DP range of oligomers and possibly other compounds as stated above. To produce more pure XO fractions used in food or pharmaceutical industries, the hydrolysis liquor must be refined by removing monosaccharides or non-saccharide compounds to obtain the highest possible XO content or a given DP range. Purification and separation of XOs from autohydrolysis liquor is complicated and may require multistage processing for reaction and/or fractionation. Depending on the degree of purity desired, a sequence of several physicochemical treatments may be needed (44).

2.4.1 Solvent extraction

Solvent extraction is frequently applied to recover XOs and also applied to preextract interfering components before chemical or enzymatic treatment to simplify purification. Vacuum evaporation may be applied first to concentrate the crude XOs solution produced by hydrothermal processing and remove volatile components. Then, as shown in Figure 2.2, solvent extraction can remove non-saccharide compounds to yield both a refined aqueous phase and a solvent-soluble fraction that mainly contains most of the phenolics and extractive-derived compounds. The recovery yields and the degree of purification depend on the solvent employed for extraction, with ethanol, acetone, and 2-propanol the most common choices to refine crude XOs solution (44-46). However, lignocellulosic materials used for XOs production may contain stabilizing non-saccharide components, especially comparatively high proportions of uronic groups and/or

compounds in autohydrolysis liquors that are influenced by the XOs substitution pattern (44). A study of solvent extraction of freeze-dried solids by 2-propanol, acetone, and ethanol showed that the highest purities were achieved with ethanol, although at the expense of lower recovery yields (44).

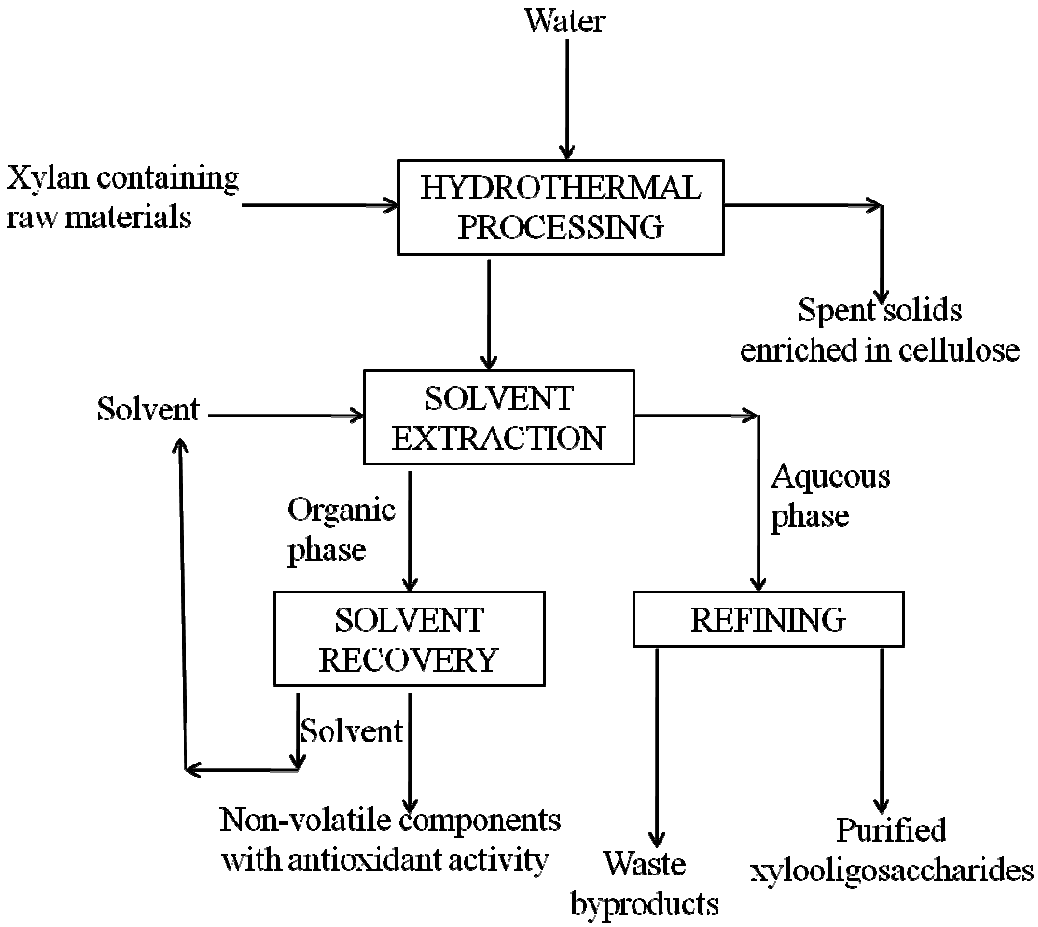

Figure 2.2. Hydrothermal treatment coupled with solvent extraction for production of purified XOs from xylan-containing lignocellulosic materials Hydrothermal treatment coupled with solvent extraction for production of purified XOs from xylan-containing lignocellulosic materials, adapted from Moure et al., 2006. (47) with permission of Elsevier.

2.4.2 Adsorption by surface active materials

Adsorption by surface active materials has been used in combination with other treatment steps to separate oligosaccharides from monosaccharides or remove other undesired compounds. The most widely used adsorbents for purification of XOs liquors include activated charcoal, acid clay, bentonite, diatomaceous earth, aluminium hydroxide or oxide, titanium, silica, and porous synthetic materials (26). For example, Pellerin et al. used activated charcoal followed by elution with ethanol to fractionate XOs based on their molecular weight (48). In the first stage, XOs were retained by activated charcoal and then released according to DP by changing the ethanol concentration during elution (48). Zhu et al.(49) employed the same approach to purify oligosaccharides from aqueous ammonia pretreated corn stover and cobs. In this case, 1-10% w/w activated carbon was added to the supernatant containing oligosaccharides, and the mixture was subsequently eluted with a solution containing 0 to 50% ethanol in water. The highest XOS yield was achieved for elution with 15-30% ethanol, but only the total oligosaccharides concentration was measured by traditional post-hydrolysis with 4% sulfuric acid at 121^{o}C for 1 hour and not the concentrations of each oligosaccharide DP fraction (50).

Montane et al. proposed that activated carbon treatment of raw XOs solutions obtained by autohydrolysis of lignocellulosic materials is feasible for removal of extractives, lignin-derived compounds, and carbohydrate degradation products (51). Selective adsorption of lignin products compared to carbohydrates was favored by three commercial activated carbons at slightly acidic pH. The results also showed that

selectivity towards lignin adsorption was higher when the carbon used was highly microporous and had smaller mesopore diameters, a low volume of mesopores, and a low concentration of basic surface groups to favor adsorption of lignin derivatives (51).

2.4.3 Chromatographic separation techniques

Although all the methods outlined above could be used to refine and concentrate XOs solutions, the resulting XOs solution may not be sufficiently pure. On the other hand, high purity XO fractions have been produced at the analytical scale by chromatographic separations. For example, samples from hydrothermally treated lignocellulosic materials were fractionated by anion-exchange or size-exclusion chromatography ((52-54). However, techniques such as ^{13}C NMR (55), matrix-assisted laser desorption/ionization-time of flight (MALDI-TOF), and nanospray mass spectrometry have usually been employed for refining samples before structural characterization of XOs(53). Katapodis et al. employed size-exclusion chromatograph (SEC) in combination with other techniques for purification of feruloylated oligosaccharides (56). Jacobs and others purified hemicellulose-derived products from hydrothermal microwave treatments of flax shive by employing ion-exchange chromatography and/or SEC in combination with enzymatic processing (57).

Industrially, charcoal chromatography is preferred for sugar purifications due to its higher loading capacity than for other separation methods. However, it is difficult to separate XOs with high DPs, and acidic oligosaccharides (XOs with uronic acid substituents) would overlap with simpler XOs on the chromatograph. As a result, Dowex

1-X4 anion-exchange resin in the acetate form was used before charcoal chromatography to avoid overlapping. Due its low efficiency and time-consuming operation, this method is less satisfactory in separation of high purity XOs. In addition, continuous operation was not applied because of the gradient elution mode used and requirement for column regeneration.

Gel permeation chromatography (GPC) with cross-linked polyacrylamide and cross-linked dextran beads has been successfully applied for fractionating oligosaccharides since the 1960s. Sugars from mannose through mannoheptose were separated from each other using Sephadex G-25, but longer oligomers were not well resolved (58).

Unlike Sephadex, Bio-Gel is composed of polyacrylamide which is not susceptible to microbial degradation and does not leak carbohydrates during elution. Pontis applied Bio-Gel P-2 to separate sucrose through the heptaoligosaccharide of fructosan, but once again, larger fractosans were not separated well (59). Havlicek and Samuelson applied a Bio-Gel P2 column to separate XOs with DP ranging from 2 to 18 from acid pretreated birchwood xylan hydrolysate after removing acidic saccharides with ion-exchange resin (60). Korner et al. fractionated XOs up to DP 7 using a Bio-Gel P4 column operated at 40°C with 0.05 M Tris/HCl buffer (pH 7.8) at a flow rate of 30 ml/hr. Under such conditions, the series of XOs were eluted according to size exclusion principles, whereas acidic saccharides composed of xylose and uronic acids were separated according to partition principles, resulting in xyloheptose being superimposed on glucuronosylxylose. Because Bio-Gel and Toyopearl gels are known to be resistant to

the permeation of acidic saccharides into pores of the gel particles, acidic saccharides are eluted near the void fraction with distilled water as eluent. Distilled water eliminates the need to remove buffer salts after separation, and the XOs fractions collected after separation could be easily concentrated by evaporation. Furthermore, columns filled with Bio-Gel with different pore sizes could be combined in series to maximize separation purity. Sun et al.(42) used three combinations of two columns connected in series to isolate xylose and XOs with DPs ranging from 2 to 15. BioGel P-4 and Toyopearl HW-40F columns proved to provide good resolution, and chromatography with BioGel P-4 and P-2 columns also achieved separation of XOs up to DP 15. However, the resolution of the latter was slightly lower than that of BioGel P-4 and Toyopearl HW-40 columns. In contrast, Toyopearl HW-50 and HW-40 columns connected in series could only separate XOs up to DP 8, as shown in Figure 2.3.

Gel-permeation chromatography is a widely used separation technique that can be easily adapted for an autopreparative system using an autosampler (or injection pump), a refractive index detector, and an auto fraction collector that responds to the detector signal. Figure 2.3 shows a simplified schematic for such a system. Depending on the Bio-Gel pore size, relatively high purity XOs fractions with different DP ranges can be collected, and more columns can be connected in series to further improve separation performance. The main disadvantage of GPC for separation of oligosaccharides is its relatively high cost. Thus, although GPC purification is frequently used to obtain fractions of XOs for structural characterization and the degree of purification of the

different DP fractions is relatively good, GPC tends to be not cost effective for large scale production of XOs.

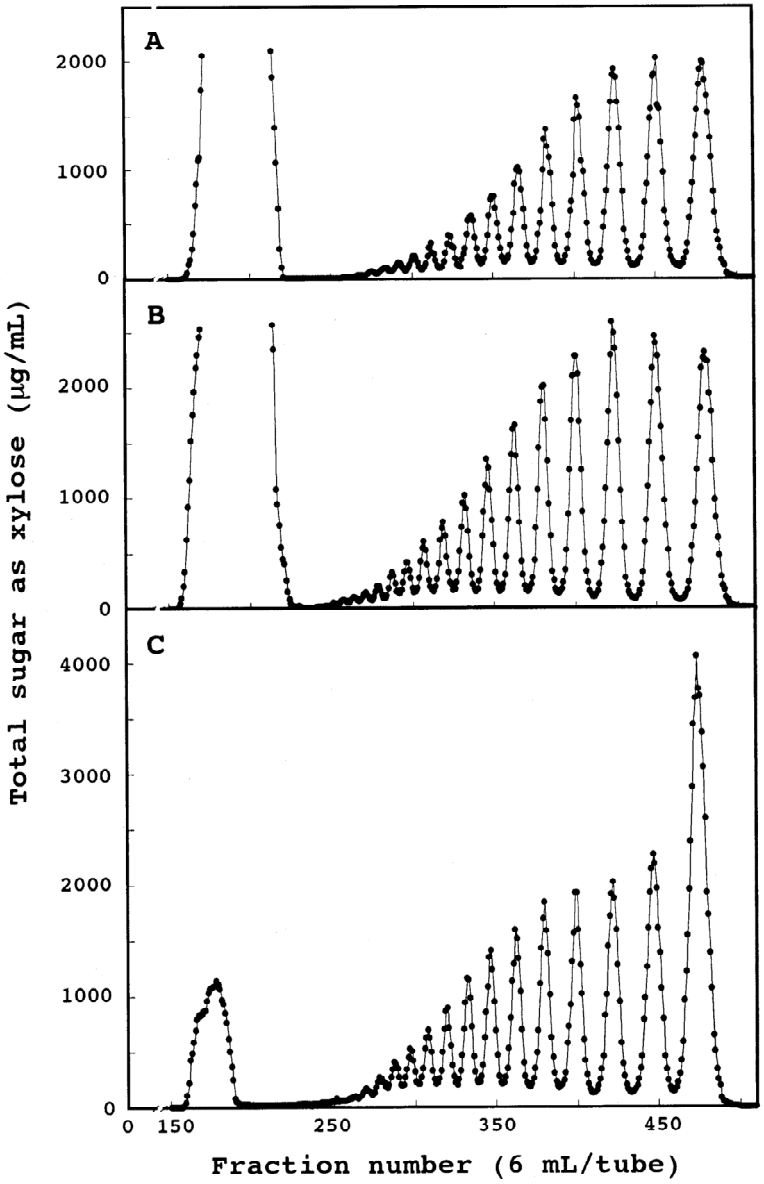

Figure 2.3. Elution profiles of hydrolysis products of three kinds of xylans on BioGel P-4 and Toyopearl HW-40F columns connected in series: (A) Cottonseed xylan; (B) Birchwood xylan; and (C) Oat spelt xylan, adapted from Sun et al. (42) with permission of Elsevier

2.4.4 Membrane separation

Membrane technology, mainly ultrafiltration and nanofiltration, is currently seen as the most promising downstream strategy for industrial manufacture of high purity and concentrated oligosaccharides. Ultrafiltration separates oligosaccharides from higher molecular weight compounds or fractionates oligosaccharides of different DP. On the other hand, nanofiltration can concentrate liquors and/or remove undesired low molecular weight compounds, such as monosaccharides or phenolics, enabling purification of oligosaccharide mixtures (61). Compared to the other purification methods discussed above, membrane separation has a number of advantages including low energy requirements, easily manipulated critical operational variables, and relatively ease of scale-up (62, 63). Certain operational variables including pressure, temperature, feed flow rate, and agitation can impact properties of the solute and membrane and physical aspects directly related to diffusion and convection of the solute, which in turn affects the overall process efficiency. In addition, oligosaccharide inhibition of enzymatic reactions can be reduced by continuous or semi-continuous product removal by membranes (61). However, membrane separation performance can be affected by structural characteristics of oligosaccharides, including the types of monosaccharides, substitutions and linkages in oligomer structure, and the final molecular weight and extent of branching. Furthermore, oligosaccharide solubility has a major impact on membrane separation performance (61).

Membrane separations have been used for preparing various concentrations of several oligosaccharides, including fructose oligosaccharides (64), maltooligosaccharides (65), soybean oligosaccharides (66), pecticoligosaccharides (67), and

chitooligosaccharide (68). However, limited literature has reported applications of membranes to refining XOs containing solutions, and some dealt with processing of solutions/slurry resulting from hydrolytic treatment followed by enzymatic reaction. Recently, some studies successfully applied membranes to XOs produced by enzymatic hydrolysis or autohydrolysis of xylan containing materials (46, 69). Yuan and others employed nanofiltration membranes for concentrating XOs obtained by enzymatic hydrolysis of xylan from steamed corn cobs, whereas concentration and fractionation of XOs by sequential membrane-based steps has been employed in multistage purification processes (70).

Although microfiltration and ultrafiltration are well established separation processes for purifying oligosaccharides from high molecular weight enzymes and polysaccharides, commercial streams often contain low molecular weight sugars that are undesirable or do not contribute to beneficial properties of the higher molecular weight oligosaccharides. In a study by Akpinar et al. (31), ultrafiltration was used to separate and purify XOs from hydrolysate generated by enzymatic hydrolysis of cotton stalk xylan. The hydrolysate was first filtered through a 10 kDa molecular weight cut off membrane to remove high molecular weight polysaccharides and enzymes, followed by filtration through a 1-3 kDa molecular weight cut off membrane to further fractionate the XOs. Permeate from the 1 and 3 kDa membranes contained mixtures of different DPs, with 43.3 and 81.6%, respectively, reported to have DPs higher than 5. Although chromatography is still the principal choice, Leiva and Guzman reported nanofiltration membranes can concentrate or purify oligosaccharide mixtures (71) as an alternative to

more expensive chromatographic techniques. The molecular weight cut-off of nanofiltration membranes is in the range of 200-1000 Da, combining ultrafiltration and reverse osmosis separation properties. However, despite its promise for industrial scale purification and concentration of oligosaccharide mixtures, its performance for fractionation of oligosaccharide mixtures has not yet been convincingly proven.

2.4.5 Centrifugal partition chromatography

Centrifugal purification chromatography (CPC), a method based on countercurrent chromatography, has recently been proposed for XOs purification (72). Separation is based on the differences in partitioning behavior of components between two immiscible liquids. CPC uses a so-called “hydrostatic mode” resulting from constant centrifugal force intensity and direction for separation. Therefore, the mobile phase penetrates the stationary phase either by forming droplets or by jets stuck to the channel walls, broken jets, or atomization. The intensity of agitation of both phases depends on centrifugal force intensity, mobile phase flow rate, and solvent physical properties. Compared to countercurrent chromatography, stationary phase retention is less sensitive to physical properties of the solvent systems, such as viscosity, density, and interfacial tension (73). Similar to other chromatographic techniques, the CPC method is able to separate broad ranges of molecular weight compounds. In addition, samples can be recovered by flushing the system since the stationary phase is also a liquid. In contrast to other chromatographic techniques such as GPC, CPC could be used for preparative separation or purification because of its large stationary phase volume (74).

CPC has been widely used as an efficient purification and separation tool for many compounds including flavonoids, flavonolignans, and macrolide antibiotics (74). Shibusawa et al. (75) employed CPC to purify apple-derived catechin oligosaccharides by operating in an ascending mode with a solvent system containing equal volumes of hexane, methyl acetate, acetonitrile, and water. Apple catechin oligosaccharides up to DP 10 were successfully fractionated by this method. However, the total mass and corresponding purity of each DP fractions were not reported.

Lau et al. (74) used CPC to separate and purify xylan-derived oligosaccharides from birchwood xylan. A CPC solvent system containing dimethyl sulfoxide (DMSO), tetrahydrofuran (THF), and water in a 1: 6: 3 volumetric ratio, respectively, was chosen for its ability to dissolve XOS of different DP. Monomeric xylose and XOS up to DP 5 (xylopentose) were collected with this separation system with relatively high purity for DP 1 and 2 (higher than 85%) and relatively low purity for other DPs (lower than 55%).

2.5 Characterization and quantification of xylooligosaccharides

2.5.1 Measuring xylooligosaccharides by quantification of reducing ends

Each oligosaccharide chain, with few exceptions, has a reducing end on its terminal sugar residue. Because the aldehyde or ketone group of this terminal sugar residue is not fixed into a ring structure, it is free to undergo oxidation-reduction reactions with chemical reagents to form products that can be detected by colorimetric methods. By measuring the number of reducing ends in a sample, the total number of oligosaccharide chains can be determined. Colorimetric methods to measure

monosaccharides as well as oligosaccharides employ a UV-Vis spectrophotometer, a simple and inexpensive instrument. Although these methods are still used today, different types of sugars cannot be differentiated.

The most widely used method for colorometric quantification of reducing ends is the dinitrosalicylic acid (DNS) assay, which was first developed to determine the concentration of monosaccharides (76-78) and then applied to quantify the total numbers of oligosaccharide chains in aqueous solution (79, 80). In the DNS assay, 3, 5-dinitrosalicylic acid reacts with sugar reducing ends to form red-brown 3-amino-5-nitrosalicylate, that is quantified by comparison of its absorbance at 560 nm or above (76-78) to that with pure sugar calibration standards. Thus, the volumetric concentration of reducing ends can be calculated by determining the intensity of color formation of 3-amino-5-nitrosalicylate. However, the equivalence between amino-nitrosalicylate produced and the number of reducing ends varies for different sugars, suggesting that the DNS assay can only be accurate for evaluation of a single sugar (76, 81). Other methods in this category, such as the arsenomolybdate (ARS; also known as Nelson-Somogyi assay) assay (82), the p-hydroxybenzoic acid hydrazide (PAHBAH) assay (83, 84), and the phenol-sulfuric acid assay (85, 86) are also used to measure reducing sugars but have similar response variance issues with different sugars as the DNS assay. When these colorimetric methods were applied to measure reducing ends of xylooligosaccharides, they responded differently to xylooligosaccharides of different DP. For example, the ARS assay showed less reactivity to higher DP xylooligosaccharides, while the DNS assay showed the opposite trend (80). The reason, however, is not well understood.

2.5.2 Characterizing xylooligosaccharide composition

The determination of structure of oligosaccharides released from biomass hydrolysis first requires knowledge of what monosaccharide components are present and in what amounts. This can be achieved by enzymatic or chemical decomposition of oligosaccharides into their monosaccharide building blocks followed by identification and quantification of each component by gas chromatography (GC) or high performance liquid chromatography (HPLC) (4). GC methods require multistep formation of volatile derivatives of monosaccharides prior to analysis, with two derivatization methods routinely used: formation of alditol acetates or TMS methyl glycosides (4).

Although GC methods have the advantage of baseline sugar resolution (50), HPLC is more widely used for analysis because sugar derivatization is not required. In standard biomass analytical procedures developed by the National Renewable Energy Laboratory (NREL), HPLC employing a refractive index (RI) detector is the default tool for determining total component monosaccharides released from post hydrolysis of oligosaccharides with 4wt% sulfuric acid at 121°C for 1 hour (87). Two columns, both from Bio-Rad, are commonly used in this application. The HPX-87P column can separate all common biomass sugars (cellobiose, glucose, xylose, galactose, arabinose, and mannose) with high resolution. However, retention times (RT) for xylose, mannose, and galactose on the HPX-87H column are close (within 0.1 min), which often results in a single peak, depending on column conditions. But considering that heteroxylans are the dominant form of hemicellulose in most lignocellulosic feedstocks (refer to Section 2.2.2), the amounts of galactose and mannose in oligosaccharides released from biomass

pretreatment are low. Thus, the HPX-87H column is widely used to measure the glycosyl composition of xylooligosaccharides, because it provides stable and near-baseline resolution of glucose, xylose, and arabinose.

2.5.3 Direct characterization of different DP xylooligosaccharides

As discussed in Section 2.2.3, there is a significant and increasing demand for reproducible, fast, and simple methods to characterize and quantify XOs released from biomass pretreatment to better understand the decomposition mechanisms of hemicellulose in major lignocellulosic feedstocks. To date, several methodologies for qualitative and quantitative analysis of XOs have been developed, which can be grouped into the following categories: HPLC, high performance anion exchange chromatography (HPAEC), and capillary electrophoresis (CE).

2.5.4 HPLC

Li et al. (2003) quantitatively analyzed XOs derived from hydrothermal pretreatment of oat spelt xylan at 200°C for 15 minutes with a 5 wt% solid loading (88). A Waters model 717 chromatography system, equipped with a RI detector and a Bio-Rad Aminex HPX-42A ion-moderated partition (IMP) column was used. At a flow rate of 0.2 ml/min and a column temperature of 85°C, xylooligosaccharides up to DP 10 were separated, but the baseline for the IMP chromatogram was difficult to resolve, especially for DP higher than 5, as shown in Figure 2.4. Commercial low DP XOs standards (xylobiose, xylotriose, xylotetraose, and xylopentaose) were used to calibrate the IMP

system for quantification of xylooligosaccharides with DPs in that same range of 2 to 5. It was also shown that xylooligosaccharides of DP from 2 to 5 could be quantified by taking the ratio of peak heights of each XO to the peak height for xylose and multiplying this ratio by the concentration of the latter. These results confirmed that peak height followed concentrations closely for xylooligosaccharides with DP less than 5 for an RI detector. This approach was extended to quantifying XOs with higher DPs from 6 to 10; however, accuracy could not be confirmed due to the lack of standards.

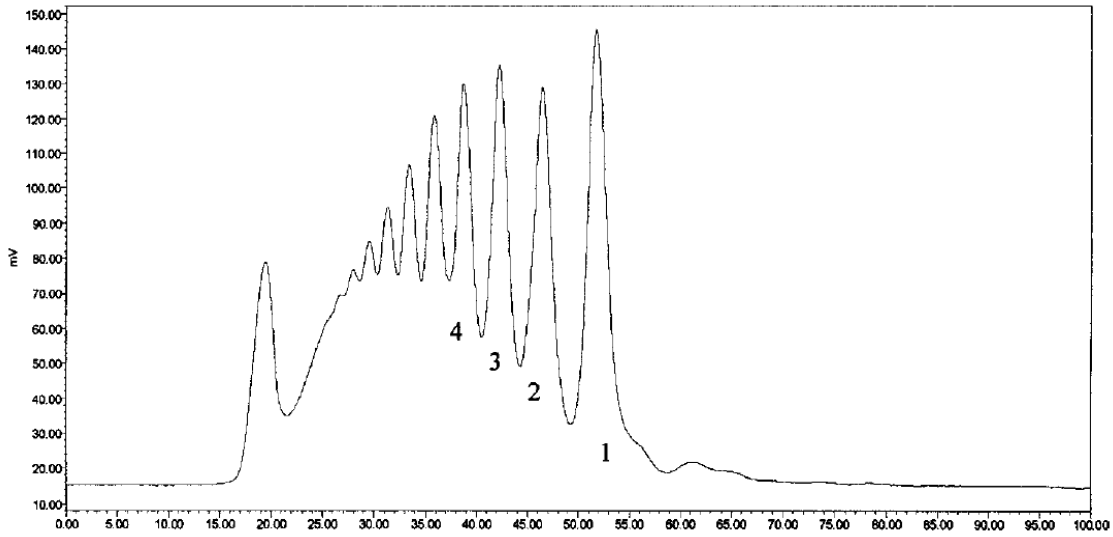

Figure 2.4. IMP chromatogram of xylooligosaccharides derived from hydrothermal pretreatment of oat spelt xylan, 1-DP 1; 2-DP2; 3-DP3; 4-DP4, adapted from Li et al. (2003), with permission of Springer.

Ohara et al. (2006) used a cation exchange column (Sugar KS-802; Showa Denko, Tokyo) with RI detector to characterize xylooligosaccharides up to DP6, which were prepared by enzymatic hydrolysis of birchwood xylan with endo-xylanase (89). The column temperature was 60°C, and the mobile phase was water with a flow rate of 0.6 ml/min.

For HPLC systems, an evaporative light scattering detector (ELSD) was reported to be more sensitive and thus provide better baseline stability than RI based detectors for measuring oligosaccharides (90). Yu and Wu (2009) identified gluco-oligosaccharides from DP2 to DP6 using a Prevail™ carbohydrate ES column with an ELSD 3300 detector from Alltech (91). Other literature on specific characterization of xylooligosaccharides using ELSD, however, is scarce.

Recently, a Waters Acquity® ultrahigh performance liquid chromatography (UPLC) equipped with a BEH HILIC column and 4000 QTrap MS detector was applied to characterize xylooligosaccharides by Tomkins et al. (92). As the chromatogram in Figure 2.5 shows, the approach was very sensitive, with detection of xylooligosaccharides at concentrations of about a pmol and very fast within only 2 min needed to separate xylooligosaccharides of DP up to 6.

2.5.5 HPAEC

The advent of HPAEC featuring pulsed amperometric detection (HPAEC-PAD) in 1980s provided a highly sensitive and selective tool for separation and detection of complex carbohydrates without derivatization. The recognition by Johnson in 1986 that oligosaccharides could be detected by PAD greatly enhanced the popularity of HPAEC (93). HPAEC-PAD is often classified as an HPLC method. However, HPAEC-PAD technology is discussed in some detail here because of its novel ability to analyze and characterize XOs over a wide DP range. The unique advantages of HPAEC were first described in the paper by Rocklin and Pohl in 1983(94). The oligosaccharides were

separated in strong alkaline eluents (pH>13), where their hydroxyl groups were of deprotonated and thus rendered anionic. The number of hydroxyl groups in a single oligosaccharide molecule varies with DP, resulting in various weakly acidic properties which the HPAEC use to separate oligosaccharides.

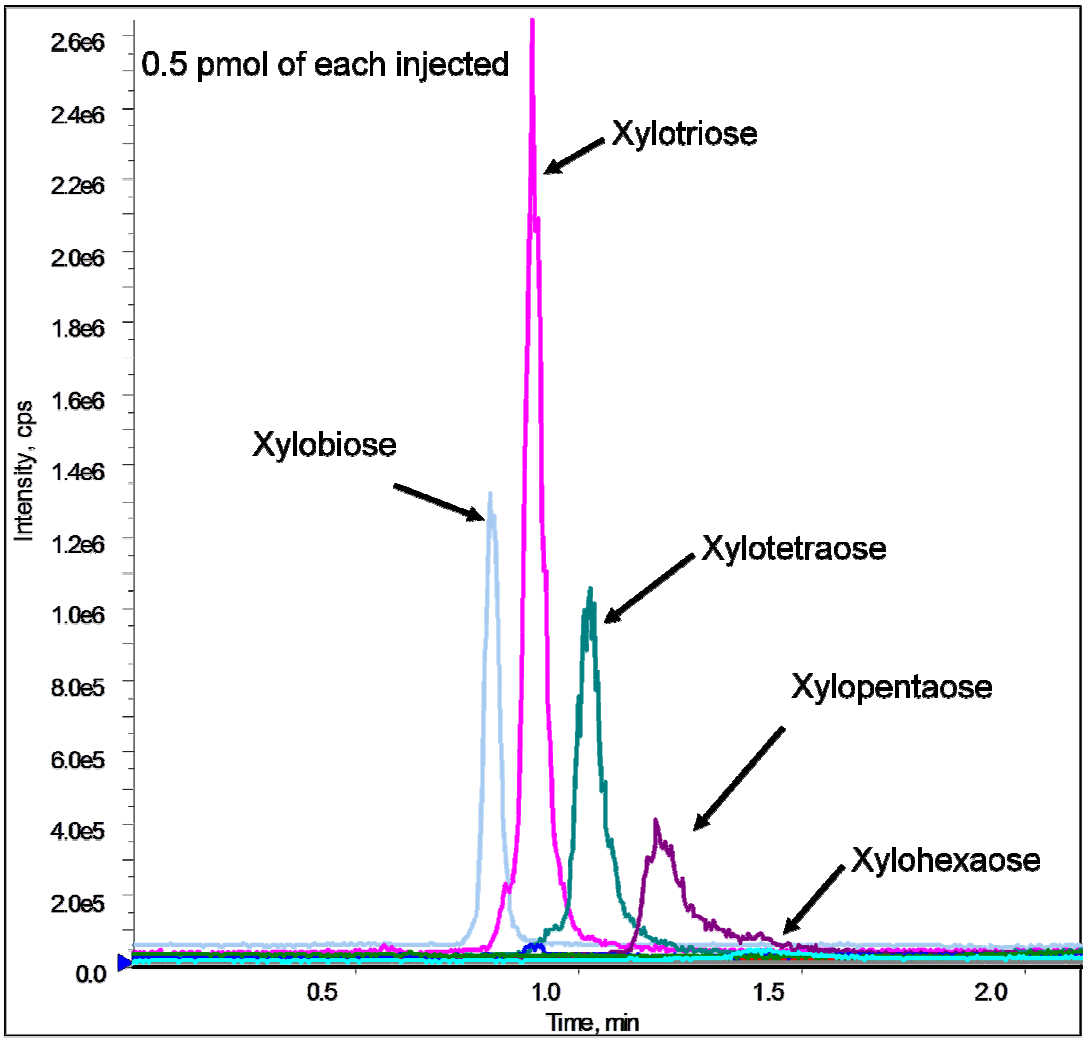

Figure 2.5. UPLC chromatogram of xylooligosaccharides of DP 2 to DP 6, adapted from Tomkins et al. (2010) with permission of the authors.

The PAD detection mechanism consists primarily of a three-step potential waveform with a frequency of 1-2 Hz. When analyte molecules are absorbed on the oxidation-free surface of the gold working electrode illustrated in Figure 2.6 (95), a detection potential (E_1) appropriate for the analyte properties as well as oxidation mechanism is applied first, and then the analyte molecules are oxidized. Thus, the anodic signal current can be measured in this step. Following detection, the electrode surface is usually oxidatively cleaned by a positive potential (E_2) and then reactivated by a negative potential (E_3). Alternatively, the cleaning potential (E_2) could be negative, as demonstrated for effectively minimizing electrode wear (96, 97). In particular, a waveform suggested by Dionex Technical Note 21 has been widely used for characterizing monosaccharides and oligosaccharides, as shown in Table 2.2 (96).

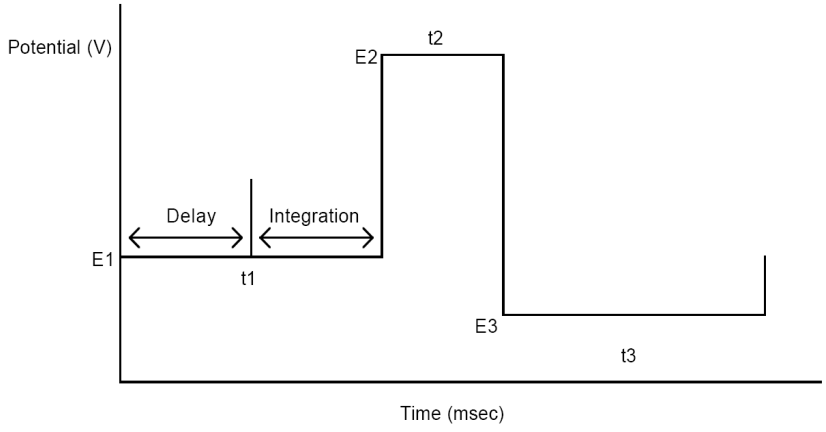

Figure 2.6. Diagram of the pulse sequence for carbohydrate detection on a PAD detector, reproduced from Dionex Technical Note 20 with permission of Dionex Corporation.

Table 2.2. Waveform of PAD for carbohydrates analysis using the Dionex IC system, reproduced with Dionex Technical Note 21 permission of Dionex Corporation.

Time (ms)	Potential (V)	Integration
0	+0.1	
200	+0.1	Begin
400	+0.1	End
410	-2.0	
420	-2.0	
430	+0.6	
440	-0.1	
500	-0.1	

Dionex Corporation recently advanced its oligosaccharides profiling using HPAEC-PAD with its CarboPac PA-100 and CarboPac PA-200 columns. Several publications have successfully profiled the DP distribution of the oligosaccharides amylopectin, maltodextrin, and inulin up to DP 60 (3, 98-102). However, HPAEC-PAD characterization of xylooligosaccharides derived from hemicellulose in lignocellulosic biomass is difficult due to their low solubility at room temperature and resulting precipitation of higher DP oligosaccharides (103). In addition, the heterogeneous glycosyl residue composition of side chains and different linkage substitutions also limit HPAEC-PAD. Yang and Wyman successfully separated XOs released from hydrothermal pretreatment of corn stover using a Dionex DX-600 module with a CarboPac PA100 column (2). The mobile phase was operated in a gradient mode (50 mM to 450 mM of sodium acetate (NaAc)) through 150 mM NaOH (102) with the same waveform shown in Table 2.2. As the chromatogram shows in Figure 2.7, xylooligosaccharides with DPs up

to 13 were separated well with near baseline resolution. Peaks suspected to represent higher DP xylooligosaccharides could also be detected, but the separation was relatively poor.

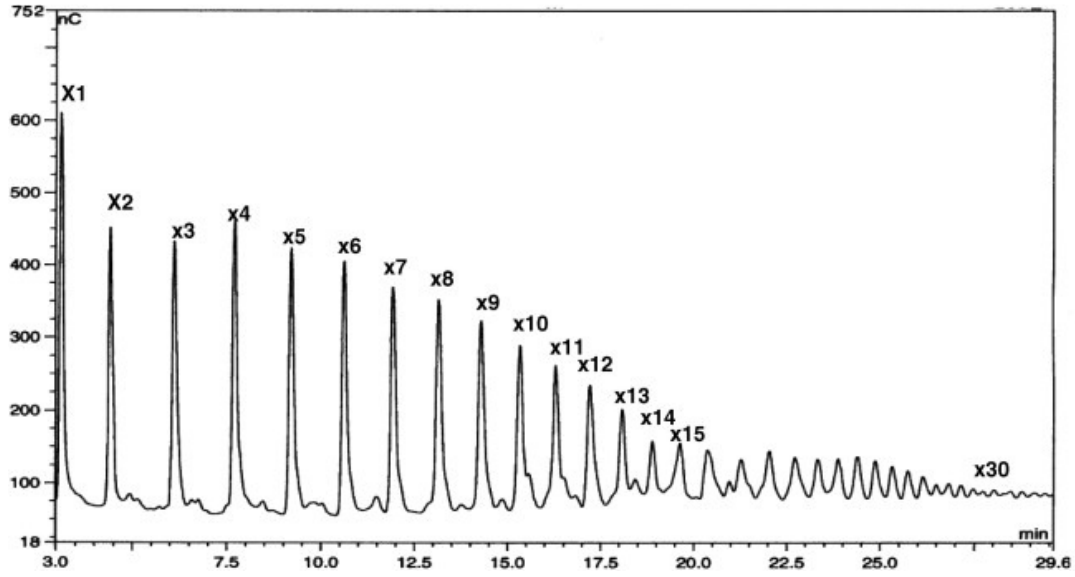

Figure 2.7. Dionex IC chromatogram of xylooligosaccharides released from hydrothermal pretreatment of corn stover, adapted from Yang and Wyman (2008) with permission of Elsevier.

The PAD response of these xylooligosaccharides is believed to depend on the size and spatial structure of analyte molecules (104, 105) and vary with DP in this situation. Koch et al. showed that relative electrochemical responses of amylopectin oligosaccharides increased with DP based on molar concentrations but decreased with DP based on mass concentrations (99). The variable detection behavior is one of the disadvantages of this technique and results in the need for sugar standards for accurate quantification of each DP fraction. However, standards of xylooligosaccharides are only available for DPs below 6 (Megazyme International Ireland Ltd., Ireland) and even then

are very expensive. Alternatively, a recent study by Li et al. defined and calculated a series of PAD response factors for xylooligosaccharides of different DP, providing a relatively accurate and rapid quantification of xylooligosaccharides up to DP 14 without the need for expensive sugar standards (106). As shown in Figure 2.8, a steep decline in the response factors for DP 2 to 7 was observed while the curve tended to level off for xylooligosaccharides with DP higher than 10, thereby demonstrating that higher DP xylooligosaccharides have lower PAD responses per microgram of sample injected.

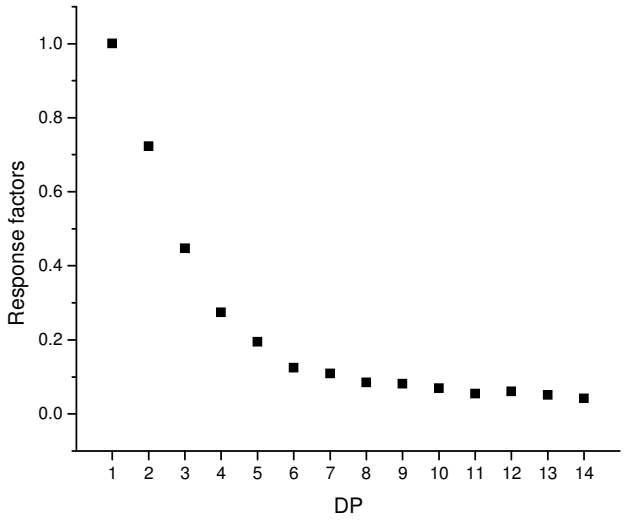

Figure 2.8. Response factors based on PAD peak height and mass concentrations for xylooligosaccharides of DP 1 to 14, with xylose as the sugar standard, adapted from Li et al. (2012).

In the case of HPAEC-PAD for oligosaccharides with the same glycosidic linkages, smaller DP molecules elute first followed by larger ones; however, the order can change when different linkage variants are mixed. For example, Morales et al. showed that isomaltohexaose eluted before maltotriose (107). In fact, factors like charge,

molecular size, sugar composition, and glycosidic linkages can impact chromatographic separation (108). Thus, the effects of these factors must be considered when measuring oligosaccharides released by lignocellulosic biomass, particularly for biomass with highly heterogeneous cell wall polysaccharides. In this situation, additional analytical techniques following HPAEC-PAD are required, such as Mass Spectroscopy (MS) or Nuclear Magnetic Resonance Spectroscopy (NMR).

2.5.6 Capillary electrophoresis

Capillary electrophoresis (CE) has been successfully applied to separate a wide range of xylooligosaccharide compounds. Since the middle of 1990s, application of CE to characterize xylooligosaccharides released from plant cell wall polysaccharides has been reported in several publications (109-112). However, due to the lack of charged groups and chromophores, applications to separation of important oligosaccharides by CE are limited (113, 114). Kabel et al. applied CE-LIF (laser induced fluorescence detector) successfully to separate xylooligosaccharides derived from hydrothermally treated *Eucalyptus* woods (115). In this case, xylooligosaccharides were derivatized with 9-aminopyrene-1,4,6-trisulfonate (APTS), which attached to the reducing end of oligosaccharide molecules to provide a fluorescent APTS tag as well as three negative charges. As shown by the LIF-electropherograms in Figure 2.9, a series of xylooligosaccharides up to DP 17 that had been derivatized with APTS were separated with very high resolution and much better than similar xylooligosaccharide samples that

were not derivatized. Coupled with MS, the minor peaks between the major peaks were identified as linear 1, 4-β-xylooligosaccharides with a different structure.

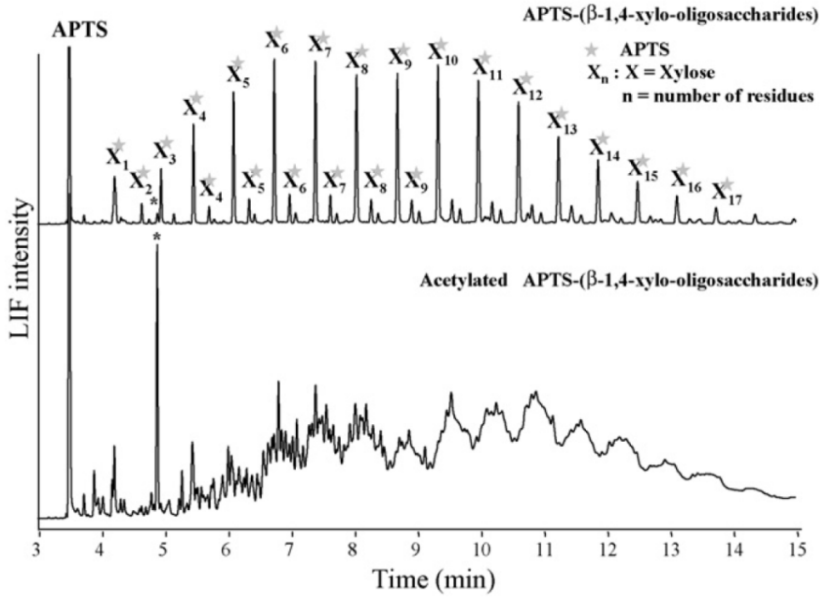

Figure 2.9. LIF-electropherograms of APTS derivatized β-(1, 4)-xylooligosaccharides (top) and (less diluted) *O*-acetylated β-(1, 4)-xylooligosaccharides (bottom) obtained from hydrothermally treated *Eucalyptus* wood (* is maltose internal standard), adapted from Kabel et al. (2006) with permission of Elsevier.

Although derivatization leads to improved sensitivity and resolution with CE, different reactivity of derivatizing reagents and formation of several byproducts result in control problems for consistent preparation of analytes (116). High pH buffer and other detection techniques have been used to avoid derivatization, but successful application on oligosaccharides profiling has not been shown.

2.5.7 Determining detailed structures of oligosaccharides by MS and NMR

The analytical techniques reviewed in previous sections are effective for characterizing glycosyl residue compositions for oligosaccharides as well as DP profiling

of oligosaccharides with the same type of glycosyl linkages. However, they cannot provide detailed structural information for oligosaccharides, such as glycosyl linkage composition, the sequence of glycosyl residues, and the anomeric configuration. MS and NMR are needed to characterize such structural features for oligosaccharides.

MS has proven to be valuable for several aspects of structural characterization of oligosaccharides. With different combinations of ionizations and analyzers, MS is often coupled to chromatography techniques, such as GC-MS, HPLC-MS, and HPAEC-MS, but many challenges remain. For example, HPAEC could provide good separation of oligosaccharides without the need for derivatization, but the eluent used in HPAEC contains a high concentration of salt which limits use with MS (115). Regardless of whether MS is online or offline, good separation of oligosaccharides prior to MS analysis will always facilitate structural characterization. Thus, preparative columns such as size exclusion (52) and ion exchange are also used to isolate oligosaccharides into different fractions for offline MS analysis. Currently, electrospray (ESI) and matrix-assisted laser desorption (MALDI) (52) are the most common ionization sources used for xylooligosaccharides characterization in combination with tandem MS analyzers (117-122). Usually, one type of MS analysis is better for a particular type of oligosaccharide; for example, MALDI-TOF (time-of-flight) MS allows routine determination of the molecular weight of oligosaccharides containing more than 10 glycosyl residues (4). As the MALDI-TOF mass spectra shown in Figure 2.10, xylooligosaccharides from *Eucalyptus* wood with different chain lengths were characterized with additional information on the degree of acetylation (123).

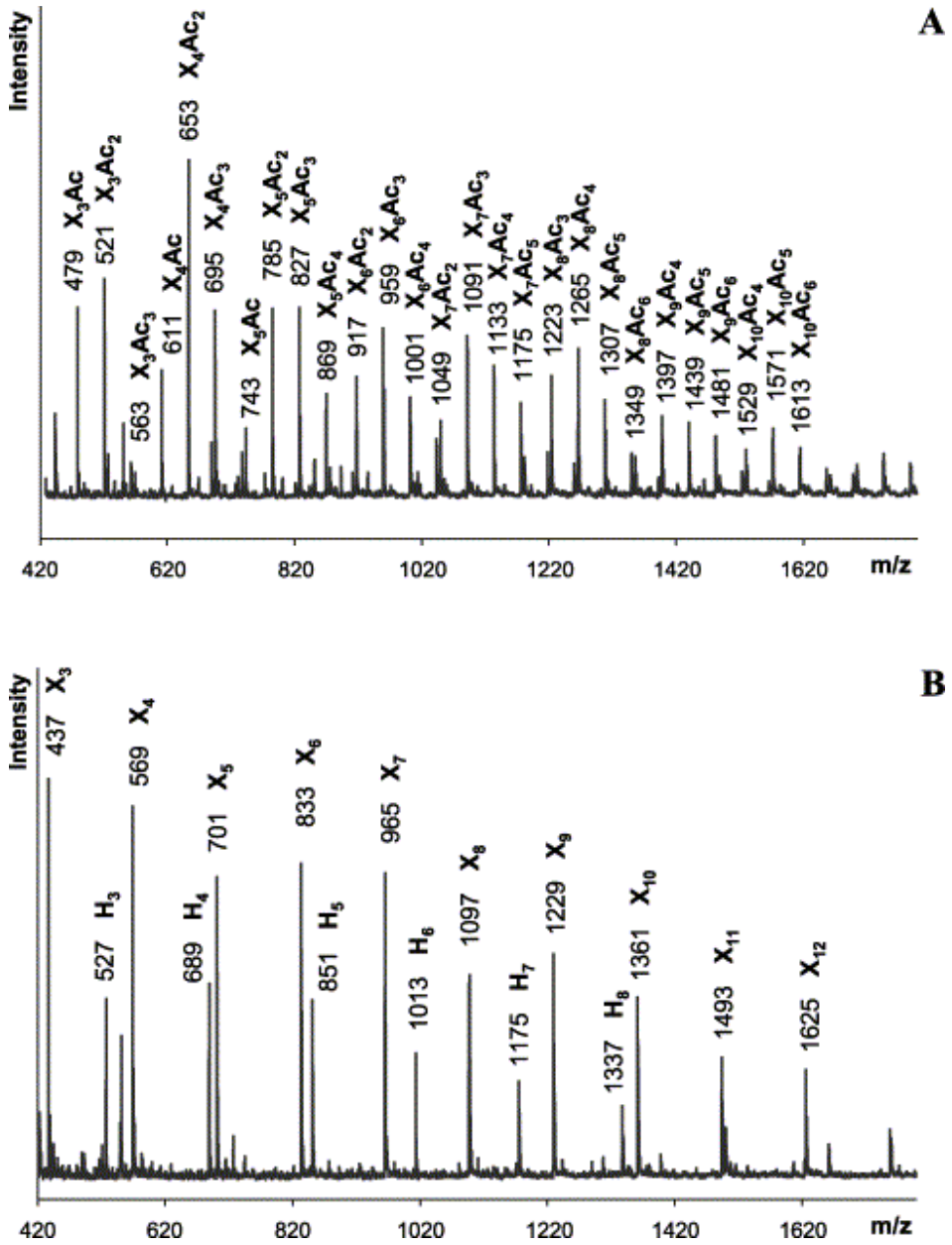

Figure 2.10. MALDI-TOF mass spectra of the neutral xylooligosaccharides obtained from *Eucalyptus* wood hydrolysate (A) before and (B) after saponification (X=xylose; Ac=acetyl-group; H=hexose), adapted from Kabel et al. (2002) with permission of Elsevier.

NMR has proven valuable for understanding oligosaccharide structures. The most used isotopes in oligosaccharides characterization are ^{1}H and ^{13}C. For example, ^{1}H-NMR

can identify the anomeric configuration of glucosyl residues in an oligosaccharide fragment (124-126), and the glycosyl sequence of oligosaccharides can be determined by both one- and two-dimensional (1-D and 2-D) NMR (4, 127). NMR provides an effective method for quick and accurate characterization of specified molecular structures or chemical bonds when the corresponding chemical shifts have been previously defined. In most cases, NMR spectra are insufficient to analyze an unknown structure, and structural information from MS and other analytical techniques must be also used.

2.6 Concluding remarks

Characterizing oligosaccharides released during biomass pretreatment or enzymatic hydrolysis can reveal important structural information about hemicellulose polysaccharides in plant cell walls and how they change during deconstruction to form sugars or other products. XOs also have excellent potential for applications in pharmaceutical, agriculture, and food industries. XOs can be produced by chemical or enzymatic methods on an industrial scale from lignocellulosic materials. Chemical methods are preferred to produce XO mixtures with a wide DP range, while enzymatic methods are preferred in the food or pharmaceutical industries to reduce formation of degradation products. With the growing importance of making fuels from cellulosic biomass and the increasing demand for xylooligosaccharides, more opportunities are emerging to process xylan-rich pretreatment hydrolyzate in a cellulosic biorefinery into high value products that could further lower the cost of cellulosic biofuels. However,

separation technologies are needed to produce high purity XO fractions that span desired DP ranges for industry applications or characterization.

2.7 Acknowledgments

We gratefully acknowledge the support by the Office of Biological and Environmental Research in the DOE Office of Science through the BioEnergy Science Center (BESC). The authors would like to thank Professor Eugene A. Nothnagel at the Botany and Plant Science Department of University of California, Riverside and Dr. Bruce A. Tomkins at Oak Ridge National Laboratory for valuable discussions and comments for this chapter. We are thankful to the Center for Environmental Research & Technology (CE-CERT) for providing the facilities and equipments. We would also like to thank Ford motor company for their support of the Chair in Environmental Engineering at the University of California Riverside (UCR).

2.8 References

1. Abballe F, Toppazzini M, Campa C, Uggeri F, Paoletti S. Study of molar response of dextrans in electrochemical detection. J. Chromatogr. A. 2007 May;1149(1):38-45.
2. Yang B, Wyman CE. Characterization of the degree of polymerization of xylooligomers produced by flowthrough hydrolysis of pure xylan and corn stover with water. Bioresource Technol. 2008 Sep;99(13):5756-62.
3. Ronkart SN, Blecker CS, Fourmanoir H, Fougnies C, Deroanne C, Van Herck J-C, et al. Isolation and identification of inulooligosaccharides resulting from inulin hydrolysis. Analytica Chimica Acta. 2007 Nov;604(1):81-7.
4. Albersheim P, Darvill A, Roberts K, Sederoff R, Staehelin A. Plant cell walls : from chemistry to biology. New York, NY: Garland Science; 2010.
5. Himmel ME. Biomass recalcitrance : deconstructing the plant cell wall for bioenergy. Oxford: Blackwell Pub.; 2008.

6. Kabyemela BM, Adschiri T, Malaluan RM, Arai K. Glucose and fructose decomposition in subcritical and supercritical water: Detailed reaction pathway, mechanisms, and kinetics. Ind Eng Chem Res. 1999 Aug;38(8):2888-95.
7. Shallom D, Shoham Y. Microbial hemicellulases. Curr Opin Microbiol. 2003 Jun;6(3):219-28.
8. Wyman CE, Decker SR, Himmel M, Brady JW, Skopec CE, Viikari L. Hydrolysis of Cellulose and Hemicellulose. In: Dumitriu S, editor. Polysaccharides : structural diversity and functional versatility. 2nd ed. New York: Marcel Dekker; 2005. p. xvii, 1204 p.
9. Kumar R, Wyman CE. Access of cellulase to cellulose and lignin for poplar solids produced by leading pretreatment technologies. Biotechnol Progr. 2009 May-Jun;25(3):807-19.
10. Studer MH, DeMartini JD, Davis MF, Sykes RW, Davison B, Keller M, et al. Lignin content in natural Populus variants affects sugar release. Proc. Natl Acad Sci USA. 2011 Apr;108(15):6300-5.
11. Wyman CE. What is (and is not) vital to advancing cellulosic ethanol. Trends Biotechnol. 2007 Apr;25(4):153-7.
12. Lynd LR, Wyman CE, Gerngross TU. Biocommodity engineering. Biotechnol Prog. 1999 Oct 1;15(5):777-93.
13. Ye ZH, Lee CH, Teng Q, Huang WL, Zhong RQ. Down-regulation of PoGT47C expression in poplar results in a reduced glucuronoxylan content and an increased wood digestibility by cellulase. Plant Cell Physiol. 2009 Jun;50(6):1075-89.
14. Azadi P, Naran R, Black S, Decker SR. Extraction and characterization of native heteroxylans from delignified corn stover and aspen. Cellulose. 2009 Aug;16(4):661-75.
15. Wyman CE. Potential synergies and challenges in refining cellulosic biomass to fuels, chemicals, and power. Biotechnol Prog. 2003 Mar-Apr;19(2):254-62.
16. Somerville C, Youngs H, Taylor C, Davis SC, Long SP. Feedstocks for lignocellulosic biofuels. Science. 2010 Aug;329(5993):790-2.
17. Wyman CE. Biomass ethanol: Technical progress, opportunities, and commercial challenges. Annu Rev Energ Env. 1999 Nov;24:189-226.
18. Wyman CE, Dale BE, Elander RT, Holtzapple M, Ladisch MR, Lee YY. Coordinated development of leading biomass pretreatment technologies. Bioresource Technol. 2005 Dec;96(18):1959-66.
19. Kumar R, Mago G, Balan V, Wyman CE. Physical and chemical characterizations of corn stover and poplar solids resulting from leading pretreatment technologies. Bioresource Technol. 2009 Sep;100(17):3948-62.
20. Selig MJ, Viamajala S, Decker SR, Tucker MP, Himmel ME, Vinzant TB. Deposition of lignin droplets produced during dilute acid pretreatment of maize stems retards enzymatic hydrolysis of cellulose. Biotechnol Progr. 2007 Nov-Dec;23(6):1333-9.
21. Kumar R, Wyman CE. The impact of dilute sulfuric acid on the selectivity of xylooligomer depolymerization to monomers. Carbohyd Res. 2008 Feb 4;343(2):290-300.
22. Hahn-Hagerdal B, Palmqvist E. Fermentation of lignocellulosic hydrolysates. II: inhibitors and mechanisms of inhibition. Bioresource Technol. 2000 Aug;74(1):25-33.

23. Ladisch M, Mosier N, Wyman C, Dale B, Elander R, Lee YY, et al. Features of promising technologies for pretreatment of lignocellulosic biomass. Bioresource Technol. 2005 Apr;96(6):673-86.
24. Kumar R, Wyman CE. Effect of enzyme supplementation at moderate cellulase loadings on initial glucose and xylose release from corn stover solids pretreated by leading technologies. Biotechnol Bioeng. 2009 Feb 1;102(2):457-67.
25. Qing Q, Yang B, Wyman CE. Xylooligomers are strong inhibitors of cellulose hydrolysis by enzymes. Bioresource Technol. 2010 Dec;101(24):9624-30.
26. Vazquez MJ, Alonso JL, Dominguez H, Parajo JC. Xylooligosaccharides: manufacture and applications. Trends Food Sci Tech. 2000 Nov;11(11):387-93.
27. Akpinar O, Erdogan K, Bostanci S. Production of xylooligosaccharides by controlled acid hydrolysis of lignocellulosic materials. Carbohyd Res. 2009 Mar 31;344(5):660-6.
28. Parajo JC, Garrote G, Cruz JM, Dominguez H. Production of xylooligosaccharides by autohydrolysis of lignocellulosic materials. Trends Food Sci Tech. 2004 Mar;15(3-4):115-20.
29. de Menezes CR, Silva IS, Pavarina EC, Dias EFG, Dias FG, Grossman MJ, et al. Production of xylooligosaccharides from enzymatic hydrolysis of xylan by the white-rot fungi Pleurotus. Int Biodeter Biodegr. 2009 Sep;63(6):673-8.
30. Brienzo M, Carvalho W, Milagres AMF. Xylooligosaccharides production from alkali-pretreated sugarcane bagasse using xylanases from thermoascus aurantiacus. Appl Biochem Biotech. 2010 Oct;162(4):1195-205.
31. Akpinar O, Ak O, Kavas A, Bakir U, Yilmaz L. Enzymatic production of xylooligosaccharides from cotton stalks. J Agr Food Chem. 2007 Jul 11;55(14):5544-51.
32. Teng C, Yan QJ, Jiang ZQ, Fan GS, Shi B. Production of xylooligosaccharides from the steam explosion liquor of corncobs coupled with enzymatic hydrolysis using a thermostable xylanase. Bioresource Technol. 2010 Oct;101(19):7679-82.
33. Nabarlatz D, Ebringerova A, Montane D. Autohydrolysis of agricultural by-products for the production of xylo-oligosaccharides. Carbohyd Polym. 2007 May 1;69(1):20-8.
34. Lloyd TA, Wyman CE. Combined sugar yields for dilute sulfuric acid pretreatment of corn stover followed by enzymatic hydrolysis of the remaining solids. Bioresource Technol. 2005 Dec;96(18):1967-77.
35. Jacobsen SE, Wyman CE. Xylose monomer and oligomer yields for uncatalyzed hydrolysis of sugarcane bagasse hemicellulose at varying solids concentration. Ind Eng Chem Res. 2002 Mar 20;41(6):1454-61.
36. Nabarlatz D, Farriol X, Montane D. Kinetic modeling of the autohydrolysis of lignocellulosic biomass for the production of hemicellulose-derived ligosaccharides. Ind Eng Chem Res. 2004 Jul 21;43(15):4124-31.
37. Nabarlatz D, Farriol X, Montane D. Autohydrolysis of almond shells for the production of xylo-oligosaccharides: Product characteristics and reaction kinetics. Ind Eng Chem Res. 2005 Sep 28;44(20):7746-55.

38. Sun RC, Tomkinson J, Ma PL, Liang SF. Comparative study of hemicelluloses from rice straw by alkali and hydrogen peroxide treatments. Carbohyd Polym. 2000 Jun;42(2):111-22.
39. Uffen RL. Xylan degradation: a glimpse at microbial diversity. J Ind Microbiol Biot. 1997 Jul;19(1):1-6.
40. Den Haan R, Van Zyl WH. Enhanced xylan degradation and utilisation by Pichia stipitis overproducing fungal xylanolytic enzymes. Enzyme Microb Tech. 2003 Oct 8;33(5):620-8.
41. Milagres AMF, Magalhaes PO, Ferraz A. Purification and properties of a xylanase from Ceriporiopsis subvermispora cultivated on Pinus taeda. Fems Microbiol Lett. 2005 Dec 15;253(2):267-72.
42. Sun HJ, Yoshida S, Park NH, Kusakabe I. Preparation of (1 -> 4)-beta-D-xylooligosaccharides from an acid hydrolysate of cotton-seed xylan: suitability of cotton-seed xylan as a starting material for the preparation of (1 -> 4)-beta-D-xylooligosaccharides. Carbohyd Res. 2002 Apr 2;337(7):657-61.
43. Qing Q, Wyman CE. Hydrolysis of different chain length xylooliogmers by cellulase and hemicellulase. Bioresource Technol. 2011 Jan;102(2):1359-66.
44. Vazquez MJ, Garrote G, Alonso JL, Dominguez H, Parajo JC. Refining of autohydrolysis liquors for manufacturing xylooligosaccharides: evaluation of operational strategies. Bioresource Technol. 2005 May;96(8):889-96.
45. Vegas R, Alonso JL, Dominguez H, Parajo JC. Manufacture and refining of oligosaccharides from industrial solid wastes. Ind Eng Chem Res. 2005 Feb 2;44(3):614-20.
46. Swennen K, Courtin CM, Van der Bruggen B, Vandecasteele C, Delcour JA. Ultrafiltration and ethanol precipitation for isolation of arabinoxylooligosaccharides with different structures. Carbohyd Polym. 2005 Dec 1;62(3):283-92.
47. Moure A, Gullon P, Dominguez H, Parajo JC. Advances in the manufacture, purification and applications of xylo-oligosaccharides as food additives and nutraceuticals. Process Biochem. 2006 Sep;41(9):1913-23.
48. Pellerin P, Gosselin M, Lepoutre JP, Samain E, Debeire P. Enzymatic Production of Oligosaccharides from Corncob Xylan. Enzyme Microb Tech. 1991 Aug;13(8):617-21.
49. Zhu YM, Kim TH, Lee YY, Chen RG, Elander RT. Enzymatic production of xylooligosaccharides from corn stover and corn cobs treated with aqueous ammonia. Appl Biochem Biotech. 2006 Mar;130(1-3):586-98.
50. Sluiter JB, Ruiz RO, Scarlata CJ, Sluiter AD, Templeton DW. Compositional analysis of lignocellulosic feedstocks. 1. review and description of methods. J Agr Food Chem. 2010 Aug 25;58(16):9043-53.
51. Montane D, Nabarlatz D, Martorell A, Torne-Fernandez V, Fierro V. Removal of lignin and associated impurities from xylo-oligosaccharides by activated carbon adsorption. Ind Eng Chem Res. 2006 Mar 29;45(7):2294-302.
52. Aad G, Abat E, Abdallah J, Abdelalim AA, Abdesselam A, Abdinov O, et al. The ATLAS experiment at the CERN large hadron collider. Journal of Instrumentation. 2008 Aug;3

53. Kabel MA, Carvalheiro F, Garrote G, Avgerinos E, Koukios E, Parajo JC, et al. Hydrothermally treated xylan rich by-products yield different classes of xylo-oligosaccharides. Carbohyd Polym. 2002 Oct 1;50(1):47-56.
54. Kabel MA, Kortenoeven L, Schols HA, Voragen AGJ. In vitro fermentability of differently substituted xylo-oligosaccharides. J Agr Food Chem. 2002 Oct 9;50(21):6205-10.
55. Christakopoulos P, Katapodis P, Kalogeris E, Kekos D, Macris BJ, Stamatis H, et al. Antimicrobial activity of acidic xylo-oligosaccharides produced by family 10 and 11 endoxylanases. Int J Biol Macromol. 2003 Jan 15;31(4-5):171-5.
56. Katapodis P, Vardakou M, Kalogeris E, Kekos D, Macris BJ, Christakopoulos P. Enzymic production of a feruloylated oligosaccharide with antioxidant activity from wheat flour arabinoxylan. Eur J Nutr. 2003 Jan;42(1):55-60.
57. Jacobs A, Palm M, Zacchi G, Dahlman O. Isolation and characterization of water-soluble hemicelluloses from flax shive. Carbohyd Res. 2003 Sep 1;338(18):1869-76.
58. Stewart TS, Mendersh.Pb, Ballou CE. Preparation of a mannopentaose mannohexaose and mannoheptaose from saccharomyces cerevisiae mannan. Biochemistry-Us. 1968;7(5):1843-&.
59. Pontis HG. Separation of fructosans by gel filtration. Anal Biochem. 1968;23(2):331-&.
60. Havlicek J, Samuelso.O. Chromatography of oligosaccharides from xylan by various techniques. Carbohyd Res. 1972;22(2):307-&.
61. Meyer AS, Pinelo M, Jonsson G. Membrane technology for purification of enzymatically produced oligosaccharides: Molecular and operational features affecting performance. Sep Purif Technol. 2009 Nov 19;70(1):1-11.
62. Cano A, Palet C. Xylooligosaccharide recovery from agricultural biomass waste treatment with enzymatic polymeric membranes and characterization of products with MALDI-TOF-MS. J Membrane Sci. 2007 Mar 15;291(1-2):96-105.
63. Czermak P, Ebrahimi M, Grau K, Netz S, Sawatzki G, Pfromm PH. Membrane-assisted enzymatic production of galactosyl-oligosaccharides from lactose in a continuous process. J Membrane Sci. 2004 Mar 15;232(1-2):85-91.
64. Li WY, Li JD, Chen TQ, Zhao ZP, Chen CX. Study on nanofiltration for purifying fructo-oligosaccharides II. Extended pore model. J Membrane Sci. 2005 Aug 1;258(1-2):8-15.
65. Slominska L, Grzeskowiak-Przywecka A. Study on the membrane filtration of starch hydrolysates. Desalination. 2004 Mar 10;162(1-3):255-61.
66. Kim S, Kim W, Hwang IK. Optimization of the extraction and purification of oligosaccharides from defatted soybean meal. Int J Food Sci Tech. 2003 Mar;38(3):337-42.
67. Iwasaki K, Matsubara Y. Purification of pectate oligosaccharides showing root-growth-promoting activity in lettuce using ultrafiltration and nanofiltration membranes. J Biosci Bioeng. 2000 May;89(5):495-7.
68. Jeon YJ, Kim SK. Production of chitooligosaccharides using an ultrafiltration membrane reactor and their antibacterial activity. Carbohyd Polym. 2000 Feb;41(2):133-41.

69. Vegas R, Luque S, Alvarez JR, Alonso JL, Dominguez H, Parajo JC. Membrane-assisted processing of xylooligosaccharide-containing liquors. J Agr Food Chem. 2006 Jul 26;54(15):5430-6.
70. Yuan QP, Zhang H, Qian ZM, Yang XJ. Pilot-plant production of xylo-oligosaccharides from corncob by steaming, enzymatic hydrolysis and nanofiltration. J Chem Technol Biot. 2004 Oct;79(10):1073-9.
71. Leiva MHL, Guzman M. Formation of Oligosaccharides during Enzymatic-Hydrolysis of Milk Whey Permeates. Process Biochem. 1995;30(8):757-62.
72. Marchal L, Legrand J, Foucault A. Centrifugal partition chromatography: A survey of its history, and our recent advances in the field. Chem Rec. 2003;3(3):133-43.
73. Armstrong DW. Theory and use of centrifugal partition chromatography. J Liq Chromatogr. 1988;11(12):2433-46.
74. Lau CS, Bunnell KA, Clausen EC, Thoma GJ, Lay JO, Gidden J, et al. Separation and purification of xylose oligomers using centrifugal partition chromatography. J Ind Microbiol Biot. 2011 Feb;38(2):363-70.
75. Shibusawa Y, Yanagida A, Shindo H, Ito Y. Separation of apple catechin oligomers by CCC. J Liq Chromatogr R T. 2003;26(9-10):1609-21.
76. Miller GL. Use of Dinitrosalicylic Acid Reagent for determination of reducing sugar. Anal Chem. 1959;31(3):426-8.
77. Sumner JB, Graham VA. Dinitrosalicylic acid: A reagent for the estimation of sugar in normal and diabetic urine. J Biol Chem. 1921 Jun;47(1):5-9.
78. Sumner JB, Noback CV. The estimation of sugar in diabetic urine, using dinitrosalicylic acid. J Biol Chem. 1924 Dec;62(2):287-90.
79. Bailey MJ, Biely P, Poutanen K. Interlaboratory testing of methods for assay of xylanase activity. J Biotechnol. 1992 May;23(3):257-70.
80. Jeffries TW, Yang VW, Davis MW. Comparative study of xylanase kinetics using dinitrosalicylic, arsenomolybdate, and ion chromatographic assays. Appl Biochem Biotech. 1998 Spr;70-2:257-65.
81. Rivers DB, Gracheck SJ, Woodford LC, Emert GH. Limitations of the DNS assay for reducing sugars from saccharified-lignocellulosics. Biotechnol Bioeng. 1984;26(7):800-2.
82. Somogyi M. Notes on sugar determination. J Biol Chem. 1952;195(1):19-23.
83. Lever M. New Reaction for Colorimetric Determination of Carbohydrates. Anal Biochem. 1972;47(1):273-&.
84. Lever M. Carbohydrate Determination with 4-Hydroxybenzoic acid hydrazide (Pahbah) - effect of bismuth on reaction. Anal Biochem. 1977;81(1):21-7.
85. Dubois M, Gilles K, Hamilton JK, Rebers PA, Smith F. A colorimetric method for the determination of sugars. Nature. 1951;168(4265):167-.
86. Saha SK, Brewer CF. Determination of the concentrations of oligosaccharides, complex type carbohydrates, and glycoproteins using the phenol sulfuric-acid method. Carbohyd Res. 1994 Feb 17;254:157-67.
87. Sluiter A, Hames B, Ruiz R, Scarlata C, Sluiter J, Templeton D. Determination of sugars, byproducts, and degradation products in liquid fraction process samples. Golden, CO, USA: National Renewable Energy Laboratory2006.

88. Li X, Converse AO, Wyman CE. Characterization of molecular weight distribution of oligomers from autocatalyzed batch hydrolysis of xylan. Appl Biochem Biotech. 2003 Spr;105:515-22.
89. Ohara H, Owaki M, Sonomoto K. Xylooligosaccharide fermentation with Leuconostoc lactis. J Biosci Bioeng. 2006 May;101(5):415-20.
90. Alltech. Carbohydrate Analysis-Prevail Carbohydrate ES HPLC Columns and ELSD. Brochure No 467A.
91. Yu Y, Wu HW. Characteristics and precipitation of glucose oligomers in the fresh liquid products obtained from the hydrolysis of cellulose in hot-compressed water. Ind Eng Chem Res. 2009 Dec 2;48(23):10682-90.
92. Tomkins BA, Van Berkel GJ, Emory JF, Tschaplinski TJ. Development and application of ultra-performance liquid chromatography/mass spectrometric methods for metabolite characterization and quantitation. 2010 DOE BioEnergy Science Center Annual Retreat; June 21; Asheville, NC2010.
93. Johnson DC. Carbohydrate detection gains potential. Nature. 1986 May 22;321(6068):451-2.
94. Rocklin RD, Pohl CA. Determination of carbohydrates by anion exchange chromatography with pulsed amperometric detection. J. Liqui Chromatogr. 1983;6(9):1577-90.
95. Dionex. Dionex Technical Note 20.
96. Dionex. Dionex Technical Note 21.
97. Jensen MB, Johnson DC. Fast wave forms for pulsed electrochemical detection of glucose by incorporation of reductive desorption of oxidation products. Anal Chem. 1997 May 1;69(9):1776-81.
98. Hanashiro I, Abe J, Hizukuri S. A periodic distribution of the chain length of amylopectin as revealed by high-performance anion-exchange chromatography. Carbohyd Res. 1996 Mar 22;283:151-9.
99. Koch K, Andersson R, Aman P. Quantitative analysis of amylopectin unit chains by means of high-performance anion-exchange chromatography with pulsed amperometric detection. J. Chromatogr A. 1998 Mar 27;800(2):199-206.
100. Koizumi K, Fukuda M, Hizukuri S. Estimation of the distributions of chain-length of amylopectins by high-performance liquid-chromatography with pulsed amperometric detection. J Chromatogr. 1991 Nov;585(2):233-8.
101. Koizumi K, Kubota Y, Tanimoto T, Okada Y. High performance anion exchange chromatography of homogeneous D-gluco-oligosaccharides and D-gluco-polysaccharides (polymerization degree-greater-than-or-equal-to-50) with pulsed amperometric detection. J. Chromatogr. 1989 Mar;464(2):365-73.
102. Dionex. Application Note 67.
103. Gray MC, Converse AO, Wyman CE. Solubilities of oligomer mixtures produced by the hydrolysis of xylans and corn stover in water at 180 degrees C. Ind Eng Chem Res. 2007 Apr 11;46(8):2383-91.
104. Cataldi TRI, Campa C, De Benedetto GE. Carbohydrate analysis by high-performance anion-exchange chromatography with pulsed amperometric detection: The potential is still growing. Fresen J Anal Chem. 2000 Dec;368(8):739-58.

105. Paskach TJ, Lieker HP, Reilly PJ, Thielecke K. High-performance anion-exchange chromatography of sugars and sugar alcohols on quaternary ammonium resins under alkaline conditions. Carbohyd Res. 1991 Aug 12;215(1):1-14.
106. Li H, Qing Q, Kumar R, Wyman CE. An Integrated chromatographic method for preparing and characterizing concentrations of 1, 4-β-xylooligosaccharide fractions with different chain lengths. Submitted to Biomass & Bioenergy. 2012.
107. Morales V, Sanz ML, Olano A, Corzo N. Rapid separation on activated charcoal of high oligosaccharides in honey. Chromatographia. 2006 Aug;64(3-4):233-8.
108. Gohlke M, Blanchard V. Separation of N-glycans by HPLC. Methods Mol Biol. 2008;446:239-54.
109. Khandurina J, Guttman A. High resolution capillary electrophoresis of oligosaccharide structural isomers. Chromatographia. 2005;62:S37-S41.
110. Rydlund A, Dahlman O. Oligosaccharides obtained by enzymatic hydrolysis of birch kraft pulp xylan: Analysis by capillary zone electrophoresis and mass spectrometry. Carbohyd Res. 1997 May 12;300(2):95-102.
111. Rydlund A, Dahlman O. Rapid analysis of unsaturated acidic xylooligosaccharides from kraft pulps using capillary zone electrophoresis. Hrc-J High Res Chrom. 1997 Feb;20(2):72-6.
112. Sartori J, Potthast A, Ecker A, Sixta H, Rosenau T, Kosma P. Alkaline degradation kinetics and CE-separation of cello- and xylooligomers. Part I. Carbohyd Res. 2003 May 23;338(11):1209-16.
113. Arentoft AM, Michaelsen S, Sorensen H. Determination of oligosaccharides by capillary zone electrophoresis. Journal of Chromatography A. 1993 Oct 22;652(2):517-24.
114. Zemann A, Nguyen DT, Bonn G. Fast separation of underivatized carbohydrates by coelectroosmotic capillary electrophoresis. Electrophoresis. 1997 Jun;18(7):1142-7.
115. Kabel MA, Heijnis WH, Bakx EJ, Kuijpers R, Voragen AGJ, Schols HA. Capillary electrophoresis fingerprinting, quantification and mass-identification of various 9-aminopyrene-1,4,6-trisulfonate-derivatized oligomers derived from plant polysaccharides. Journal of Chromatography A. 2006 Dec 22;1137(1):119-26.
116. Lee YH, Lin TI. Determination of carbohydrates by high-performance capillary electrophoresis with indirect absorbance detection. Journal of Chromatography B-Biomedical Applications. 1996 May 31;681(1):87-97.
117. Harvey DJ. Matrix-assisted laser desorption/ionization mass spectrometry of carbohydrates. Mass Spectrom Rev. 1999 Nov-Dec;18(6):349-450.
118. Reis A, Coimbra MA, Domingues P, Ferrer-Correia AJ, Domingues MRM. Fragmentation pattern of underivatised xylo-oligosaccharides and their alditol derivatives by electrospray tandem mass spectrometry. Carbohyd Polym. 2004 Mar 15;55(4):401-9.
119. Reis A, Pinto P, Coimbra MA, Evtuguin DV, Neto CP, Correia AJF, et al. Structural differentiation of uronosyl substitution patterns in acidic heteroxylans by electrospray tandem mass spectrometry. J Am Soc Mass Spectr. 2004 Jan;15(1):43-7.
120. Reis A, Domingues MRM, Domingues P, Ferrer-Correia AJ, Coimbra MA. Positive and negative electrospray ionisation tandem mass spectrometry as a tool for structural characterisation of acid released oligosaccharides from olive pulp glucuronoxylans. Carbohyd Res. 2003 Jul 4;338(14):1497-505.

121. Reis A, Domingues MRM, Ferrer-Correia AJ, Coimbra MA. Structural characterisation by MALDI-MS of olive xylo-oligosaccharides obtained by partial acid hydrolysis. Carbohyd Polym. 2003 Jul 1;53(1):101-7.
122. Reis A, Coimbra MA, Domingues P, Ferrer-Correia AJ, Domingues MRM. Structural characterisation of underivatised olive pulp xylo-oligosaccharides by mass spectrometry using matrix-assisted laser desorption/ionisation and electrospray ionisation. Rapid Commun Mass Sp. 2002;16(22):2124-32.
123. Kabel MA, Schols HA, Voragen AGJ. Complex xylo-oligosaccharides identified from hydrothermally treated Eucalyptus wood and brewery's spent grain. Carbohyd Polym. 2002 Nov 1;50(2):191-200.
124. Hoffmann RA, Geijtenbeek T, Kamerling JP, Vliegenthart JFG. H-1-Nmr Study of enzymatically generated wheat-endosperm arabinoxylan oligosaccharides - structures of hepta-saccharides to tetradeca-saccharides containing 2 or 3 branched xylose residues. Carbohyd Res. 1992 Jan;223:19-44.
125. Kormelink FJM, Hoffmann RA, Gruppen H, Voragen AGJ, Kamerling JP, Vliegenthart JFG. Characterization by H^1 NMR spectroscopy of oligosaccharides derived from alkali-extractable wheat-flour arabinoxylan by digestion with endo-(1-]4)-beta-D-xylanase from aspergillus-awamori. Carbohyd Res. 1993 Nov 3;249(2):369-82.
126. York WS, Vanhalbeek H, Darvill AG, Albersheim P. The Structure of Plant-Cell Walls .29. Structural analysis of xyloglucan oligosaccharides by H^1 NMR spectroscopy and fast-atom-bombardment mass-spectrometry. Carbohyd Res. 1990 Apr 25;200:9-31.
127. Hoffmann RA, Leeflang BR, de Barse MMJ, Kamerling JP, Vliegenthart JFG. Characterisation by H^1 NMR spectroscopy of oligosaccharides, derived from arabinoxylans of white endosperm of wheat, that contain the elements →4)[α-l-Araf-(1-ar3)]-β-d-Xylp-(1→ or →4)[α-l-Araf-(1→2)][α-lAraf-(1→3)]-β-d-Xylp-(1→. Carbohyd Res. 1991;221(1):63-81.

Chapter 3

Chromatographic Determination of 1,4-β-Xylooligosaccharides of Different Chain Lengths to Follow Xylan Deconstruction in Biomass Conversion*

*This whole chapter will be submitted under the following citation:
Li H, Qing Q, Kumar R, Wyman CE. "Chromatographic determination of 1, 4-β-xylooligosaccharides of different chain lengths to follow xylan deconstruction in biomass conversion"

3.1 Abstract

Xylooligosaccharides released in hydrothermal pretreatment of lignocellulosic biomass can be purified for high value products or further hydrolyzed into sugars for fermentation or chemical conversion. In addition, characterization of xylooligosaccharides is vital to understand hemicellulose structure and removal mechanisms in pretreatment of cellulosic biomass. In this study, gel permeation chromatography (GPC) was applied to fractionate xylooligosaccharides produced from birchwood xylan according to their specific degree of polymerization (DP). Then, each fraction was identified by high performance anion exchange chromatography with pulsed amperometric detection (HPAEC-PAD) and matrix-assisted laser desorption/ionization-time of flight mass spectrometry (MALDI-TOF-MS); and their concentrations were determined by a downscaled post hydrolysis method. Based on PAD responses and sugar concentrations for each fraction, a series of response factors were developed that can be used to quantify xylooligosaccharides of DP from 2 to 14 without standards. The resulting approach can profile xylooligosaccharides and help gain new insights into biomass deconstruction.

3.2 Introduction

For the majority of lignocellulosic feedstocks for production of bioethanol and other biofuels, heteroxylans are the predominant component in hemicellulose, the second most abundant polysaccharide in nature (1, 2). When heated up with water, the structure of biopolymers within plant cell walls is disturbed, and heteroxylans are depolymerized into numerous xylooligosaccharides with different chain lengths (3-5). With the growing commercial importance of hemicellulose, these soluble oligosaccharides can be either purified for high value-added products such as ingredients in functional foods, cosmetics, and pharmaceuticals due to their prebiotic activity (6) or further hydrolyzed into fermentable sugars as platform molecules for biofuels (7-9). However, the reactions of heteroxylans to soluble xylooligosaccharides and monomeric sugars also involve degradation to byproducts, which reduce sugar recovery and inhibit or prevent subsequent bioconversion processes (10, 11). Detailed study of xylooligosaccharide hydrolysis kinetics and degradation pathways is essential to understand hemicellulose decomposition mechanisms and can aid in designing low cost processes.

Unfortunately, quantification of xylooligosaccharides is very challenging, and the conventional post hydrolysis method conducted with 4wt% acid at 121^{o}C for 1 hour remains dominant for quantifying oligosaccharides in liquid hydrolyzates (12). However, this approach only determines the total equivalent monomeric xylose concentration and does not characterize the distribution of xylooligosaccharide concentrations according to chain length. It also suffers from sugar degradation during the procedure, and although

sugar recovery standards can be applied in an attempt to account for such losses, it introduces additional uncertainties into the measurement (13).

HPAEC-PAD promises to be a sensitive and selective tool for analysis of complex carbohydrates without derivatization (14-16) and has proved effective in separating xylooligosaccharides released from hydrothermal pretreatment of corn stover (5). The HPAEC-PAD takes advantage of the weakly acidic properties of carbohydrates in alkaline eluents (pH >13) to separate carbohydrates and detects the corresponding aldehyde and hydroxyl groups by electro-oxidation reactions under a multistep potential waveform (17, 18). PAD detection has been suggested to directly detect oligosaccharides at oxide-free surfaces (18) by absorbing analyte molecules on a gold electrode surface where they are anodically oxidized under a positive potential. However, previous studies have shown that the PAD response of carbohydrates is a complicated function of certain chemical and physical variables such as pK_a and structural features such as molecular dimensions and spatial structure (14, 19). For a series of oligosaccharides with a range of DPs, such factors can result in different reaction rates for electro-catalytic oxidation on the electrode surface and further impact PAD responses. Thus, corresponding sugar standards are needed to quantify oligosaccharide fractions with different DPs. Unfortunately, because xylooligosaccharide standards are only available for DPs less than 6, accurate quantification of higher DP xylooligosaccharides released by biomass pretreatment has not been possible with HPAEC-PAD.

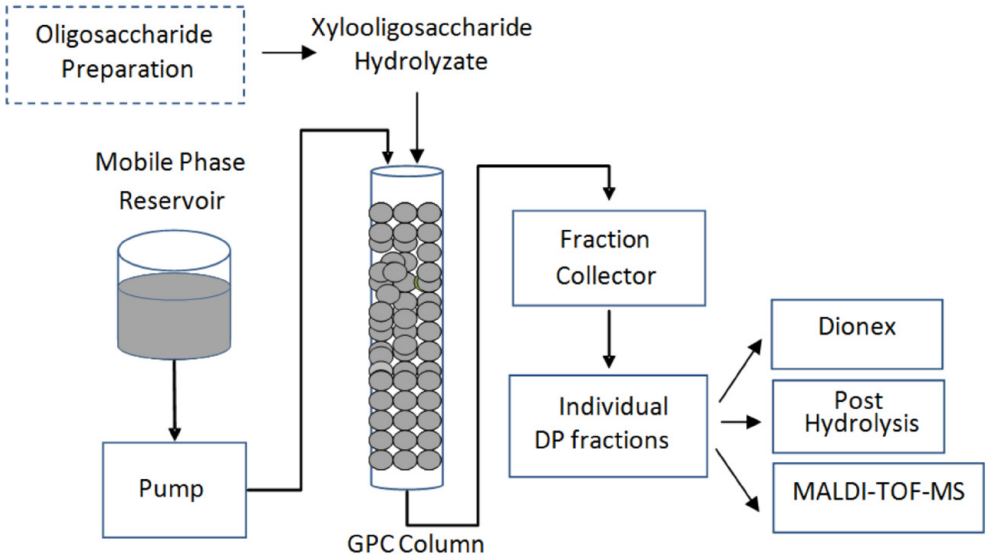

Figure 3.1. Diagram of the integrated chromatographic system used to isolate and characterize xylooligosaccharides resulting from hydrothermal pretreatment of birchwood xylan.

This study sought to calibrate the HPAEC-PAD technique by developing a series of coefficients we term response factors to more precisely characterize xylooligosaccharides according to their DP when standards are not available. First, xylooligosaccharides from hydrothermally hydrolyzed birchwood xylan were separated into individual DP fractions by size exclusion GPC, and the purity of these fractions was checked by HPAEC-PAD and MALDI-TOF-MS. A sketch of the major steps in this integrated system is shown in Figure 3.1. The PAD responses of these isolated fractions were then compared to their sugar concentrations quantified by a downscaled post hydrolysis approach, and a series of response factors were established for xylooligosaccharides with DP from 2 to 14. These response factors allow fast and more precise quantification of xylooligosaccharides produced by lignocellulosic biomass pretreatment on HPAEC-PAD without expensive, and in many cases, unavailable,

xylooligosaccharide standards. They also provide valuable new insight into the mechanism of sugar release and new opportunities to advance pretreatment and other biomass deconstruction technologies.

3.3 Materials and Methods

3.3.1 Materials

Birchwood xylan (Lot No. 038K0751) was purchased from Sigma-Aldrich (St. Louis, MO) and was measured to have a xylan content of ~85% by a two-step acid hydrolysis method (12); D-xylose with a xylose purity > 99% was also obtained from Sigma-Aldrich (Batch No. 1403673). Xylobiose, xylotriose, and xylotetraose standards (Cat No. O-XBI, O-XTR, O-XTE) of over 95% purity were purchased from Megazyme International Ireland Ltd. (Bray Business Park, Bray, Co. Wicklow, Ireland). Sodium acetate (Cat No. S7545) and 50 wt% sodium hydroxide solution (Cat No. 72064) were purchased from Sigma-Aldrich (St. Louis, MO).

3.3.2 Xylooligosaccharide production

Xylooligosaccharide hydrolyzate was produced by hydrothermal pretreatment of 15% (w/v) birchwood xylan at 200^{o}C for 15 minutes in 6 in. long cylindrical tube reactors made of Hastelloy C276 (Industrial Alloys Plus Inc., Utica, KY). This condition was previously found to maximize xylooligosaccharide concentrations and minimize degradation (20). After the fifteen minutes reaction time, the tubes were quenched quickly in room temperature water. The hydrolyzate was then filtered through a glass

fiber filter (Fisherbrand, Cat No. 09-804-110A). To avoid further degradation or precipitation of higher DP xylooligosaccharides, fresh stock was always generated just before analysis.

3.3.3 Xylooligosaccharide separation by GPC

To fractionate the xylooligosaccharide mixture into its individual components according to their DP, a 5 cm inner diameter by 1 m long low-pressure glass column with an acrylic water jacket (Cat No. XK50/100, GE Healthcare, Piscataway, NJ) was filled with ultra fine Biogel P-4 (Bio-Rad, Hercules, CA). Gel preparation was based on the instruction manual by Bio-Rad. After that, 400 mL of degassed, deionized (DI) water was slowly poured along the inner wall of the glass column to fill 20% of the column. The gel slurry was then slowly poured evenly into the column in the same way as water to avoid splashing and trapping air bubbles. After a 5 cm high bed was formed, the column outlet was opened to allow water to flow until all the gel was packed. A 7 cm I.D. adjustable length flow adapter (GE Healthcare, Piscataway, NJ) was then connected to a peristaltic pump (Masterflex, Model 7518-00). Degassed DI water was pumped through the column at a flow rate of 1.6 mL/min overnight to complete packing. A Fisher Scientific immersion circulator (Pittsburgh, PA) was used to heat water to 50°C and pump it through the 7 cm I.D. x 100 cm acrylic water jacket (GE Healthcare, Piscataway, NJ). After the column reached equilibrium at the flow rate and temperature, 10 mL of xylooligosaccharide hydrolyzate prepared as above was injected into the column. The

outflow from the column passed into a Waters Fraction Collector II (Waters Corporation, Milford, MA) to automatically collect sample fractions at 6 minutes intervals.

3.3.4 Xylooligosaccharide identification

Unfractionated xylooligosaccharide hydrolyzate and xylooligosaccharide fractions separated by the GPC system and collected by the Waters fraction collector were analyzed by the HPAEC-PAD technique on a Dionex DX-600 Ion Chromatograph system equipped with a ED50 electrochemical detector, a CarboPac PA100 (4×250mm) anion exchange column, and a guard cartridge (Dionex Corp., Sunnyvale, CA). The mobile phases were operated in the gradient mode from 50 mM to 450 mM of sodium acetate through 150 mM sodium hydroxide (Dionex Application Note 67). An example Dionex IC chromatogram of the distribution of chain lengths for unfractionated xylooligosaccharide hydrolyzate resulting from the preparation method described in Section 3.3.2 is shown in Figure 3.2. Peaks of xylose, xylobiose, xylotriose, and xylotetraose were determined by retention time of corresponding commercial sugar standards. Assignment of chromatographic peaks for xylooligosaccharides with DP > 4 was based on the generally accepted assumption that retention time of a homologous series of xylooligosaccharides increases with DP (21) and that each successive peak represents an oligosaccharide with one more xylose residue than for the previous peak. Xylooligosaccharide fractions that displayed the highest purity in the Dionex analysis were selected for each DP from 2 to 14. A Bruker Microflex LT mass spectrometer in the positive ion mode was employed to further confirm the purity of the selected

xylooligosaccharide fractions on MALDI-TOF-MS. 1µL of a mixture prepared by mixing 5µL of each sample with 5µL 10 mM NaCl was then added to 1µL DHB (dihydroxybenzoic acid matrix 10 mg/mL in 50% acetonitrile) on the stainless steel MALDI target plate and dried with warm air.

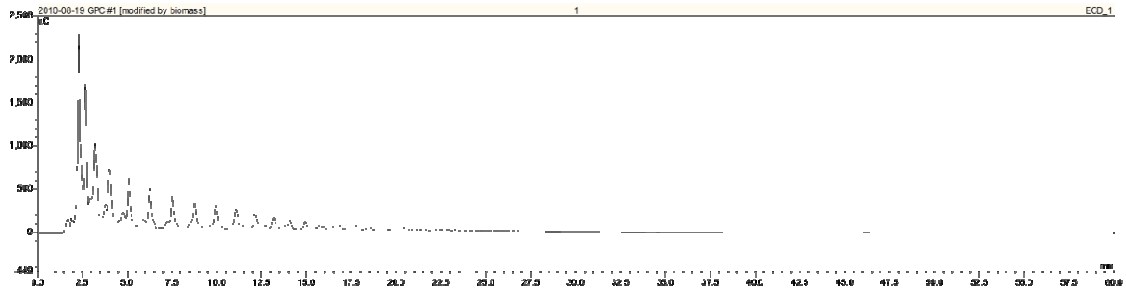

Figure 3.2. Example chromatogram from HPAEC-PAD analysis of xylooligosaccharide hydrolyzate produced by hydrothermal pretreatment of birchwood xylan as detected by the Dionex IC system coupled with a CarboPac PA-100 column.

3.3.5 Determination of isolated xylooligosaccharide concentrations

Concentrations of the individual isolated xylooligosaccharide DP fractions collected with the GPC were measured according to the NREL post hydrolysis method (12). However, due to the small volumes of each fraction that could be collected, these measurements were scaled down by a factor of 100 in our custom-made 96 well plates made of Hastelloy 276 steel (22). 400 µL of liquid sample was transferred into each vial, followed by 14 µL of 72 wt% sulfuric acid to bring the acid concentration to 4 wt%. Then, the resulting mixture was hydrolyzed at 121°C for 1 hour to breakdown the oligosaccharides to xylose (12). Sugar recovery standards containing xylose at a concentration close to that in the samples were also run in parallel to estimate sugar degradation in calculating the final xylose concentration. The validity of the downscaled

method for quantification of sugars was previously established (23). Monomeric sugars were analyzed with a Waters Alliance HPLC system (Model 2695, Waters Corporation, Milford, MA) equipped with a refractive index detector (Waters 2414). The sugars were separated on an Aminex HPX-87H column (Bio-Rad Laboratories, Hercules, CA) heated to 65°C with 0.005 M sulfuric acid as the eluent at 0.6 mL/min in an isocratic mode.

3.3.6 Definition and calculation of response factors

PAD response factor α_n to quantify higher DP xylooligosaccharides for which no standards are available was determined through calibration with existing xylose standard based on basic HPLC quantitative analysis theory:

$$\frac{H_n}{C_n} = \alpha_n \times \frac{H_1}{C_1} \qquad \text{(Equation 3.1)}$$

in which C_1 is the concentration of the xylose standard in g/L, H_1 is the corresponding xylose peak height from the HPAEC-PAD chromatogram, C_n is the concentration of the xylooligosaccharide of DP_n as measured by downscaled post hydrolysis, and H_n is the peak height measured for that xylooligosaccharide. To calculate α_n, a linear curve passing through the origin was fit to C_n vs. H_n measurements for three different injection concentrations of each xylooligosaccharide DP fraction. As shown in Equation 3.2, the slope of the resulting calibration curve, M_n, relates the concentration C_n to the PAD response H_n for each DP xylooligosaccharide.

$$C_n = M_n \times H_n \qquad \text{(Equation 3.2)}$$

If n equals 1, Equation 3.2 corresponds to a xylose calibration curve:

$$C_1 = M_1 \times H_1 \qquad \text{(Equation 3.3)}$$

By dividing Equation 3.3 by Equation 3.2, the response factor α_n defined above can be calculated as the ratio of M_1 to M_n for each DP xylooligosaccharide:

$$\frac{M_1}{M_n} = \frac{C_1}{H_1} \times \frac{H_n}{C_n} = \alpha_n \quad \text{(Equation 3.4)}$$

In this study, all sugar concentrations were measured in g/L.

3.4 Results and discussion

3.4.1 Isolation and characterization of individual DP xylooligosaccharides

After injection of the xylooligosaccharide hydrolyzate into the GPC column, the fraction collector was set to collect liquid samples in 15 mL plastic test tubes at 6 minutes intervals. The first isolated xylooligosaccharide fraction was detected at around 770 minutes and identified as DP 14 based on the retention time from the Dionex IC chromatogram of mixed DP xylooligosaccharide hydrolyzate (Figure 3.2). Injection of 10 mL of xylooligosaccharide hydrolyzate into the GPC resulted in the best separation of xylooligosaccharide fractions over a DP range from 14 to 2 during the retention period from 770 to 1560 minutes. Based on analysis of the results from the Dionex IC system, 13 individual fractions corresponding to xylooligosaccharide from DP 2 to 14 were selected for subsequent experiments. As shown in the chromatograms in Figure 3.3, these fractions were selected to maximize the proportion of the dominant DP xylooligosaccharide in each fraction. The separation purity of each DP fraction was calculated based on Equation 3.5 to gauge the separation efficacy of the GPC system:

$$\text{Separation purity} = \frac{\text{Peak area of desired DP xylooligosaccharide}}{\text{Sum of peak areas in chromatogram}} \times 100\% \quad \text{(Equation 3.5)}$$

The separation purity values calculated in this manner are shown in Figure 3.4. Although the purity for DP 14 was somewhat low at 87%, the separation purities calculated for xylooligosaccharide fractions from DP 13 to 2 were all above 90%, indicating good purity of the samples in this DP range.

Figure 3.3. Analytical HPAEC-PAD chromatograms of 13 individual DP xylooligosaccharide fractions isolated from GPC system, from right to left corresponding to (A) DP 14 to 11, (B) DP 10 to 6, and (C) DP 5 to 2.

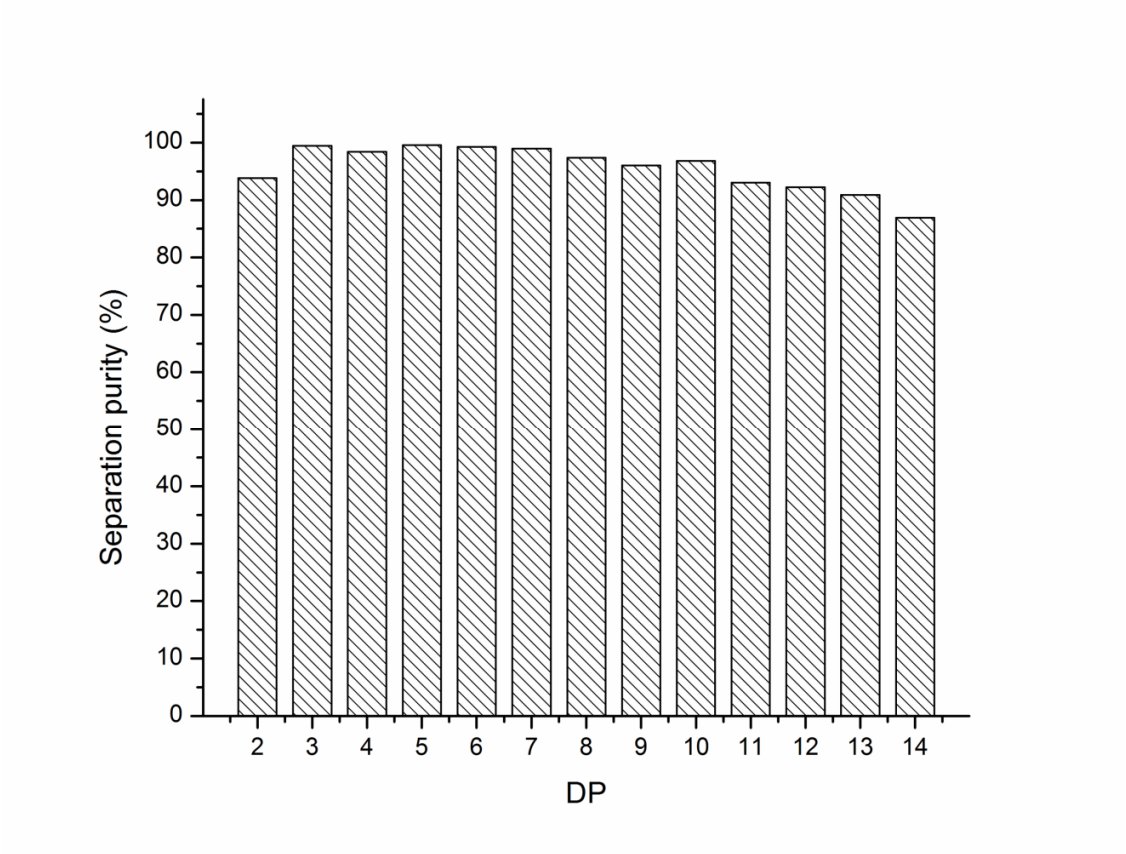

Figure 3.4. Separation purities of individual DP xylooligosaccharide fractions isolated by the GPC system.

We assumed that the xylooligosaccharides were composed of xylose as backbone (dehydrated molecular weight of 132) with few glucuronic acid residues (GlcA, dehydrated molecular weight of 176). However, to test these assumptions, we developed mass spectrograms for each fraction, as illustrated in Figure 3.5 for xylooligosaccharide fractions with DP 4, 7, 10, and 13. The neutral oligosaccharides gave pseudo-molecular ions $[M+Na]^+$ and oligosaccharides containing GlcA gave $[M+Na]^+$ and $[M+2Na]^+$ ions. Results from MALDI-TOF-MS supported the successful isolation of the selected

xylooligosaccharide fractions by GPC with reasonably high purity. Thus, they should serve as good standards to calculate response factors for xylooligosaccharides.

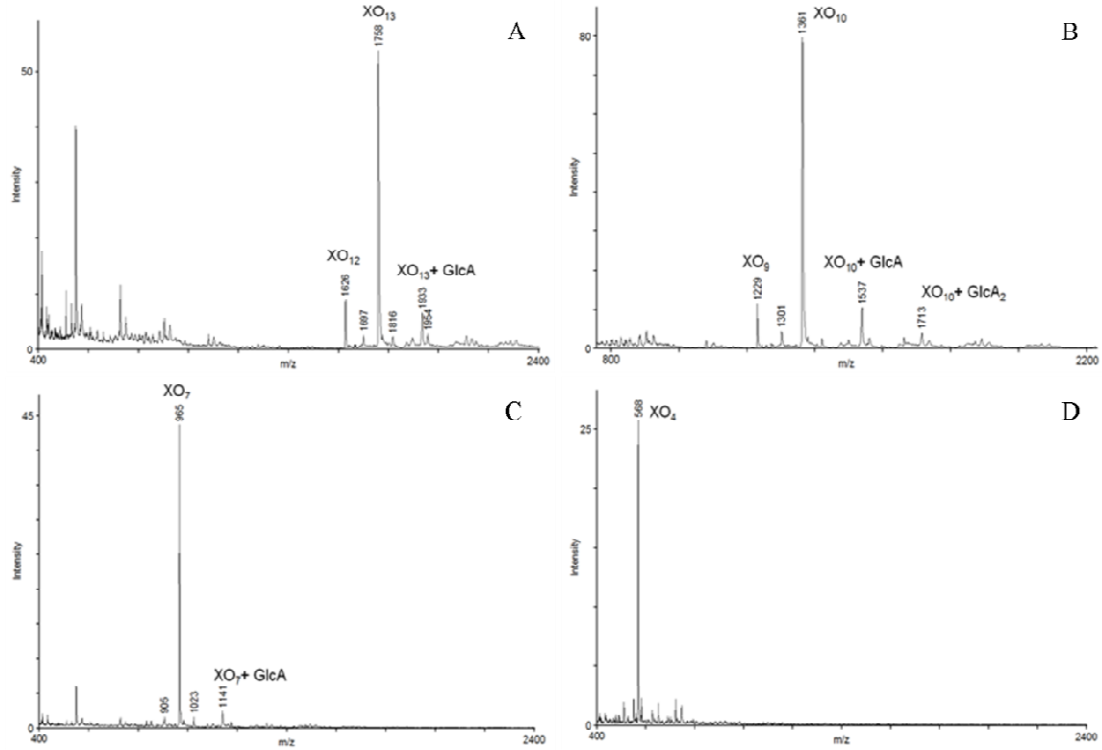

Figure 3.5. Selected MALTI-TOF-MS spectra of individual DP xylooligosaccharides isolated by the GPC system: (A) DP 13, (B) DP 10, (C) DP 7 and (D) DP 4.

3.4.2 Concentrations of isolated xylooligosaccharide fractions

As shown in Fig 3.6, the concentrations of isolated DP fractions covered a range of 0.5-1.1 g/L. Although concentrations of lower DP xylooligosaccharide fractions, such as xylobiose and xylotriose, were lower than those of higher DP fractions, these results did not represent the actual concentration distribution in mixed DP xylooligosaccharide hydrolyzate produced by hydrothermal pretreatment.

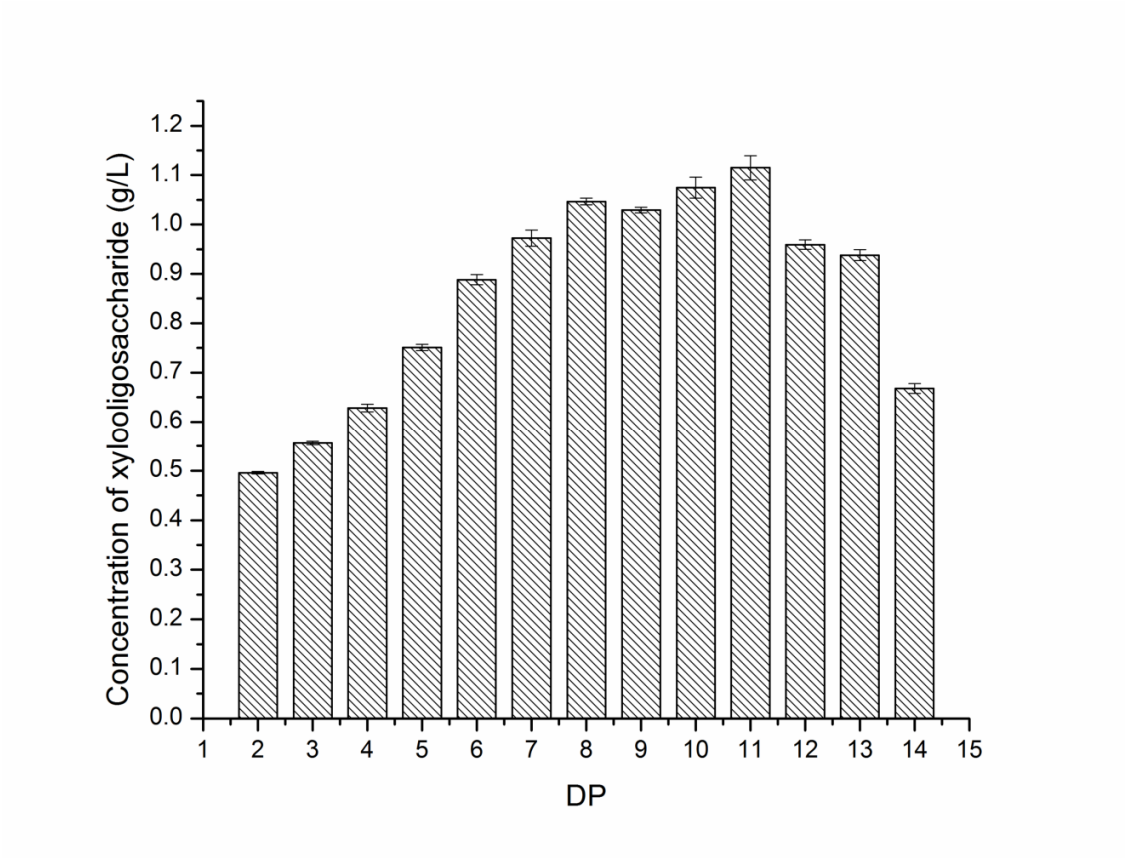

Figure 3.6. Concentration of isolated xylooligosaccharide fractions over a DP range from 2 to 14 as determined by downscaled post hydrolysis. The error bars represent the standard deviation for three replicates.

3.4.3 Xylooligosaccharide response factors

Each DP fraction was analyzed by Dionex IC for application of three different injection concentrations (including two and four fold dilution with DI water) to obtain the linear fit calibration curves described in Section 3.3.7. Table 3.1 shows the linear fit slope (M_n, according to Equation 3.2) and the squares of correlation coefficients (R^2) based on peak height and peak area. Slope values based on peak height showed a significant decreasing trend with DP; thus, the PAD response per unit concentration of

xylooligosaccharides decreased as chain length increased. The R^2 values for the slopes calculated from peak heights also showed very good linear relationships for xylose standard and xylooligosaccharides up to DP 10, demonstrating that values calculated from the response factor agreed well with experimental data. For xylooligosaccharides from DP 11 to 14, the R^2 values resulting from a linear fit of peak height were not as good as those for lower DPs but still followed a predictable trend of higher DP xylooligosaccharides having lower PAD responses.

Table 3.1 Slopes and squares of the correlation coefficients for lines drawn from the origin to each concentration and its PAD response for the range of xylooligosaccharide DPs considered. The slopes on the left are based on response values calculated according to the height of the peaks while those on the right side are calculated based on the area under the curve.

	Peak height based[a]		Peak area based[b]	
DP	Slope	R^2	Slope	R^2
1	7394.8	0.9899	1113.9	0.7816
2	5345.8	0.9755	920.7	0.7233
3	3307.5	0.9249	649.9	0.6620
4	2023.8	0.9947	562.0	0.7321
5	1441.1	0.9463	405.0	0.5616
6	919.3	0.8544	316.6	0.6854
7	804.3	0.9715	303.9	0.6846
8	629.7	0.9588	288.3	0.6986
9	601.4	0.9340	238.8	0.7146
10	513.1	0.9574	191.8	0.6667
11	401.2	0.7675	131.4	0.6329
12	448.0	0.7583	153.6	0.6138
13	373.7	0.7214	119.6	0.6039
14	309.1	0.6359	86.2	0.6023

a: linear relationship between concentration and peak height

b: linear relationship between concentration and peak area

As also shown in Table 3.1, slope values based on peak area, decreasing with DP, are consistent with results based on peak height. The corresponding results for R^2, however, indicate that the linear fit through zero was not good for the isolated xylooligosaccharide fractions. Thus, PAD response based on peak height provided a better fit for the calculation model defined in this study than those based on peak area.

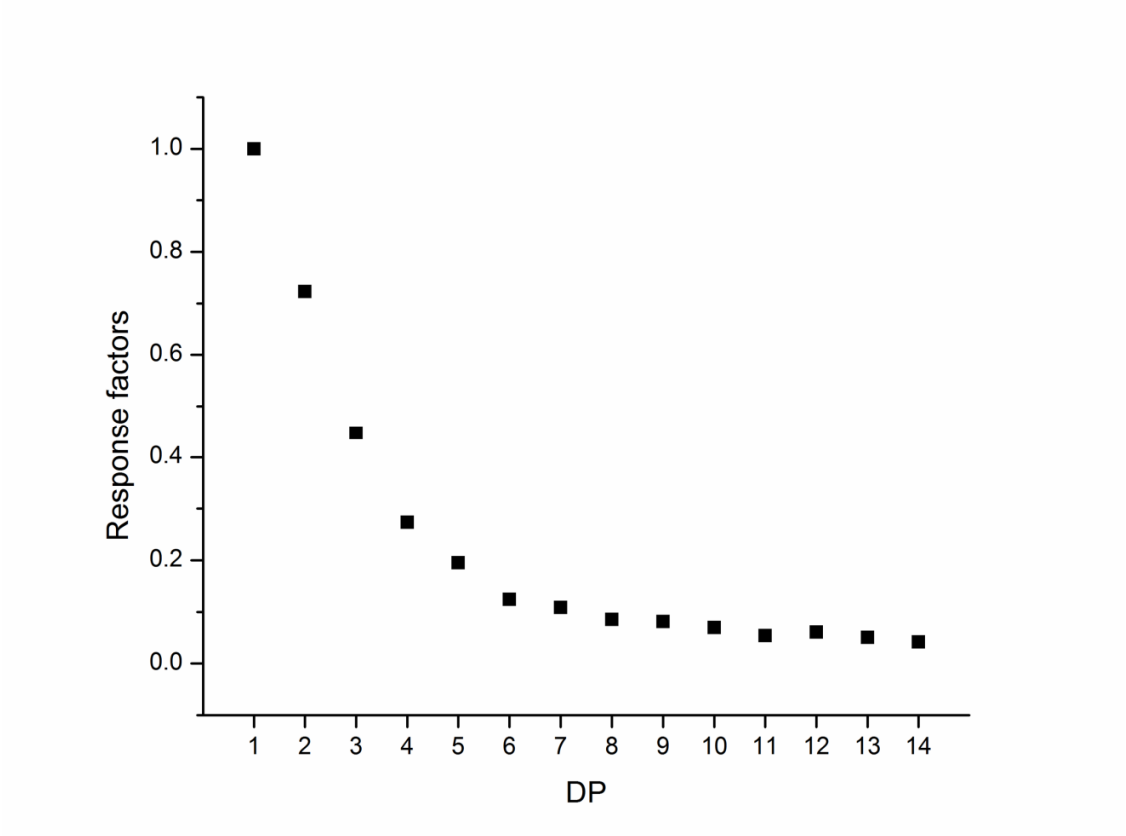

Figure 3.7. Response factors based on PAD response peak height for xylooligosaccharides from DP 2 to 14, with xylose as the sugar standard.

Response factors were quantitatively calculated from the measured slopes for each DP fraction according to Equation 3.4. As shown in Figure 3.7, response factors

based on peak height decreased according to an exponential pattern from xylose to the xylooligosaccharide with DP 14. Because xylose was selected as the calibration basis, its response factor value α_1 was set as 1. The PAD detection response of xylooligosaccharides dropped dramatically from 1 to 0.1 as the DP increased from 1 to 7. This result indicates that even if the PAD peak height of xylooligosaccharide of DP 7 was only one-tenth of that for xylose, the mass concentrations of these two samples might be similar. The decreasing trend of response factors became milder after DP of 8, dropping from α_8 of 0.085 to α_{14} of 0.042.

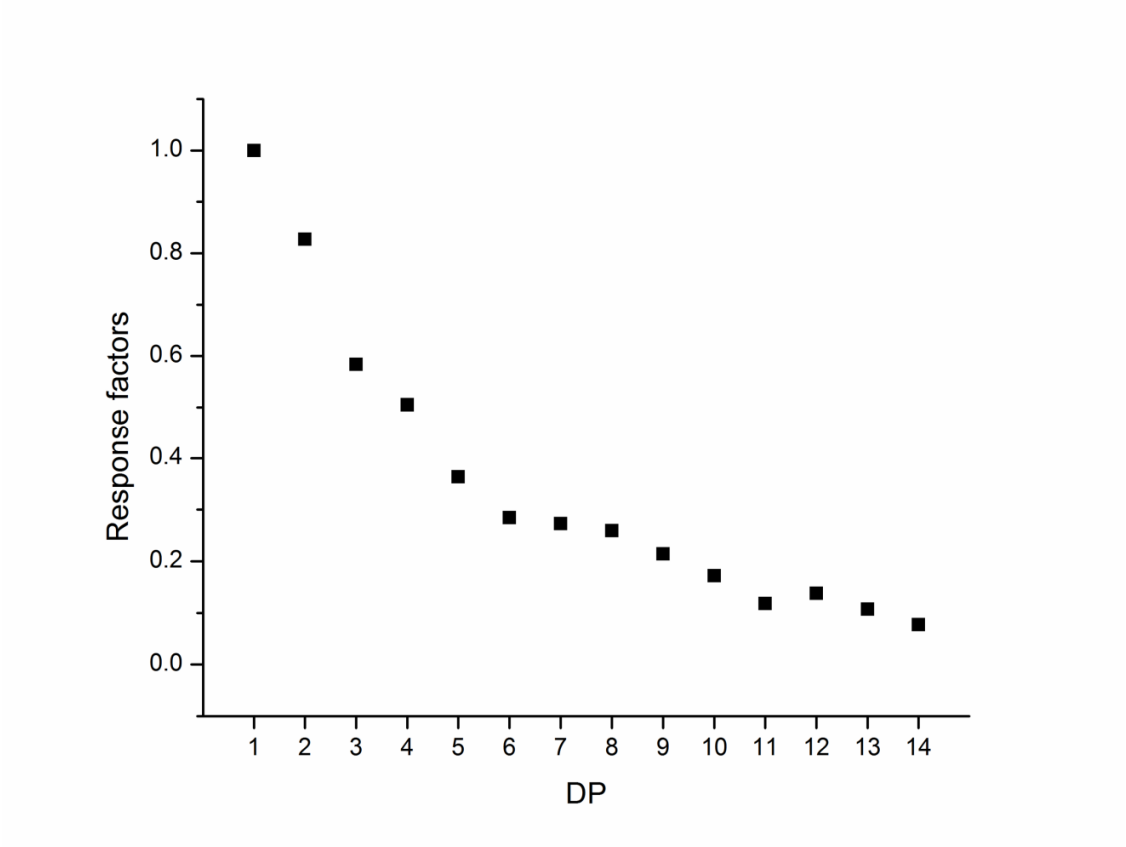

Figure 3.8. Response factors based on PAD response peak area for xylooligosaccharides from DP 2 to 14, with xylose as the sugar standard.

Response factors based on peak area were also calculated and are shown in Figure 3.8. Although both sets of α_n also dropped with increasing oligosaccharide chain length, the values did not follow a smooth trend with increasing DP in addition to not showing good linearity for the PAD response according to the definition in section 3.3.7. Thus, use of response factors based on peak area is not recommended for application of this analytical method.

The numerical value of each response factor depended on the sugar standard from which other response factors were calibrated. For example, if we chose xylobiose as the standard, Equation 3.4 would be modified to Equation 3.6 for calculation of α_n:

$$\frac{M_2}{M_n} = \frac{C_2}{H_2} \times \frac{H_n}{C_n} = \alpha_n \quad \text{(Equaiton 3.6)}$$

According to Equation 3.6, the value of α_2 would be set equal to 1, and the response factor for DP 7 would shift to 0.15 instead of the value of 0.1 calculated when xylose was used as the basis, as shown in solid triangles in Figure 3.9. Thus, the ratio between any two of response factors remained the same. This result allows flexibility in choosing a sugar standard other than xylose if interference by other compounds corrupts the xylose peak, with commercial xylooligosaccharide sugar standards currently available over a DP range from 2 to 6. However, because lower DP oligosaccharides cost less, it is generally advisable to use the lowest DP possible while still assuring good accuracy.

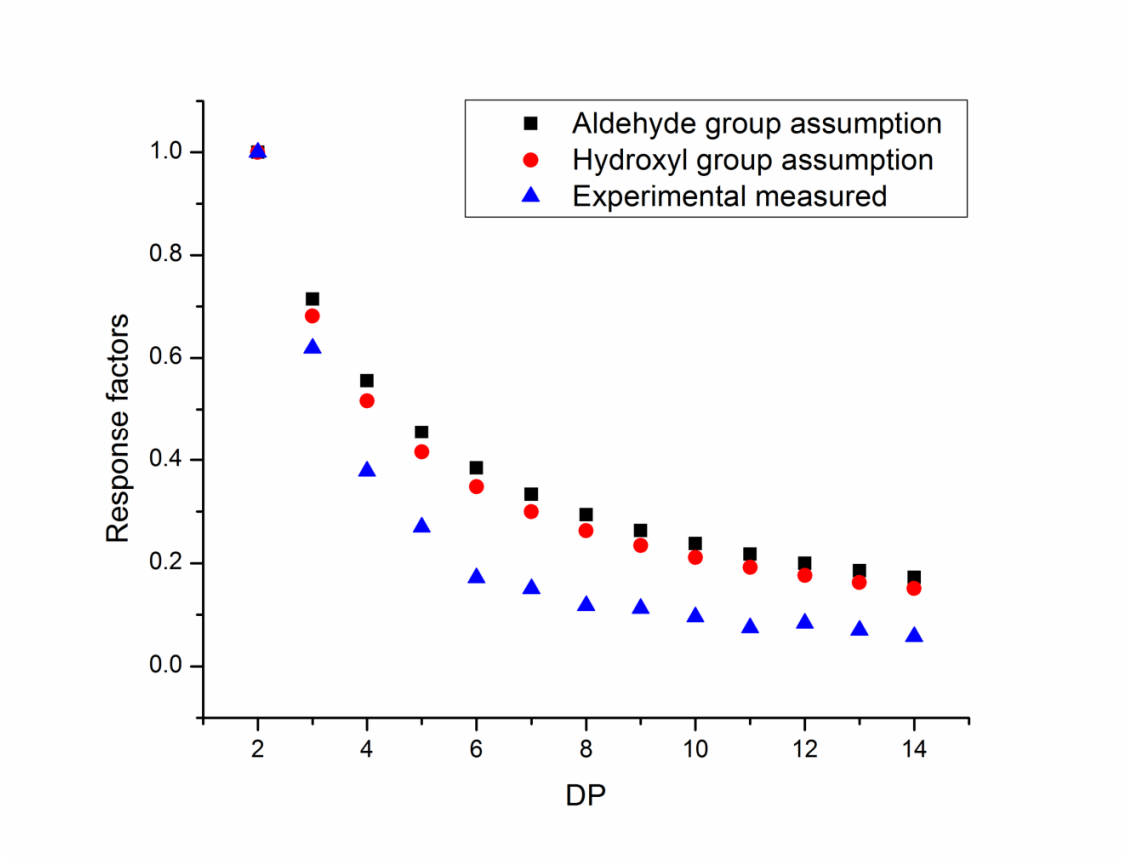

Figure 3.9. Comparison of two assumption models with the experimental measured response factors in this study based on PAD peak height for xylooligosaccharides from DP 2 to 14, with xylobiose as the sugar standard.

Consistent with our response factor results for xylooligosaccharides, Koch et al. found an exponential decline in PAD response per µg of glucan chains with increasing DP (24), and Timmermans et al. found a similar pattern for fructooligosaccharides derived from inulin (25). However, the factor responsible for such a sharp decline in PAD response has not been well defined. Johnson and LaCourse suggested aldehydes, including reducing sugars, were anodically detected by PAD during the potential region of -0.6 V to 0.2 V (18). Because there is only one reducing aldehyde group per oligosaccharide molecule, PAD responses of xylooligosaccharides could be in inversely

proportion to molecular weight and thus decline with DP. Based on this assumption, a series of response factors for xylooligosaccharides covering DP 2 to 14 were calculated and compared to our measured response factors, as shown in solid squares in Figure 3.9. Alternatively, Koch et al. proposed that the ratio of the most acidic hydroxyl group in the C_1 position on the reducing end to other hydroxyl groups in oligosaccharide molecule is larger for short chains than for long ones, resulting in more effective oxidation at the gold electrode for the former (24). Corresponding response factors calculated from this assumption are also presented in Figure 3.9 (solid cycles). Although all three response factor series follow a similar pattern, our experimentally measured response factors had a lower PAD response than predicted by either mechanism. Several explanations could be offered to account for the lower value of experimentally measured response factors compared to those calculated by either "ideal assumption." First, random coiling of xylooligosaccharides of higher DP could reduce detection of reducing aldehyde groups or hydroxyl groups, lowering the detection response. Second, the presence of methyl groups (26) and side chain substitution by GlcA could hinder interactions between xylooligosaccharide molecules and the gold PAD electrode. Diffusion of analyte molecules might also impact surface reaction on the PAD electrode (27), and diffusion coefficients measured for our selected individual DP xylooligosaccharide fractions decreased with DP (data not shown).

The response factors determined in this study can provide a relatively accurate basis for application of HPAEC-PAD technology for fast quantification of the degree of polymerization of xylooligosaccharides released from biomass pretreatment and

enzymatic hydrolysis. Although the response factors are currently limited to xylooligosaccharides with DP less than 14, further study could extend the range of accurate PAD response factors as well as improve the detection response for higher DP xylooligosaccharides.

3.5 Conclusions

High purity xylooligosaccharide fractions with DP values from 2 to 14 were chromatographically isolated from hydrothermal pretreatment hydrolyzate of birchwood xylan. PAD responses measured for each fraction dropped with increasing DP. Response factors calculated from PAD response values and corresponding xylooligosaccharide concentrations also dropped with DP. Response factors calculated from PAD peak heights followed a more consistent trend than those based on area and provided a good basis for accurately calculating xylooligosaccharide concentrations for DP values up to 14. Experimentally determined response factors followed the trend predicted from hydroxyl and aldehyde group models but were lower, particularly for higher DP.

3.6 Acknowledgements

This research was funded by the BioEnergy Science Center (BESC), a U.S. Department of Energy Bioenergy Research Center supported by the Office of Biological and Environmental Research in the DOE Office of Science. We want to also acknowledge support for some of this research by Mascoma Corporation in Lebanon, NH. The authors especially appreciate Malcolm O'Neil and Trina D. Saffold at the Complex

Carbohydrate Research Center of the University of Georgia for MALDI-TOF-MS characterization. We would also like to thank Professor Eugene A. Nothnagel in the Botany and Plant Science Department of the University of California, Riverside for valuable discussion on response factors. Gratitude is extended to the Ford Motor Company for funding the Chair in Environmental Engineering at the Center for Environmental Research and Technology of the Bourns College of Engineering at UCR that augments support for many projects such as this.

3.7 References

1. Ebringerova A, Heinze T. Xylan and xylan derivatives - biopolymers with valuable properties, 1 - Naturally occurring xylans structures, procedures and properties. Macromol Rapid Comm. 2000 Jun 20;21(9):542-56.
2. Himmel ME. Biomass recalcitrance : deconstructing the plant cell wall for bioenergy. Oxford: Blackwell Pub.; 2008.
3. Li X, Converse AO, Wyman CE. Characterization of molecular weight distribution of oligomers from autocatalyzed batch hydrolysis of xylan. Appl Biochem Biotech. 2003 Spr;105:515-22.
4. Gray MC, Converse AO, Wyman CE. Solubilities of oligomer mixtures produced by the hydrolysis of xylans and corn stover in water at 180 degrees C. Ind Eng Chem Res. 2007 Apr 11;46(8):2383-91.
5. Yang B, Wyman CE. Characterization of the degree of polymerization of xylooligomers produced by flowthrough hydrolysis of pure xylan and corn stover with water. Bioresource Technol. 2008 Sep;99(13):5756-62.
6. Vazquez MJ, Alonso JL, Dominguez H, Parajo JC. Xylooligosaccharides: manufacture and applications. Trends Food Sci Tech. 2000 Nov;11(11):387-93.
7. Wyman CE. Biomass ethanol: Technical progress, opportunities, and commercial challenges. Annu Rev Energ Env. 1999;24:189-226.
8. Wyman CE. Twenty years of trials, tribulations, and research progress in bioethanol technology - Selected key events along the way. Appl Biochem Biotech. 2001 Spr;91-3:5-21.
9. Wyman CE. What is (and is not) vital to advancing cellulosic ethanol. Trends in Biotechnology. 2007;25(4):153-7.
10. Luo C, Brink DL, Blanch HW. Identification of potential fermentation inhibitors in conversion of hybrid poplar hydrolyzate to ethanol. Biomass and Bioenergy. 2002;22(2):125-38.

11. Cantarella M, Cantarella L, Gallifuoco A, Spera A, Alfani F. Effect of inhibitors released during steam-explosion treatment of poplar wood on subsequent enzymatic hydrolysis and SSF. Biotechnol Progr. 2004 Jan-Feb;20(1):200-6.
12. Sluiter A, Hames B, Ruiz R, Scarlata C, Sluiter J, Templeton D. Determination of Sugars, Byproducts, and Degradation Products in Liquid Fraction Process Samples. Golden, CO, USA: National Renewable Energy Laboratory2006.
13. Zhang YHP, Moxley G. More accurate determination of acid-labile carbohydrates in lignocellulose by modified quantitative saccharification. Energ Fuel. 2007 Nov-Dec;21(6):3684-8.
14. Cataldi TRI, Campa C, De Benedetto GE. Carbohydrate analysis by high-performance anion-exchange chromatography with pulsed amperometric detection: The potential is still growing. Fresen J Anal Chem. 2000 Dec;368(8):739-58.
15. Rocklin RD, Pohl CA. Determination of carbohydrates by anion exchange chromatography with pulsed amperometric detection. J Liqui Chromatogr. 1983;6(9):1577 - 90.
16. Johnson DC. Carbohydrate detection gains potential. Nature. 1986 May 22;321(6068):451-2.
17. Jensen MB, Johnson DC. Fast wave forms for pulsed electrochemical detection of glucose by incorporation of reductive desorption of oxidation products. Anal Chem. 1997 May 1;69(9):1776-81.
18. Johnson DC, Lacourse WR. Liquid-chromatography with pulsed electrochemical detection at gold and platinum-electrodes. Anal Chem. 1990 May 15;62(10):A589-A97.
19. Paskach TJ, Lieker HP, Reilly PJ, Thielecke K. High-Performance Anion-Exchange Chromatography of Sugars and Sugar Alcohols on Quaternary Ammonium Resins under Alkaline Conditions. Carbohyd Res. 1991 Aug 12;215(1):1-14.
20. Gray MC. Heterogeneous dissolution fundamentals for water-only pretreatment of biomass. Hanover: Dartmouth College; 2005.
21. Corradini C, Bianchi F, Matteuzzi D, Amoretti A, Rossi M, Zanoni S. High-performance anion-exchange chromatography coupled with pulsed amperometric detection and capillary zone electrophoresis with indirect ultra violet detection as powerful tools to evaluate prebiotic properties of fructooligosaccharides and inulin. Journal of Chromatography A. 2004 Oct 29;1054(1-2):165-73.
22. Studer MH, DeMartini JD, Brethauer S, McKenzie HL, Wyman CE. Engineering of a high-throughput screening system to identify cellulosic biomass, pretreatments, and enzyme formulations that enhance sugar release. Biotechnol Bioeng. 2010 Feb 1;105(2):231-8.
23. DeMartini JD, Studer MH, Wyman CE. Small-scale and automatable high-throughput compositional analysis of biomass. Biotechnol Bioeng. 2011 Feb;108(2):306-12.
24. Koch K, Andersson R, Aman P. Quantitative analysis of amylopectin unit chains by means of high-performance anion-exchange chromatography with pulsed amperometric detection. Journal of Chromatography A. 1998 Mar 27;800(2):199-206.

25. Timmermans JW, Vanleeuwen MB, Tournois H, Dewit D, Vliegenthart JFG. Quantitative-analysis of the molecular-weight distribution of inulin by means of anion-exchange hplc with pulsed amperometric detection. J Carbohyd Chem. 1994;13(6):881-8.
26. Koizumi K, Kubota Y, Ozaki H, Shigenobu K, Fukuda M, Tanimoto T. Analyses of isomeric mono-O-methyl-D-glucoses, D-glucobioses and D-glucose monophosphates by high-performance anion-exchange chromatography with pulsed amperometric detection. J Chromatogr. 1992 Mar;595(1-2):340-5.
27. DeLisi C. The biophysics of ligand-receptor interactions. Q Rev Biophys. 1980 May;13(2):201-30.

Chapter 4

Application of High Throughput Pretreatment and Co-Hydrolysis System to Thermochemical Pretreatment, Part 2: Dilute Alkali*

*This whole chapter will be submitted under the following citation:
Li H, Gao X, DeMartini JD, Kumar R, Wyman CE. "Application of high throughput pretreatment and co-hydrolysis system to thermochemical pretreatment, Part 2: dilute alkali"

4.1 Abstract

High throughput pretreatment and enzymatic hydrolysis (HTPH) systems are now vital for screening large numbers of biomass samples to investigate biomass recalcitrance over various pretreatment and enzymatic hydrolysis conditions. Although hydrothermal pretreatment is currently being employed in most high throughput applications, thermochemical pretreatment at low and high pH conditions can offer additional insights to better understand the roles of hemicellulose and lignin, respectively, in defining biomass recalcitrance . Thus, after successfully applying the HTPH approach to dilute acid pretreatment (1), extension to dilute alkali pretreatment was also achieved using a similar single-step neutralization and buffering concept. In the latter approach, poplar and switchgrass were pretreated with 1 wt% sodium hydroxide at 120^{o}C for different reaction times. Following pretreatment, a H_2Cit^-/$HCit^{2-}$ buffer with a pH of 4.5 was used to condition the pretreatment slurry to a pH range of 4.69-4.89, followed by enzymatic hydrolysis for 72 h of the entire mixture. Sugar yields showed different trends for poplar and switchgrass with increases in pretreatment times, demonstrating the method provided a clearly discernible screening tool at alkali conditions. This method was then applied to selected *Populus tremuloides* samples to follow ring-by-ring sugar release patterns. Observed variations were compared to results from hydrothermal pretreatments, providing new insights in understanding the influence of biomass structural differences on recalcitrance.

4.2 Introduction

Biomass recalcitrance is collective resistance of plant cell wall structural polymers, including lignin, hemicellulose, and cellulose, to chemical or biological deconstruction (2, 3). Pretreatment of lignocellulosic biomass is a critical prerequisite to reduce biomass recalcitrance and achieve high enough sugar yields by enzymes and microorganisms to be economically viable (4-6). Researchers are also working to reduce biomass recalcitrance through two other major approaches: genetic modification of plant cell walls to reduce their recalcitrance and consolidating processing of enzymes and microorganisms to overcome biomass recalcitrance. To connect these three approaches, interactions and impacts among cell wall modification, pretreatment conditions, and biological deconstruction are very important to understand. However, a large number of factors must be considered in this integration: 1) numerous energy crop species and genetic modification options provide thousands of biomass samples that need to be tested; 2) various pretreatment pH, temperature, and reaction times have to be considered; and 3) numerous enzyme and/or microorganism combinations and formulations need to be evaluated. In response to this challenge, high throughput pretreatment and enzymatic hydrolysis (HTPH) systems have been developed and applied to much more efficiently evaluate the vast number of combinations of variables that can affect sugar release from biomass in a fast and automatable manner (7).

Although hydrothermal pretreatment is currently applied in most current HTPH systems, operation with chemicals at high temperature is also desirable to evaluate whether dilute alkali and/or dilute acid pretreatment alter biomass differently and expand

the range of pretreatment conditions that can be applied to large numbers of biomass materials and enzyme/organism combinations. For example, alkaline conditions are more effective in removing lignin from the cell wall polysaccharide matrix while acidic conditions usually facilitate hemicellulose removal (8-11). To date, several alkaline pretreatments have been developed including those based on sodium hydroxide, wet alkaline oxidation, aqueous ammonia, lime, and ammonia fiber expansion (AFEX) (12-17). Sodium hydroxide is perhaps the most widely used base, with Table 4.1 summarizing typical conditions that have been reported for this approach (9, 12, 18-23). Compared to hydrothermal and dilute acid pretreatments, alkaline pretreatments tend to employ lower temperatures but relatively longer reaction times.

Table 4.1. Typical conditions reported to give high sugar yields from sodium hydroxide pretreatment.

Biomass	Pretreatment conditions	Reference
Cotton	1, 2, 5, and 10 wt% NaOH; 100°C; 60 min	(Farid et al., 1983)
Cotton stalks	2 wt% NaOH, 121°C, 90 min	(Silverstein et al., 2007)
Sugarcane bagasse	10 wt% NaOH, 90°C, 90 min	(Zhao et al., 2009)
Switchgrass	1 and 5 wt% NaOH; 60 and 80°C; 24 h	(Gupta and Lee, 2010a)
Corn stover, poplar	1, 1.5, and 5 wt% NaOH; 25, 60, and 120°C; 24 h	(Gupta and Lee, 2010b)
Switchgrass	0.5, 1, and 2 wt% NaOH; 121°C; 1 h	(Xu et al., 2010)
Bermuda grass	1 wt% NaOH, 121°C, 30 min	(Wang et al., 2010)
Wheat straw	2 wt% NaOH, 121°C, 30 min	(McIntosh and Vancov, 2011)

Because most HTPH systems based on a “co-hydrolysis” approach in which the whole slurry from pretreatment is subjected to enzymatic hydrolysis without an intermediate step for liquid/solid separation, the high pH slurry (usually over 12) from

sodium hydroxide pretreatment needs to be neutralized prior to hydrolysis to maintain enzyme activity. One approach is to neutralize the slurry with acid; however, neutralization by acid titration is time and labor intensive and impractical for high throughput applications. To avoid this problem, a very low sodium hydroxide concentration (0.025 wt%) was employed (24), but the concentration was so dilute that the results did not reflect the true benefits of alkaline pretreatment. Therefore, in this study, an $H_2Cit^-/HCit^{2-}$ buffer with pH 4.5 was developed that successfully adjusted the pH value of biomass slurries from about 12 for 1 wt% sodium hydroxide pretreatment to a range appropriate for enzymatic hydrolysis. Then, this one step neutralization and buffering method was applied to whole slurries produced by sodium hydroxide pretreatment of poplar and switchgrass prior to 72 h co-hydrolysis. Relatively high sugar yields from poplar and switchgrass over a range of reaction times demonstrated that 1 wt% sodium hydroxide can be effectively used in HTPH systems, thereby offering a much less labor-intensive and timely route to evaluate the effectiveness of alkaline pretreatments for releasing sugar from biomass. Finally, the dilute alkali HPTH system was applied to selected Aspen (*Populus tremuloides*) cross-section samples to investigate ring-by-ring differences in recalcitrance, and sugar release was compared to prior results from hydrothermal and dilute acid pretreatments.

4.3 Materials and methods

4.3.1 Plant material

Poplar (*Populus trichocarpa*) was grown at Oak Ridge National Laboratory (ORNL) and provided through BioEnergy Science Center (BESC), Oak Ridge, TN. The logs were debarked, split, and chipped (Yard Machine 10HP, MTD Products Inc., Cleveland, OH) at the National Renewable Energy Laboratory (NREL) in Golden, CO. Switchgrass (*Panicum virgatum*) was grown at Pierre, South Dakota, dried, and shipped to the University of California at Riverside (UCR). Both poplar and switchgrass samples were knife milled (Model 4, Wiley Mill, Thomas Scientific, Swedesboro, NJ), and fractions between 20-mesh (<0.85 mm) and 80-mesh (>0.180 mm) (RX-29, W.S. Tyler, Mentor, OH) were collected for subsequent experiments. The moisture content of biomass samples was determined by an automatic infrared moisture analyzer (Model No. HB43-S, Mettler-Toledo, LLC, Columbus, OH). As determined according to the NREL two-step strong acid hydrolysis procedure (25), poplar was found to contain 46.5% glucan and 20.3% xylan; and switchgrass contained 32.4 % glucan and 21.2 % xylan.

Trembling Aspen (*Populus tremuloides*) samples were prepared by fractioning a 20-30 years old cross-section, which was obtained from Benchmark International in Alberta, Canada, into its individual annual rings, as discussed in detail elsewhere (26). Samples were labeled as 1 to 26 from pith to bark, according to the relative year in which that ring was formed and knife milled through a 20-mesh screen (<0.85 mm). Samples corresponding to Year 2, Year 15, Year 20, as well as bark were selected for this study.

4.3.2 Pretreatment in tube reactors

Poplar and switchgrass were first subjected to pretreatment with three sodium hydroxide concentration (1 wt%, 2 wt%, and 5 wt%) and two pretreatment temperatures (60^{o}C and 120^{o}C) to determine the pH range of the pretreated biomass slurry. Before pretreatment, 0.1 g of biomass material was soaked overnight in a 0.9 ml of sodium hydroxide solution at room temperature to allow full penetration. Then 0.1 g biomass on a dry basis was loaded into 14 mL Hastelloy tube reactors (150 mm length, 12.5 mm OD, 0.8255 mm wall thickness) with stainless steel end caps (Swaglok, San Diego, CA). The 60^{o}C pretreatment was conducted in a water bath, while the 120^{o}C pretreatment was conducted in an autoclave chamber (Model HA300MII, Hirayama Manufacturing Corporation, Japan), for a total reaction time of 24 h. After pretreatment, the reactors were quenched in cold water prior to opening. The pretreated slurry was next mixed with 9 mL of deionized (DI) water to reach a 1 wt% solids concentration, and the resulting slurry was centrifuged (Allegra X-15R, Beckman Coulter, Fullerton, CA) in a 15 mL centrifuge tube (Corning Life Science, Fisher Scientific) for 10 min at 4,200 g, and the clear hydrolyzate was then transferred into 2 ml high recovery glass vials (Agilent, Santa Clara, CA, USA) for pH measurement. The pH values were determined by a Core Module robotics platform (Freeslate, Sunnyvale, CA) using a MI-414 Micro-combination pH electrode (Microelectrodes, Bedford, NH), with details described elsewhere (1).

4.3.3 Buffer preparation and effectiveness test

1 M citrate buffer (pH 4.5) was prepared by titration of 50 wt% sodium hydroxide solution (Cat No. 72064, Sigma-Aldrich, St-Louis, MO) into sodium citrate monobasic (Cat No. 71498, Sigma-Aldrich, St-Louis, MO) water solution, while monitoring the pH (Model Seven Easy, Mettler Toledo, Columbus, OH). To test the buffering ability of this citrate buffer, slurries were produced by pretreatment of poplar and switchgrass in a 1% wt sodium hydroxide at 120^{o}C for 10 min, 70 min, 3 h, and 24 h in tube reactors that were heated in a custom-built steam chamber (27). After pretreatment, the pretreatment slurry was mixed with a 9 mL of deionized (DI) water to reach a 1 wt% solids concentration. The slurry was then centrifuged as described above. After that, 1.425 ml of clear hydrolyzate was transferred into a 2 ml high recovery glass vial, and then 75 µL of the prepared 1M citrate buffer was added to adjust the pH of the pretreatment slurry to the proper pH range while keeping the final buffer concentration at 0.05 M. The corresponding pH value was also measured with the micro pH electrode coupled to the robotic platform.

4.3.4 Sodium hydroxide pretreatment and enzymatic co-hydrolysis HTPH system

Sodium hydroxide pretreatment and enzymatic co-hydrolysis was performed in a high throughput pretreatment and enzymatic hydrolysis (HTPH) system (1, 27-29), using a customized 96-well plate reactor. 4.5 mg of dry biomass was added to each well by an automated solid and liquid dispensing robotics platform (Core Module II, Freeslate Inc., Sunnyvale, CA) followed by 40.5 µL of 1wt% sodium hydroxide solution. The well

plates were then clamped together and allowed to soak overnight at room temperature. After that, the plate reactors were placed in a custom-built steam chamber for pretreatment, as described in detail elsewhere (27), at 120 ^{o}C for different pretreatment times. Because the objective was to evaluate the effectiveness of pretreatment on sugar release from the combined operations of pretreatment and enzymatic hydrolysis, low cellulose concentrations and high enzyme loadings were employed in enzymatic hydrolysis to minimize sugar inhibition from obscuring determination of pretreatment effectiveness. Accordingly, following pretreatment, 405 μL of DI water was added to each vial to bring the solids loading for enzymatic co-hydrolysis to 1 wt%, followed by addition of 30.5 μL of prepared citrate buffer (1 mol/L, pH 4.5), sodium azide (10 g/L), and dilute enzyme mixture, resulting in final buffer and sodium azide concentrations of 0.05 mol/L and 0.2 g/L, respectively. Cellulase (Spezyme® CP, protein concentration 116 mg/ml, Lot # 3016295230) and xylanase (Multifect® xylanase, protein concentration 42 mg/ml, Lot # 4900667792) enzymes from Genencor (DuPont™ Genencor® Science, Palo Alto, CA) were added at a protein ratio of 3:1 and a high protein loading of 100 mg/g structural carbohydrates in the raw materials. The well plates were then incubated at 50^{o}C in a Multitron shaker (Multitron Infors-HT, ATR Biotech, MD) at 150 rpm for 72 h. Following 72 h of incubation, the plates were centrifuged at 2700 rpm for 30 min, and the hydrolyzate was transferred into HPLC vials for analysis. All enzymatic hydrolysis experiments were performed in quadruplicate. Sugar concentrations were determined by a Waters Alliance e2695 HPLC with a 2414 refractive index (RI) detector (Waters Corporation, Milford, MA) and a BioRad Aminex HPX-87H column (Bio-Rad Life

Science, Hercules, CA). Reported sugar yields reflect the amount of sugars released as a percent of the maximum possible sugar in raw biomass.

4.4 Results and discussion

4.4.1 pH range of sodium hydroxide pretreatment slurry

During sodium hydroxide pretreatment of lignocellulosic biomass, hydroxide groups are consumed in several types of reactions, such as C-O-C bond cleavage within lignin polymers as well as between lignin and hemicellulose, deprotonation of phenol units, and removal of acetyl groups from hemicellulose, reducing the pH of the pretreatment slurry (17). In addition, some inorganic salts in biomass can also "neutralize" hydroxide groups. Thus, the pH change at typical sodium hydroxide pretreatment conditions must be accounted for to select proper sodium hydroxide concentrations for HPTH applications. In light of this, poplar and switchgrass were first pretreated in tube reactors using 10 wt% solids loading for three sodium hydroxide concentrations (1 wt%, 2 wt%, and 5 wt%) and two temperatures (60^{o}C and 120^{o}C). The corresponding pretreatment slurries were collected, and the pH values determined, as reported in Table 4.2. Overall, the pH values of hydrolyzates from 120^{o}C pretreatment were lower than those from 60^{o}C pretreatment; suggesting pretreatment at 120^{o}C consumed more hydroxide groups. At 120^{o}C, perhaps the most widely used temperature for sodium hydroxide pretreatment, the hydrolyzate pH values following pretreatment of poplar and switchgrass for 24 h were 8.97, 11.92, 12.61 and 8.97, 11.72, 12.63, respectively, under corresponding tested sodium hydroxide concentrations of 1 wt%, 2

wt%, and 5wt%. Considering that the low total citric ion concentration in the citrate buffer of 0.05 mol/L appropriate for enzymatic hydrolysis limits the buffering ability, pretreatment hydrolyzate with relatively low pH is more promising to achieve simple one step neutralization and buffering by the prepared citrate buffer. In addition, because co-hydrolysis is performed in the HPTH system, conditions with high sodium hydroxide concentration should be avoided to minimize enzyme inhibition. Thus, pretreatment with1 wt% sodium hydroxide at 120°C was selected for subsequent experiments.

Table 4.2. pH values of hydrolyzates produced by sodium hydroxide pretreatment of switchgrass and poplar following dilution to prepare for enzymatic co-hydrolysis.

NaOH concentration	Poplar		Switchgrass	
	60°C	120°C	60°C	120°C
1 wt%	11.66	8.97	10.63	8.97
2 wt%	12.28	11.92	12.09	11.72
5 wt%	12.76	12.61	12.70	12.63

24 h pretreatment with 10 wt% solid loading.
Prior to pH measurement, hydrolyzate was diluted with DI water to 1 wt% solid loading.

4.4.2 Preparation and verification of the new citrate buffer

For hydrothermal pretreatment with the HTPH system, sodium citrate buffer with pH of 4.8 was used to control the pH of hydrolyzate for enzymatic hydrolysis (7, 27, 28, 30). However, its buffering capacity is insufficient to neutralize the extra hydroxide groups in the hydrolyzate following sodium hydroxide pretreatment and maintain a pH appropriate to maximize enzyme activity. For a citrate buffer with a pH around 4.5-5, H_2Cit^-/$HCit^{2-}$ are the major conjugate acid base pairs with a pKa of 4.77. Approximate pH calculations based on buffering chemistry (data not shown) indicated that a slight

reduction in the pH of the citrate buffer could provide greater buffering capacity for high pH pretreatment hydrolyzates. Thus, an alternative citrate buffer (1 mol/L) was prepared by quantitative titration of aqueous sodium hydroxide into sodium citrate monobasic solution to obtain a pH of 4.5. To verify its buffering ability, a 10% solids loading of both poplar and switchgrass was pretreated with 1.0 wt% sodium hydroxide in tube reactors at 120°C. The pH values measured before and after adding this new pH 4.5 buffer to hydrolyzates from 10 min, 70 min, 3 h, and 24 h pretreatments are shown in Table 4.3. The hydrolyzate pH dropped continually with pretreatment time, with the result that pH following the 24 h pretreatment was significantly lower than that from the 10 min pretreatment, suggesting that hydroxide groups were continuously consumed over the pretreatment time.

Table 4.3. pH of hydrolyzates produced by sodium hydroxide pretreatment of switchgrass and poplar following dilution to prepare for enzymatic co-hydrolysis before and after addition of new citrate buffer.

Pretreatment time	Poplar		Switchgrass	
	Before	After	Before	After
10 min	11.09	4.87	11.16	4.89
70 min	10.64	4.82	10.73	4.83
3 h	9.92	4.77	10.10	4.76
24 h	8.97	4.69	8.97	4.72

1 wt% sodium hydroxide concentration and 10 wt% solid loading for pretreatment at 120°C. Prior to pH measurement and buffer addition, hydrolyzate was diluted with DI water to 1 wt% solid loading.

After adding citrate buffer, the hydrolyzate pH values were in the range of 4.69-4.87 and 4.72-4.89 for poplar and switchgrass, respectively. These results demonstrated that the prepared citrate buffer with a pH of 4.5 had sufficient buffering capacity to be

effective for pretreatment with 1 wt% sodium hydroxide over a wide range of pretreatment times. In this way, neutralization of the slurry from high pH alkaline pretreatment and buffering of the hydrolyzate for enzymatic hydrolysis were accomplished simultaneously for application to the HPTH system.

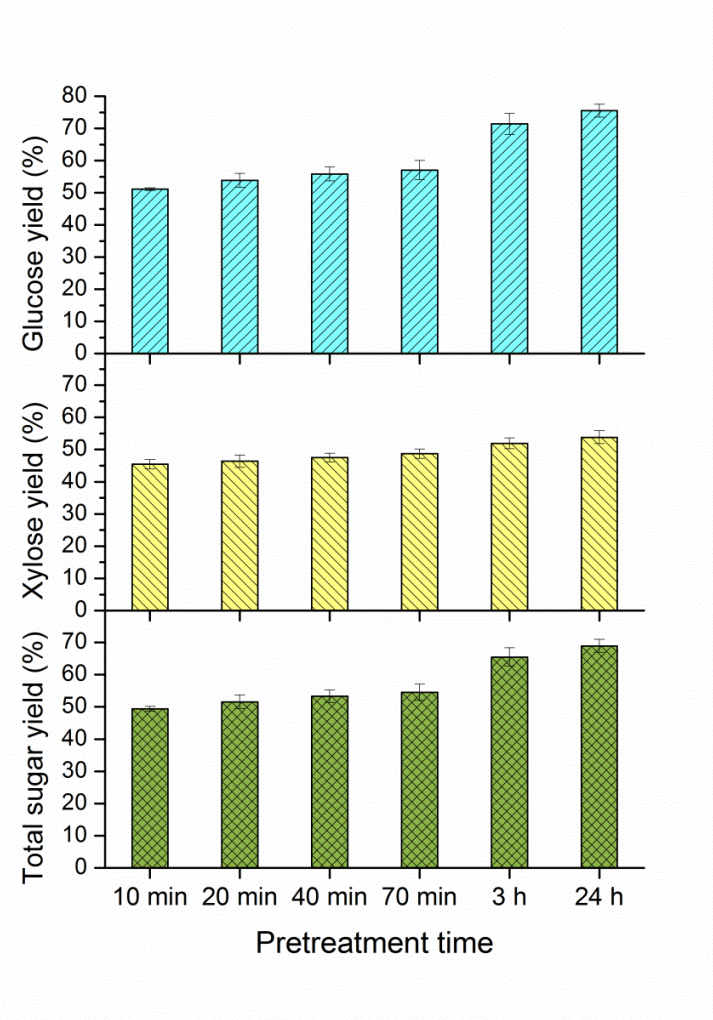

Figure 4.1. Glucose, xylose, and total sugar (glucose+xylose) yields from sodium hydroxide pretreatment and co-hydrolysis of poplar. Pretreatment was performed at 120℃ at a 1 wt% sodium hydroxide concentration, followed by enzymatic hydrolysis of the entire pretreated slurry at 50°C for 72 h using 75 mg cellulase +25 mg xylanase /g glucan+xylan in the unpretreated raw material. The error bars represent the standard deviation of four replicates.

4.4.3 Application of HTPH to sodium hydroxide pretreatment

After demonstrating that the pH 4.5 citrate buffer effectively adjusted and controlled the pH of hydrolyzates resulting from 1% sodium hydroxide pretreatment in tube reactors for 10 min to 24 h, 1 wt% sodium hydroxide was applied to the HTPH system at similar 10 wt% solids loading. In this case, both poplar and switchgrass were pretreated in the 96 well plate HTPH system at 120℃ for 10 min, 20 min, 40 min, 70 min, 3 h, and 24 h. After pretreatment, a mixture of DI water, pH 4.5 citrate buffer, sodium azide, and enzymes were added to each well, as described previously. 72 h co-hydrolysis was then performed at an enzyme loading of 75 mg cellulase +25 mg xylanase/g structural carbohydrates in the original untreated biomass. Figure 4.1 shows the glucose, xylose, and total sugar (glucose + xylose) yields from combined pretreatment and co-hydrolysis of poplar. Overall, sugar yields increased slightly with pretreatment time. In contrast to results from hydrothermal HTPH (27-29) and dilute acid HTPH (1), which were conducted at 180℃ and 160℃, respectively, sugar yields from 120℃ sodium hydroxide pretreatment changed more slowly with pretreatment time. Glucose and xylose yields for high pH pretreatment of poplar ranged between 51.1-75.5% and 45.4-53.8%, respectively, corresponding to a range of glucose plus xylose yields of 49.4 to 68.8%. Results for switchgrass, however, showed a different trend than for poplar, as shown in Figure 4.2. The maximum glucose yield of 85.1% appeared following pretreatment for 3 h, while the highest xylose yield of 71.1%was observed for pretreatment for 70 min. However, sugar yield results did drop significantly at 24 h, indicating degradation reactions at longer pretreatment times.

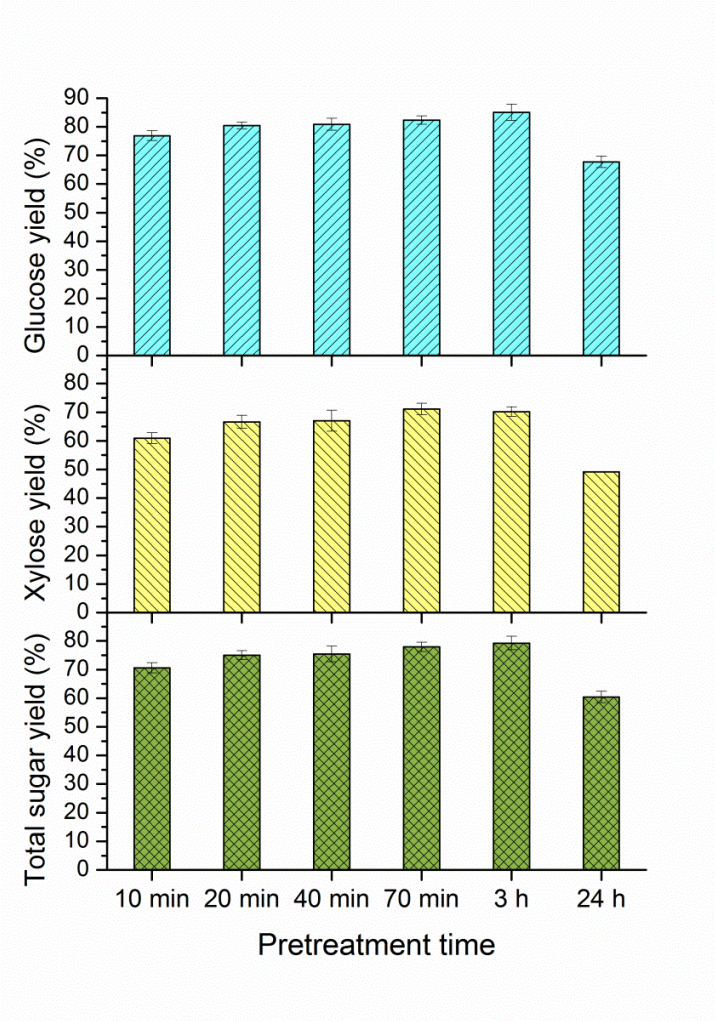

Figure 4.2. Glucose, xylose, and total sugar (glucose+xylose) yields from sodium hydroxide pretreatment and co-hydrolysis of switchgrass. Pretreatment was performed at 120℃ with a 1 wt% sodium hydroxide concentration, followed by enzymatic hydrolysis of the entire pretreated slurry at 50°C for 72 h using 75 mg cellulase +25 mg xylanase /g glucan+xylan in the unpretreated raw material. The error bars represent the standard deviation of four replicates.

To confirm the effects of sodium hydroxide on sugar release from the HTPH system, pretreatment without sodium hydroxide were also conducted for pretreatment times of 10 min, 20 min, 40 min, and 70 min at 120^{o}C, followed by enzymatic co-hydrolysis. As shown in Figure 4.3, glucose and xylose yields were very low without

addition of sodium hydroxide, demonstrating the effectiveness of the sodium hydroxide pretreatment conditions applied to obtain the high sugar yields in Figures 4.1 and 4.2 in the HTPH co-hydrolysis system. In addition, the different trends in sugar yields from poplar and switchgrass also showed that the HTPH system can effectively screen for dilute alkali pretreatment conditions that realize high sugar yields from different biomass types.

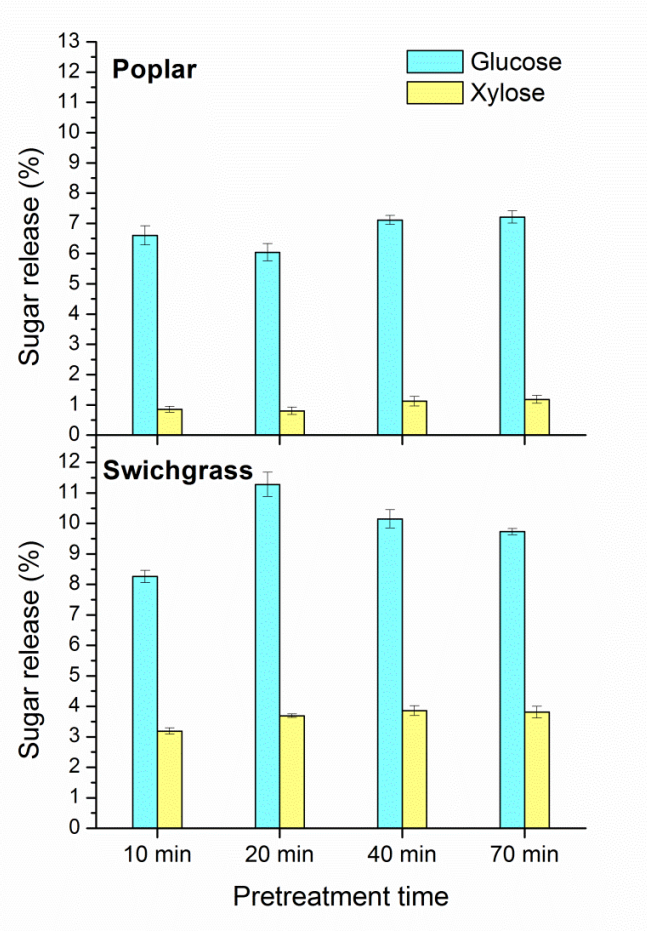

Figure 4.3. Glucose and xylose yields from hydrothermal (water only) pretreatment and co-hydrolysis of poplar (upper) and switchgrass (bottom). Pretreatment was performed at 120℃, followed by enzymatic hydrolysis at 50°C for 72 h using 75 mg cellulase +25 mg xylanase /g glucan+xylan in the unpretreated raw material. The error bars represent the standard deviation of four replicates.

4.4.4 Application of dilute alkali HTPH to Aspen wood rings

An important application of the HTPH system is to screen large number of biomass samples to identify differences in recalcitrance as measured by sugar yields following application of different biomass-pretreatment-enzyme combinations. Thus, four Aspen samples that were fractionated from different annual rings (26) were selected to investigate their sugar release performance for the sodium hydroxide HTPH system, with their compositions summarized in Table 4.4. In this case, a short pretreatment time of 10 min was applied to look for biomass that could release sugars at milder conditions where degradation would be less and containment costs lower. Also, shorter pretreatment time reduces release of degradation products and inhibitors in pretreatment that interfere with co-hydrolysis.

Table 4.4. Chemical compositions of selected rings of Aspen wood (wt %)

	Glucan	Xylan	Lignin
Bark	16.4	8.8	36.7
Year 2	33.9	16.1	33.3
Year 15	48.2	17.7	22.4
Year 20	42.5	18.5	22.5

Full dataset reported elsewhere (DeMartini and Wyman, 2011).

Figure 4.4 shows how 72 h glucose, xylose, and total sugar yields varied for pretreatment with 1% sodium hydroxide followed by co-hydrolysis of different Aspen samples. Sugar yields from hydrothermal HTPH experiments (26), which used the same protein loading for co-hydrolysis, are also shown for comparison. These results clearly show that sodium hydroxide gave different sugar yields than hydrothermal pretreatment

from Aspen wood rings. For example, although hydrothermal pretreatment resulted in sample 2 (juvenile wood), which had high lignin content, releasing less glucose than samples 15 and 20, sodium hydroxide pretreatment gave the opposite results. Xylose yields from application of the HTPH system at hydrothermal conditions to samples 2, 15, and 20 were quite high at 97.2%, 91.8%, and 95.4%, respectively, but the sodium hydroxide HTPH system resulted in the xylose yield from sample 2 being about 15% higher than that from samples 15 and 20. These differences indicate that sodium hydroxide is more effective in achieving higher sugar yields for biomass with high lignin content, consistent with expectations (17).

Application of the HTPH system to the bark sample provided some additional interesting observations. Because the bark contained higher lignin but significantly less carbohydrates than the woody samples, we might expect higher yields with base than from hydrothermal pretreatment based on the trends above. However, although hydrothermal HTPH achieved reasonable glucose (63.0%) and xylose (77.6%) yields from bark, glucose and xylose yields were only 47.2% and 13.8%, respectively, from sodium hydroxide HTPH. These results support other observations that lignin content alone does not control recalcitrance, but that other differences in cell wall structure are also important (31).

Overall, sugar yields from the four Aspen samples demonstrated that sodium hydroxide HTPH was capable of discerning differences in recalcitrance among samples. In addition, the different sugar release performance between hydrothermal HTPH and

sodium hydroxide HTPH reveal that application of dilute alkali HTPH system can offer new insights in screening biomass recalcitrance.

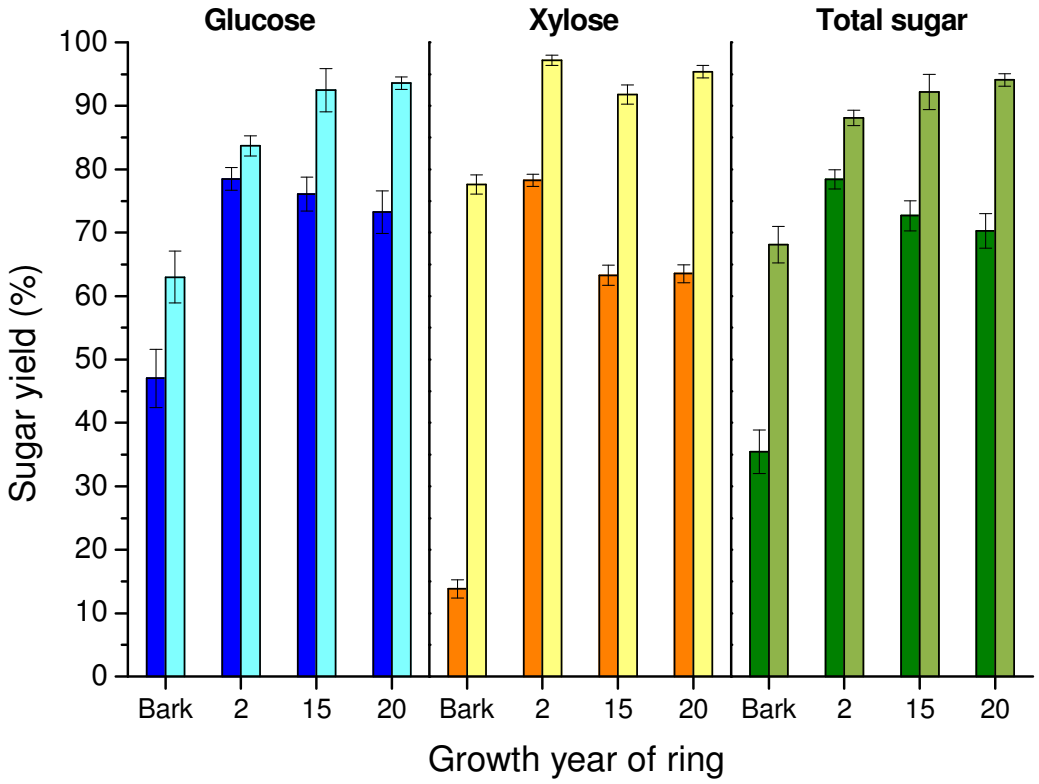

Figure 4.4. Glucose, xylose, and total sugar (glucose+xylose) yields from pretreatment of aspen wood samples 2, 15, and 20 and bark with 1% wt NaOH at 120℃ for 10 min (darker bars on the left of each pair) and hydrothermal pretreatment with just water at 160℃ for 70 min (right lighter colored bar of each pair). The co-hydrolysis enzyme loading for both was 75 mg+25 mg of cellulase+xylanase/g glucan+xylan in the unpretreated raw material. The error bars represent the standard deviation of three replicates for the experiments in the well-plate. Data for hydrothermal pretreatment are from DeMartini and Wyman, 2011.

4.5 Conclusions

Pretreatment with 1 wt% sodium hydroxide at 120℃ of 10 wt% solids loadings of poplar and switchgrass was successfully combined with enzymatic co-hydrolysis in the HTPH system. The one step buffering and neutralizing method developed with a pH 4.5 citrate buffer for a dilute acid HTPH system (1) effectively neutralized and adjusted the pH of sodium hydroxide pretreatment slurries to a range of 4.69-4.89 prior to whole slurry enzymatic co-hydrolysis. Sugar yields showed different trends for poplar and switchgrass with increasing pretreatment times, demonstrating the method was capable of clearly discerning differences in the susceptibility of different feedstocks to alkali pretreatment. The variations observed in sugar yields from Aspen wood ring and bark samples for hydrothermal and sodium hydroxide pretreatments show that HTPH pretreatment at alkali conditions can effectively screen for materials that deserve more detailed study to gain better insights into understanding the influence of biomass structural differences on recalcitrance.

4.6 Acknowledgements

This research was funded by the BioEnergy Science Center (BESC), a U.S. Department of Energy Bioenergy Research Center supported by the Office of Biological and Environmental Research in the DOE Office of Science. Gratitude is also extended to the Ford Motor Company for funding the Chair in Environmental Engineering at the Center for Environmental Research and Technology of the Bourns College of Engineering at UCR that augments support for many projects such as this.

4.7 References

1. Gao X, Kumar R, DeMartini JD, Li H, Wyman CE. Application of high throughput pretreatment and co-hydrolysis system to thermochemical pretreatment. Part1: Dilute acid. Biotechnol Bioeng. 2012:n/a-n/a.
2. Lynd LR, Wyman CE, Gerngross TU. Biocommodity Engineering. Biotechnol Prog. 1999 Oct 1;15(5):777-93.
3. Himmel ME. Biomass recalcitrance : deconstructing the plant cell wall for bioenergy. Oxford: Blackwell Pub.; 2008.
4. Lynd LR, Cushman JH, Nichols RJ, Wyman CE. Fuel Ethanol from Cellulosic Biomass. Science. 1991 Mar 15;251(4999):1318-23.
5. Wyman CE. Ethanol from Lignocellulosic Biomass - Technology, Economics, and Opportunities. Bioresource Technol. 1994;50(1):3-16.
6. Wyman CE. What is (and is not) vital to advancing cellulosic ethanol. Trends in Biotechnology. 2007 Apr;25(4):153-7.
7. DeMartini JD, Wyman CE. High Throughput Pretreatment and Hydrolysis Systems for Screening. In: Wyman CE, editor. Aqueous Pretreament of Plant Biomass for Biological and Chemical Conversion to Fuels and Chemicals. Oxford, UK: Wiley Blackwell; 2012.
8. Kumar R, Mago G, Balan V, Wyman CE. Physical and chemical characterizations of corn stover and poplar solids resulting from leading pretreatment technologies. Bioresource Technol. 2009 Sep;100(17):3948-62.
9. Gupta R, Lee YY. Pretreatment of corn stover and hybrid poplar by sodium hydroxide and hydrogen peroxide. Biotechnol Prog. 2010 Jul-Aug;26(4):1180-6.
10. Ragauskas AJ, Williams CK, Davison BH, Britovsek G, Cairney J, Eckert CA, et al. The path forward for biofuels and biomaterials. Science. 2006 Jan 27;311(5760):484-9.
11. Mosier N, Wyman C, Dale B, Elander R, Lee YY, Holtzapple M, et al. Features of promising technologies for pretreatment of lignocellulosic biomass. Bioresource Technol. 2005 Apr;96(6):673-86.
12. Xu JL, Cheng JJ, Sharma-Shivappa RR, Burns JC. Sodium Hydroxide Pretreatment of Switchgrass for Ethanol Production. Energ Fuel. 2010 Mar;24:2113-9.
13. Kim TH, Kim JS, Sunwoo C, Lee YY. Pretreatment of corn stover by aqueous ammonia. Bioresource Technol. 2003 Oct;90(1):39-47.
14. Kaar WE, Holtzapple MT. Using lime pretreatment to facilitate the enzymic hydrolysis of corn stover. Biomass Bioenerg. 2000;18(3):189-99.
15. Holtzapple MT, Jun JH, Ashok G, Patibandla SL, Dale BE. The ammonia freeze explosion (AFEX) process - a practical lignocellulose pretreatment. Appl Biochem Biotech. 1991 Spr;28-9:59-74.
16. Alizadeh H, Teymouri F, Gilbert TI, Dale BE. Pretreatment of switchgrass by ammonia fiber explosion (AFEX). Appl Biochem Biotech. 2005 Spr;121:1133-41.
17. Sierra R, Holtzapple M, Piamonte N. Fundamentals of biomass pretreatment at high pH. In: Wyman CE, editor. Aqueous Pretreament of Plant Biomass for Biological and Chemical Conversion to Fuels and Chemicals. Oxford, UK: Wiley Blackwell; 2012.
18. Gupta R, Lee YY. Investigation of biomass degradation mechanism in pretreatment of switchgrass by aqueous ammonia and sodium hydroxide. Bioresource Technol. 2010 Nov;101(21):8185-91.
19. Wang Z, Keshwani DR, Redding AP, Cheng JJ. Sodium hydroxide pretreatment and enzymatic hydrolysis of coastal Bermuda grass. Bioresour Technol. 2010 May;101(10):3583-5.

20. Farid MA, Shaker HM, Eldiwany AI. Effect of peracetic-acid, sodium-hydroxide and phosphoric-acid on cellulosic materials as a pretreatment for enzymatic-hydrolysis. Enzyme Microb Tech. 1983;5(6):421-4.
21. McIntosh S, Vancov T. Enhanced enzyme saccharification of sorghum bicolor straw using dilute alkali pretreatment. Bioresource Technol. 2010 Sep;101(17):6718-27.
22. Silverstein RA, Chen Y, Sharma-Shivappa RR, Boyette MD, Osborne J. A comparison of chemical pretreatment methods for improving saccharification of cotton stalks. Bioresource Technol. 2007 Nov;98(16):3000-11.
23. Zhao XB, Peng F, Cheng K, Liu DH. Enhancement of the enzymatic digestibility of sugarcane bagasse by alkali-peracetic acid pretreatment. Enzyme Microb Tech. 2009 Jan 6;44(1):17-23.
24. Santoro N, Cantu SL, Tornqvist CE, Falbel TG, Bolivar JL, Patterson SE, et al. A high-throughput platform for screening milligram quantities of plant biomass for lignocellulose digestibility. Bioenergy Research. 2010;3(1):93-102.
25. Sluiter A, Hames B, Ruiz R, Scarlata C, Sluiter.J., Templeton D, et al. Determination of structural carbohydrates and lignin in biomass. NREL Laboratory Analytical Procedure. 2008;NREL/TP-510-42618.
26. DeMartini JD, Wyman CE. Changes in composition and sugar release across the annual rings of Populus wood and implications on recalcitrance. Bioresource Technol. 2011 Jan;102(2):1352-8.
27. Studer MH, DeMartini JD, Brethauer S, McKenzie HL, Wyman CE. Engineering of a high-throughput screening system to identify cellulosic biomass, pretreatments, and enzyme formulations that enhance sugar release. Biotechnol Bioeng. 2010 Feb 1;105(2):231-8.
28. Studer MH, Brethauer S, Demartini JD, McKenzie HL, Wyman CE. Co-hydrolysis of hydrothermal and dilute acid pretreated populus slurries to support development of a high-throughput pretreatment system. Biotechnol Biofuels. 2011;4(1):19.
29. DeMartini JD, Wyman CE. Composition and hydrothermal pretreatment and enzymatic saccharification performance of grasses and legumes from a mixed-species prairie. Biotechnol Biofuels. 2011 Nov 15;4.
30. Selig M, Weiss N, Ji Y. Enzymatic Saccharification of Lignocellulosic Biomass. NREL Laboratory Analytical Procedure. 2008;NREL/TP-510-42629.
31. Chundawat SPS, Donohoe BS, Sousa LD, Elder T, Agarwal UP, Lu FC, et al. Multi-scale visualization and characterization of lignocellulosic plant cell wall deconstruction during thermochemical pretreatment. Energy & Environmental Science. 2011 Mar;4(3):973-84.

Chapter 5

Investigation of Lignin Deposition on Cellulose during Hydrothermal Pretreatment, its Effect on Cellulose Hydrolysis, and Underlying Mechanisms*

*This whole chapter will be submitted under the following citation:
Li H, Pu Y, Kumar R, Ragauskas AJ, Wyman CE. "Investigation of lignin deposition on cellulose during hydrothermal pretreatment, its effect on cellulose hydrolysis, and underlying mechanisms"

5.1 Abstract

In dilute acid pretreatment of lignocellulosic biomass, lignin has been shown to form droplets that deposit on the cellulose surface and retard enzymatic digestion of cellulose (1, 2). However, studies of this nature are limited for hydrothermal pretreatment, with the result that the corresponding mechanisms that inhibit cellulolytic enzymes are not well understood. In this study, scanning electron microscope (SEM) and wet chemical analysis of solids formed by hydrothermal pretreatment of a mixture of Avicel cellulose and poplar wood showed that lignin droplets from poplar wood relocated onto the Avicel surface. In addition, nuclear magnetic resonance (NMR) showed higher S/G ratios in deposited lignin than the initial lignin in poplar wood. Furthermore, the lignin droplets deposited on Avicel significantly impeded cellulose hydrolysis. A series of tests confirmed that blockage of the cellulose surface by lignin droplets was the main cause of cellulase inhibition. The results give new insights into the fate of lignin in hydrothermal pretreatment and its effects on enzymatic hydrolysis.

5.2 Introduction

In order to overcome the recalcitrance of lignocellulosic biomass for large scale, low cost biofuels production, pretreatment is a critical prerequisite to achieve high sugar yields from plant cell wall deconstruction by enzymes and microorganisms (3-5). The role of pretreatment is to disrupt and/or remove lignin and hemicellulose, the major plant cell wall structural polymers that protect cellulose microfibrils, to create high cellulose accessibility that facilitates enzymatic saccharification (6, 7). In light of this, several leading pretreatments have been developed, most of which involve high temperatures and pressures, mostly with addition of chemicals such as acids and bases (8). But high temperature pretreatments also result in formation of various inhibitory intermediates and byproducts that can slow down subsequent enzymatic hydrolysis. For example, xylooligosaccharides, important hemicellulose hydrolysis intermediates, were shown to strongly inhibit cellulose hydrolysis (9, 10). However, the highly hydrophobic, complex, and heterogeneous nature of lignin still limits understanding of its role in enzymatic hydrolysis.

Lignin in plant cell walls appears to cycle between the solid and liquid phase during pretreatment, resulting in both morphological and structural changes (11-13). Other studies on dilute acid pretreatment of corn stover and purified lignin in the presence of filter paper reported that during thermochemical pretreatment above the lignin glass transition temperature, lignin could coalesce on cell walls and migrate into the bulk liquid phase to form droplets that deposit back on the cell wall surface, negatively impacting cellulose hydrolysis (1, 2). These results indicate that

understanding the effects of lignin relocalization/deposition is as important as lignin removal in improving cellulose digestibility. It has been generally agreed that lignin reduces enzyme efficiency in two possible ways (14-17): enzyme binds nonspecifically to lignin (nonspecific binding mechanism) and lignin acts as a physical barrier that blocks enzyme access to the cellulose surface (surface blockage mechanism). However, such studies are still limited, and the mechanism of deposited lignin droplets formed during hydrothermal pretreatment in inhibiting the subsequent enzymatic hydrolysis is not yet clear.

In this study, lignin deposited Avicel (LDA) was prepared by batch hydrothermal pretreatment of Avicel PH-101 cellulose mixed with poplar wood as a lignin source. Avicel cellulose without poplar was also pretreated at similar conditions as a control. Lignin droplets deposited on LDA were characterized by SEM, wet chemistry, and ^{13}C-^{1}H HSQC NMR. Enzymatic hydrolysis at different protein loadings was performed on both the control Avicel and LDA to investigate inhibition patterns to cellulase. In addition, isolated lignin deposited Avicel (iLDA) was prepared by mixing lignin chemically extracted from poplar with Avicel to confirm the enzymatic inhibition pattern of LDA. Two possible mechanisms for such inhibition, non-specific binding and surface blockage, were evaluated; and surface blockage of enzyme to cellulose was proposed to be main mechanism responsible for the inhibition pattern of enzymatic hydrolysis of cellulose by deposited lignin droplets.

5.3 Materials and methods

5.3.1 Materials

Pure cellulose, Avicel PH-101 (Lot No. 1094627) was purchased from FMC Corporation (Philadelphia, PA), 1,4-dioxane (J.T.Baker, Lot No. K06622) was purchased from Avantor Performance Materials Inc (Phillipsburg, NJ), and bovine serum albumin (BSA, 98% purity, Batch No. 078K0730) was purchased from Sigma-Aldrich (St. Louis, MO). Debarked poplar (*Populus trichocarpa*) was provided by the National Renewable Energy Laboratory (NREL) in Golden, CO and then knife milled (Wiley Laboratory Mill Model 4, Arthur H. Thomas Company, Philadelphia, PA) to pass through a 20-mesh screen (<0.85 mm). As determined by following the NREL two-step strong acid hydrolysis procedure, the poplar was found to contain 25.1% lignin, 42.4% glucan, and 18.2% xylan.

Lignin was also extracted from poplar according to reported methods (18, 19). Briefly, the poplar was refluxed with ethanol:toluene (1:2, v/v) for 24 h in a Soxhlet apparatus to remove extractives, followed by washing with water and air drying. The extractives-free dry poplar was placed in a porcelain ball mill jar, along with porcelain grinding media and ground in a rotary ball mill for 120 h under an inert (nitrogen) atmosphere. The ground poplar powder was then extracted with *p*-dioxane: water (96:4, v/v) under stirring at room temperature for 48 h in the dark. The extracted mixture was centrifuged and the supernatant was collected, roto-evaporated, and freeze dried; the crude ball milled lignin was collected and purified.

5.3.2 LDA and iLDA preparation

Knife milled poplar was first sieved using USA Standard Testing Sieves (Fisher Scientific Company, Pittsburg, PA) to isolate -20/+40 mesh (425~850 µm) particle-size fractions that were then washed with room temperature deionized (DI) water to remove fines and dust and dried in a conventional oven at 65°C (Model No. 6520, Thermo electron corporation, Marietta, Ohio). Then, 60 g of this poplar wood and 20 g of Avicel cellulose were hydrothermally pretreated in a 1 L high pressure, mechanically stirred Parr reactor (Model No. 236HC, Parr Instrument, Moline IL) at 200°C for 15 min with a solid loading of 10 wt%. After pretreatment, this lignin deposited Avicel (LDA) was separated from poplar particles using a 100 mesh screen (150 µm, vendor), washed with room temperature DI water, and filtered until the moisture dropped to about 50%.

The steps applied to prepare isolated lignin deposited Avicel (iLDA) are summarized in Figure 5.1. In brief, 11.5 mg of isolated lignin was first dissolved in a 11 mL mixture of 1,4-dioxane and water (10:1 v/v) in a 50 mL glass vial with screw cap. 0.5 g Avicel PH-101 was then added, and the mixture was kept in an incubation shaker (Multitron Infors-HT, ATR Biotech, Laurel, MD) at 30°C for 3 h. The slurry was then transferred to an aluminum weighing dish and allowed to dry overnight in a fume hood. For comparison, Avicel control samples were also prepared without poplar wood and lignin adding at otherwise the same conditions as LDA and iLDA. The moisture content of Avicel cellulose control, LDA, and iLDA was determined by an automatic infrared moisture analyzer (Model No. HB43-S, Mettler-Toledo Inc., Columbus, OH).

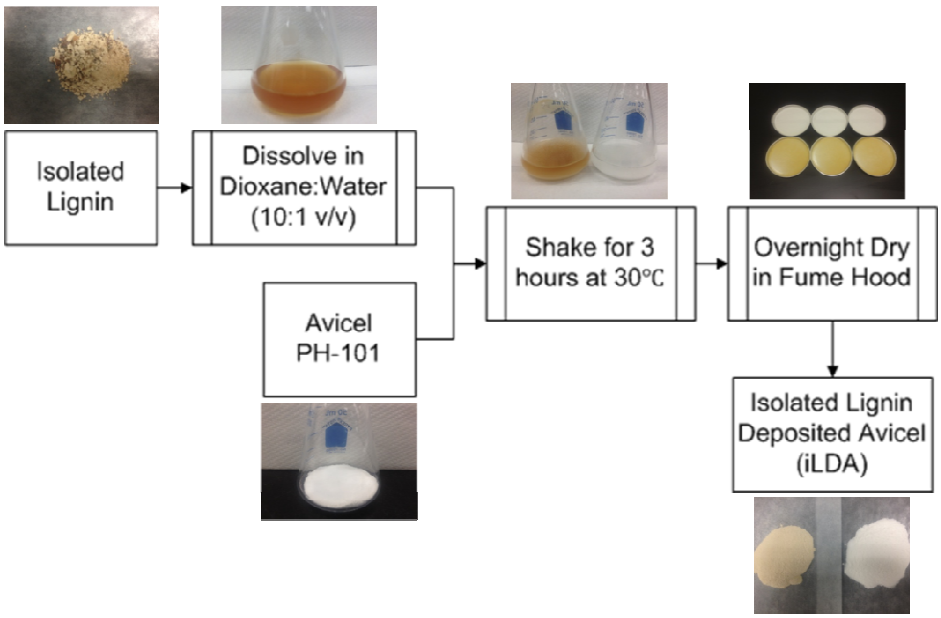

Figure 5.1. Flowchart of major steps for preparation of isolated lignin deposited Avicel (iLDA) from lignin isolated from poplar wood and Avicel cellulose.

5.3.3 LDA and iLDA characterizations

Prior to compositional analysis, the solids were dried at 105°C overnight in conventional oven (EW-52501-03, Cole-Parmer Instrument Company, Vernon Hills, IL). The glucan, xylan, and acid-insoluble lignin (Klason lignin) contents in LDA were measured by NREL standard biomass analysis procedures (20). Sugar concentrations were determined with a Waters Alliance e2695 HPLC outfitted with a 2414 refractive index (RI) detector (Waters Corporation, Milford, MA) and a BioRad Aminex HPX-87H column (Bio-Rad Life Science, Hercules, CA).

For SEM, samples were first coated with gold for one min under a 20 μA current by a Sputter Coater Cressington 108 Auto. Then, SEM images were developed using XL30 FEG SEM (Philips, address) at 5kV accelerating voltage.

For NMR, the deposited lignin from LDA was isolated with a dioxane/water (96:4, v/v) mixture with stirring for overnight. The mixture was filtered, and the filtrate was roto-evaporated and freeze-dried. The freeze dried lignin was dissolved in deuterated dimethyl sulfoxide for NMR analysis. NMR experiments were performed using a Bruker Avance-400 spectrometer operating at a frequency of 100.59 MHz for ^{13}C (21, 22). Conditions for the two-dimensional heteronuclear single quantum coherence (HSQC) analysis were as follows: 13-ppm spectra width in F2 (^{1}H) dimension with 1024 data points (95.9-ms acquisition time), 210-ppm spectra width in F1 (^{13}C) dimension with 256 data points (6.1-ms acquisition time); a 0.5-s pulse delay; and a $^{1}J_{C-H}$ of 145 Hz and 380 scans. A Shigemi NMR tube (Shigemi, Inc., Allison Park, PA) was used for the deposited poplar lignin. The central solvent peak (δ_C 39.5 ppm; δ_H 2.5 ppm) was used for chemical shift calibration. NMR data was processed using TopSpin 2.1 (Bruker BioSpin) and MestreNova (Mestre Labs) software packages.

5.3.4 Enzymatic hydrolysis

Enzymatic hydrolysis was performed according to NREL standard biomass analysis procedures (23), using 1 wt% glucan loading in a 0.05 M citrate buffer (pH 4.8) with 0.2 g/L sodium azide at 50^{o}C and 200 rpm. All hydrolysis experiments were run in triplicates in 25 ml Erlenmeyer flasks with 15 ml total volume in a temperature controlled incubation shaker (Multitron Infors-HT, ATR Biotech, Laurel, MD). Accellerase® 1500 (Lot No.4901131618, BCA protein content- 86 mg/ml) cellulase and Accellerase® XY (Lot No.1681198062, BCA protein content- 51mg/ml) xylanase were from DuPont™

Genencor® (Science, Palo Alto, CA). For LDA and the control Avicel cellulose hydrolysis, a low (30 mg total protein/g glucan) and high (120 mg total protein/g glucan) total protein loadings were applied at 1:1 protein mass ratio of cellulase to xylanase, respectively. BSA blocking experiments were performed by adding BSA (10 g/L) to the hydrolysis slurry at room temperature 30 min prior (16, 24) to adding enzymes (30 mg enzyme protein per gram of glucan at a 1:1 protein mass ratio of cellulase to xylanase). For iLDA and control hydrolysis, 20 mg of enzyme protein per gram of glucan was added at a 3:1 ratio of cellulase to xylanase. To analyze sugar release, about 1 ml samples were collected in 2 ml microcentrifuge tubes at selected time points and centrifuged at 14,600 rpm for 3min. The liquid hydrolyzate samples along with appropriate calibrations standards were run on a Waters HPLC as discussed previously to determine the sugar concentrations. Glucose yield (GY) reflects the amount of glucose released out of available sugar in raw biomass. Relative inhibition was calculated as:

$$Relative\ inhibition\ (\%) = \frac{GY(control)\text{-}GY(sample)}{GY(control)} \times 100\%$$

where GY(sample) is glucose yield of LDA or iLDA, and GY(control) is glucose yield of the corresponding Avicel control.

5.3.5 Ultraviolet (UV) absorbance

iLDA hydrolyzates collected at different time points were centrifuged at 12000 rpm in 2 mL microcentrifuge filter tubes (Cat No. 24137, Grace) for 5 min. The liquid samples were diluted by 100 times using DI water, and UV absorbance was measured on a SpectraMax M5e UV-Vis spectrophotometer (Molecular Devices, Sunnyvale, CA) at

240 nm. The corresponding hydrolyzates of Avicel control at each hydrolysis time point were also centrifuged and diluted using the method above as a background blank. Relative UV absorbance was calculated as:

$$Relative\ UV\ absorbance = \frac{Sample\ absorbance(t)\text{-}Absorbance\ of\ control\ blank\ (t)}{Sample\ absorbance(t=1)\text{-}Absorbance\ of\ control\ blank\ (t=1)}$$

where t is the hydrolysis time with a unit of hour.

5.4 Results and discussion

5.4.1 LDA and iLDA characterization

The compositional analysis results show that LDA contained approximately 2.3±0.1 % acid insoluble lignin, 90.0±2.3 % glucan, and 1.2±0.2 % xylose equivalents, while its Avicel control sample contained about 93.5±3.1 % glucan. SEM images presented in Figure 5.2 clearly show that numerous droplets were deposited on LDA while the surface of the Avicel control was very smooth. Compositional analysis by wet chemistry and SEM imaging confirmed that lignin droplets were deposited from poplar wood onto Avicel cellulose at the hydrothermal condition tested, although minor amounts of xylan was also measured for the LDA sample. These results are consistent with several previous studies that observed and identified lignin droplets on various biomass, including corn stover, switchgrass, wheat straw, and *Tamarix ramosissima*, following hydrothermal or dilute acid pretreatments (1, 2, 25-27). Lignin droplets deposited on iLDA sample were characterized by SEM only, with the image also shown in Figure 5.2. The size of lignin droplets on iLDA was relatively small compared to that found on LDA.

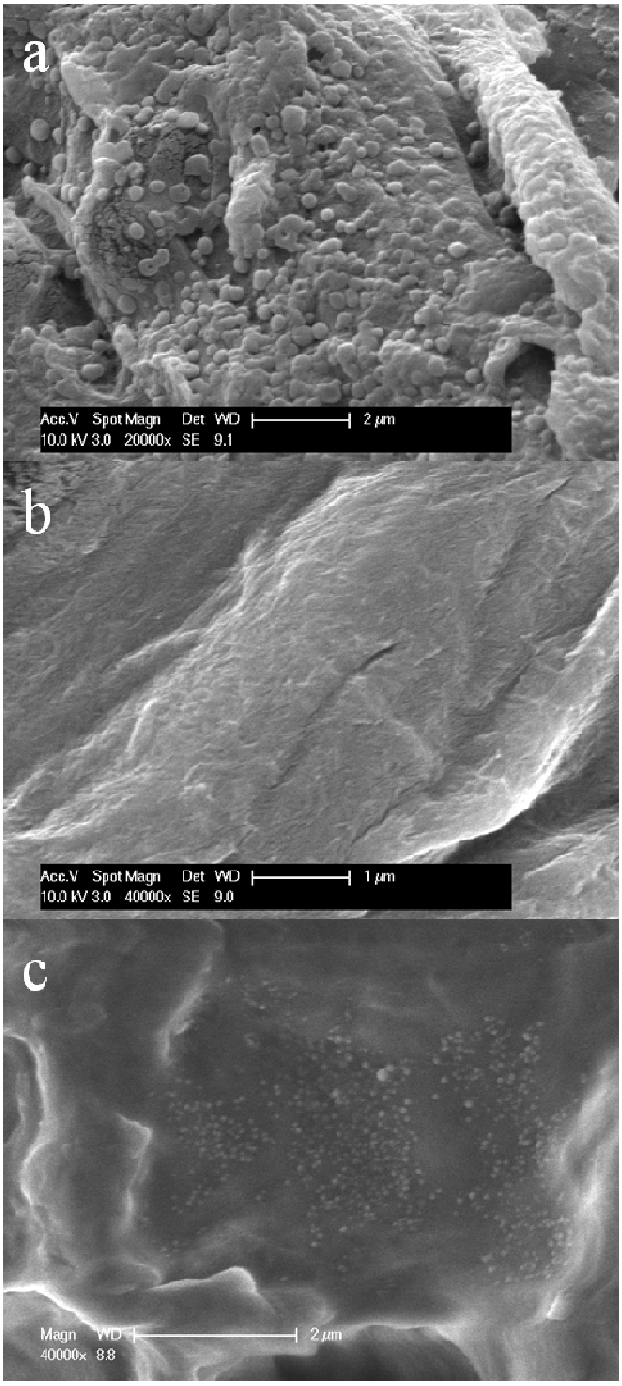

Figure 5.2. SEM images of (a) lignin deposited Avicel (LDA; magnification 20k×), (b) Avicel control (magnification 40k×), and isolated lignin deposited Avicel (iLDA; magnification 40k×) (iLDA).

Figure 5.3 shows aromatic and aliphatic regions of 2D ^{13}C-^{1}H HSQC spectra for the lignin sample isolated from LDA. The NMR spectra of lignin sample isolated from LDA showed typical poplar lignin structural features, further confirming that lignin was migrated from poplar wood and then deposited on Avicel during hydrothermal pretreatment. The aromatic region of HSQC spectrum showed prominent correlation signals for lignin syringyl (S) and guaiacyl (G) units along with p-hydroxyphenyl benzoate (PB) substructure. The aliphatic region of HSQC spectrum showed that the signals for β-O-4 substructure (A) were well resolved for C_α/H_α, C_β/H_β, and C_γ/H_γ correlations. The presence of phenylcoumaran substructures (B) was confirmed by C-H correlations for α-, β-, and γ-C positions centered around δ_c/δ_H 86.8/5.43, 53.1/3.42 and 62.8/3.74 ppm, respectively. The lignin resinol subunit (C) was also evidenced by its C/H correlations around $\delta c/\delta_H$ 84.9/4.66 (C_α/H_α), 53.5/3.04 (C_β/H_β), and 71.1/4.15 (C_γ/H_γ) ppm. The presence of phenylcoumaran and resinol subunits in lignin isolated from LDA demonstrated that such structures were also dissolved during hydrothermal pretreatment and deposited onto Avicel cellulose. The HSQC analysis also revealed that the signal of β-O-4 substructure which was linked to syringyl units was stronger than that linking with guaiacyl units, suggesting the relative higher abundance of syringyl units in the deposited lignin. One explanation is that the lignin syringyl units were more prone to cleavage/acidic degradation (28) in hydrothermal pretreatment, thereby being preferably dissolved and relocated onto the Avicel surface.

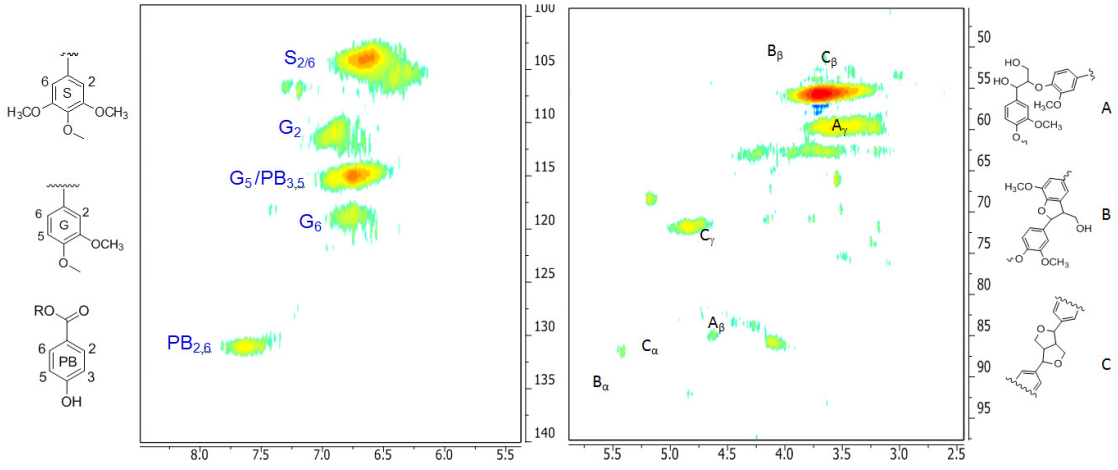

Figure 5.3. Aromatic (left) and aliphatic (right) region of 2 D ^{13}C-^{1}H HSQC spectrum for the lignin re-isolated from LDA

5.4.2 Enzymatic hydrolysis

Enzymatic hydrolysis of LDA and the Avicel control were conducted at both low and high protein loadings of 15 mg cellulase + 15 mg xylanase per gram of glucan and 60 mg cellulase + 60 mg xylanase per gram of glucan, respectively. Cellulase was supplemented with xylanase to avoid interferences from residue xylose equivalents that deposited on LDA as well. Glucose yields from enzymatic hydrolysis of LDA and the Avicel control shown in Figure 5.4 indicate that the deposition of lignin droplets did negatively affect enzymatic digestion of cellulose, especially in the early stages of hydrolysis. The relative inhibition for 1 h hydrolysis was 39.7% and 29.3% for low and high enzyme loadings, respectively. More interestingly, inhibition by deposited lignin droplets decreased with hydrolysis time and was relieved when cellulose conversion reached over 80-90%.

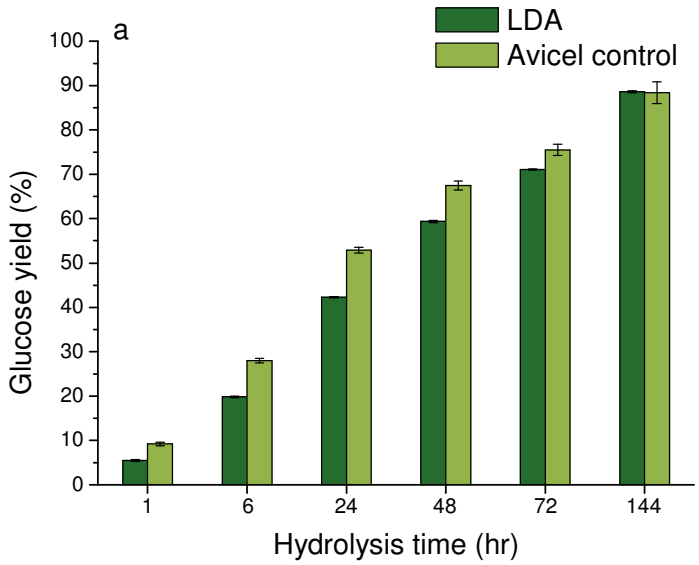

Relative inhibition (%)	
1h	39.7
6h	29.3
24h	20.0
48h	12.0
72h	5.9
144h	0

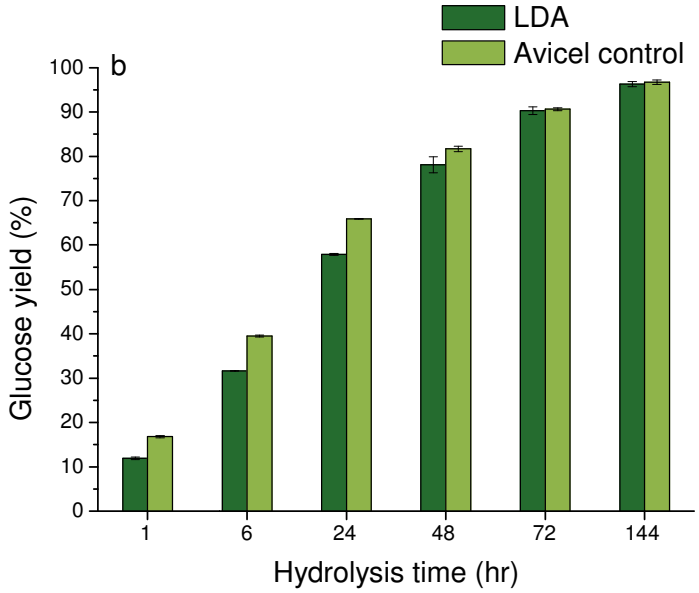

Relative inhibition (%)	
1h	29.3
6h	20.1
24h	12.3
48h	4.5
72h	0.6
144h	0

Figure 5.4. Glucose yields from enzymatic hydrolysis of Avicel cellulose control and lignin deposited Avicel (LDA) and percentage relative inhibition at different time points of enzymatic hydrolysis performed at enzyme loadings of (a) 15 mg cellulase + 15 mg xylanase protein/ g glucan and (b) 60 mg cellulase + 60 mg xylanase protein / g glucan. Error bars represent standard deviation of three replicates

In order to confirm this finding, iLDA, which was prepared with isolated lignin using the organic solvent method, was also enzymatically hydrolyzed. Although a similar inhibition pattern was observed for iLDA to that for LDA, as shown in Figure 5.5, the initial relative inhibition appeared to be lower than for LDA. These results demonstrate that the observed slowdown in the enzymatic hydrolysis rate and the drop in inhibition of LDA with extended hydrolysis time were indeed caused by the deposition of lignin droplets.

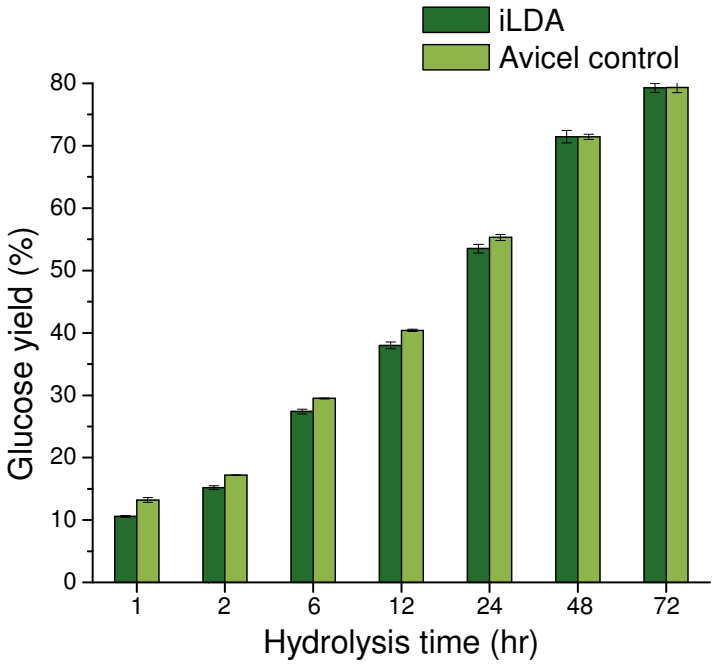

Relative inhibition (%)	
1h	19.7
2h	11.6
6h	7.2
12h	5.9
24h	3.2
48h	0
72h	0

Figure 5.5. Glucose yields from enzymatic hydrolysis of Avicel cellulose control and isolated lignin deposited Avicel (iLDA) and percentage relative inhibition at different time points of enzymatic hydrolysis for a total protein loading of 15 mg cellulase + 5 mg xylanase / g glucan. Error bars represent standard deviation of three replicates.

5.4.3 Mechanism for inhibition by nonspecific binding

To investigate the key mechanism responsible for enzyme inhibition by deposited lignin droplets, the theoretical amount of enzyme protein that could adsorb on lignin droplets in the LDA sample was first estimated based on the reported maximum cellulase adsorption capacity of lignin (56.8-126.9 mg cellulase protein/ g lignin) prepared by leading pretreatments (29). In this study, an upper limit of 127 mg enzyme protein/ g lignin was assumed for a calculation based on the 2.3% lignin content in LDA. As shown in Table 5.1, the protein adsorbed by lignin droplets on LDA was estimated to be about 3 mg/g glucan, leading to a protein loss of 10% and 2.5% for low and high enzyme loadings, respectively. However, a 2.5wt% loss in protein should not result into a 29.3% loss in hydrolysis rate at 1 h for high enzyme loading, suggesting that the nonspecific binding of enzyme on lignin droplets was not the main mechanism retarding enzymatic hydrolysis of LDA.

Table 5.1. Estimated maximum protein loss due to nonspecific binding to lignin droplets versus 1 h relative inhibition

Protein loading (mg/g glucan)	Estimated maximum protein loss	Percent protein loss	1 h relative inhibition
15 + 15 (cellulase + xylanase)	3.0 mg/g glucan	10.0 wt%	39.7 %
60 + 60 (cellulase + xylanase)	3.0 mg/g glucan	2.5 wt%	29.3 %

To confirm this deduction, BSA protein was added to LDA slurry prior to adding enzymes to prevent lignin from competitively binding enzymes because BSA was previously shown to irreversibly adsorb onto lignin binding sites without interfering with cellulose hydrolysis (16, 24, 30). Figure 5.6 shows results for enzymatic hydrolysis of

LDA with BSA blocking. Strong initial inhibition as well as the similar drop in inhibition with LDA hydrolysis without BSA blocking was observed, confirming that nonspecific binding of enzyme to deposited lignin droplets was not the primary inhibition mechanism. Further support is provided by one previous study published by our group, in which the relative inhibition increased with hydrolysis time when a significant amount of enzyme was adsorbed onto lignin (29), in contrast to the results in this study. Therefore, the results demonstrated that the role of enzyme nonspecific binding to lignin droplets in cellulose hydrolysis inhibition is highly limited.

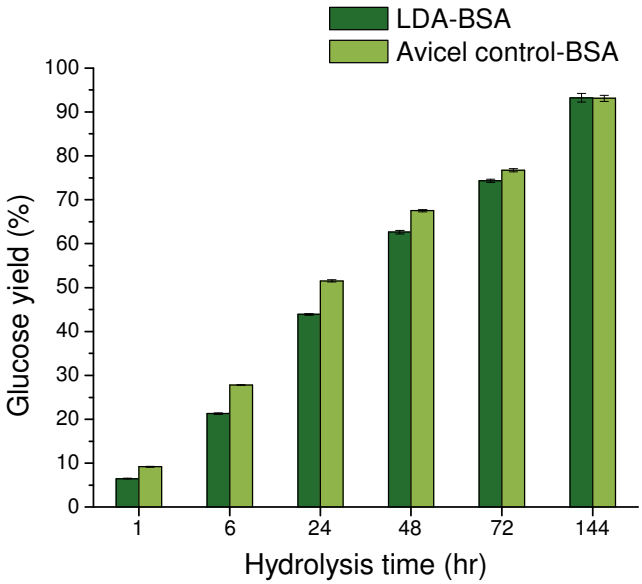

Relative inhibition (%)	
1h	29.4
6h	23.5
24h	14.8
48h	7.2
72h	3.1
144h	0

Figure 5.6. Glucose yields from enzymatic hydrolysis of BSA blocked Avicel cellulose control and BSA blocked lignin deposited Avicel (LDA-BSA) and relative inhibition at different time points of enzymatic hydrolysis conducted at a total protein loading of 15 mg cellulase + 15 mg xylanase / g of glucan. Error bars represent standard deviation of three replicates.

5.4.4 Mechanism for inhibition by surface blockage

Evidence reported in the literature suggests that cellulase hydrolyzes cellulose microfibrils layer by layer starting from surface (31, 32), sliding unidirectionally as one enzyme molecule moves along one cellulose chain (32). Thus, according to this mechanism, it appears that when lignin droplets deposit on the cellulose surface, their inhibitory effects on enzymatic hydrolysis arise not only from blocking enzymes from moving along the surface layer but also by preventing accessibility to inner layers. In this context, cellulose surface blockage can be another mechanism responsible for cellulose hydrolysis slowdown by the deposited lignin droplets. However, the drop in inhibition with extended conversion suggests that the physical barrier imposed by these lignin droplets was relieved with more cellulose conversion, leaving a question of how lignin droplets drop off from the cellulose surface? Two previous findings/theories appear to provide support to address this question. One is that a "traffic jam" of enzyme linear movements was observed when there was disturbance on the cellulose surface, resulting in a stop and/or slowdown in enzymatic digestion of cellulose. More interestingly, accumulation of subsequent enzyme molecules was found to lead a "push" that eliminated the obstacle and restarted hydrolysis (32). The other one is usually termed "enzymatic deinking" as used to recover paper in the pulp and paper industry. In this theory, ink particles are believed to be "peeled-off" with small fibrils which are loosened by enzymatic hydrolysis of the cellulose surface, and the alteration of surface chemistry, such as hydrophobicity, by hydrolysis of adjacent cellulose chains could also facilitate ink detachment from the fiber surface (33-35). Although it is still very difficult to

determine which mechanism could account for the results observed in this study, experimental results support the "drop off" of lignin droplets with hydrolysis. As shown in Figure 5.7, the relative UV absorbance of filtered iLDA hydrolyzate increased significantly with increased hydrolysis time, indicating more lignin droplets were removed from the cellulose surface and moved into bulk liquid phase.

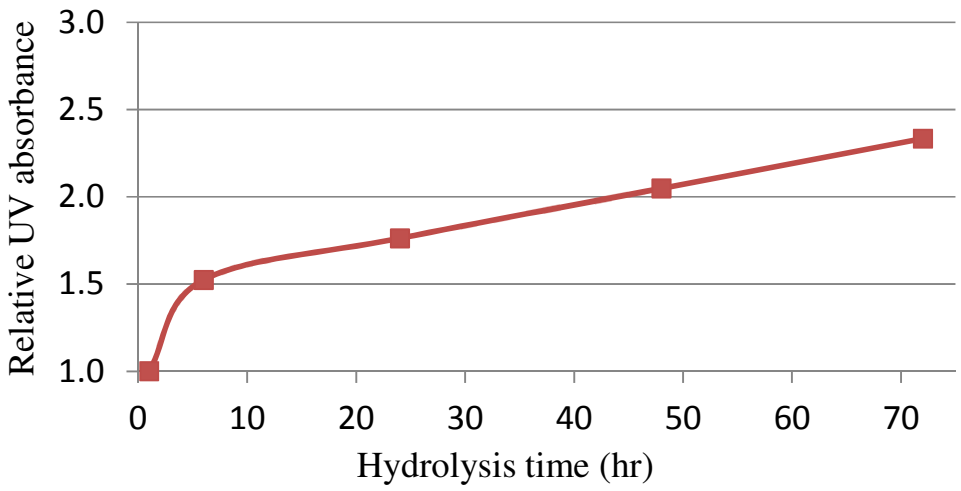

Figure 5.7. Relative UV absorbance at 240 nm of filtered hydrolyzate of isolated lignin deposited Avicel (iLDA) at different hydrolysis times.

5.4.5 Hypothesis explaining initial slowdown of hydrolysis

On the basis of the experimental results in this study and previous reported theories, a hypothesis was developed to explain how deposited lignin droplets retard cellulose enzymatic hydrolysis, especially in the early stages, as schematically represented in Figure 5.8. This hypothesis suggests that inhibition starts with lignin droplets blocking enzymes that are traveling in line with the blocked area (Figure 5.8a). Then a "traffic jam" forms, delaying more enzymes and aggravating inhibition (Figure

5.8b). With enzyme accumulation and alteration of surface chemistry by hydrolysis of adjacent cellulose chains, the lignin droplets are either "pushed off" or "peeled off" from the cellulose surface, allowing hydrolysis to continue (Figure 5.8c). As more droplets drop off with cellulose conversion, inhibition is reduced with increased hydrolysis time (Figure 5.8d). When cellulose conversion is relatively high and all initial surfaces have been hydrolyzed, inhibition virtually stops (Figure 5.8e).

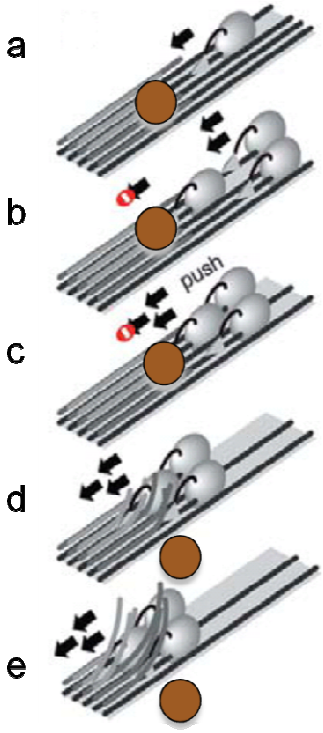

Figure 5.8. Schematic presentation of possible mechanism of deposited lignin droplets inhibition of enzymatic hydrolysis, modified from Igarashi et al., (2011).

5.5 Conclusions

Similar to observations for dilute acid pretreatment reported in previous studies (2) , lignin migrated out of the poplar wood cell wall and deposited on the Avicel

cellulose surface during hydrothermal pretreatment as well. The lignin droplets deposited on the surface of Avicel cellulose retarded enzymatic hydrolysis initially, but inhibition decreased with increased hydrolysis time and was virtually eliminated at high cellulose conversion. Experimental results demonstrated that nonspecific binding of enzymes to lignin droplets was not the primary mechanism for inhibition. Instead, surface blockage of cellulose by lignin droplets was proposed to be responsible for the inhibition pattern of enzymatic hydrolysis of LDA and iLDA. By comparing experimental results from this study to those from previous studies, the key mechanisms responsible for inhibition of cellulose hydrolysis by lignin, nonspecific binding or surface blockage or both, are believed to depend on the chemical nature and particle size of lignin polymer molecules. Although enzymatic hydrolysis in this study was performed at relatively high enzyme loadings to understand the inhibition mechanism, it is likely that lignin droplets would have an even greater impact on conversion for hydrolysis at low enzyme loadings.

5.6 Acknowledgements

This research was funded by the BioEnergy Science Center (BESC), a U.S. Department of Energy Bioenergy Research Center supported by the Office of Biological and Environmental Research in the DOE Office of Science. Gratitude is also extended to the Ford Motor Company for funding the Chair in Environmental Engineering at the Center for Environmental Research and Technology of the Bourns College of Engineering at UCR that augments support for many projects such as this.

5.7 References

1. Donohoe BS, Decker SR, Tucker MP, Himmel ME, Vinzant TB. Visualizing lignin coalescence and migration through maize cell walls following thermochemical pretreatment. Biotechnol Bioeng. 2008 Dec 1;101(5):913-25.
2. Selig MJ, Viamajala S, Decker SR, Tucker MP, Himmel ME, Vinzant TB. Deposition of lignin droplets produced during dilute acid pretreatment of maize stems retards enzymatic hydrolysis of cellulose. Biotechnol Progr. 2007 Nov-Dec;23(6):1333-9.
3. Wyman CE. Ethanol from lignocellulosic biomass - technology, economics, and opportunities. Bioresource Technol. 1994;50(1):3-16.
4. Wyman CE. What is (and is not) vital to advancing cellulosic ethanol. Trends in Biotechnology. 2007 Apr;25(4):153-7.
5. Lynd LR, Cushman JH, Nichols RJ, Wyman CE. Fuel ethanol from cellulosic biomass. Science. 1991 Mar 15;251(4999):1318-23.
6. Mosier N, Wyman C, Dale B, Elander R, Lee YY, Holtzapple M, et al. Features of promising technologies for pretreatment of lignocellulosic biomass. Bioresource Technol. 2005 Apr;96(6):673-86.
7. Kumar R, Mago G, Balan V, Wyman CE. Physical and chemical characterizations of corn stover and poplar solids resulting from leading pretreatment technologies. Bioresource Technol. 2009 Sep;100(17):3948-62.
8. Wyman CE, Dale BE, Elander RT, Holtzapple M, Ladisch MR, Lee YY. Coordinated development of leading biomass pretreatment technologies. Bioresource Technol. 2005 Dec;96(18):1959-66.
9. Kumar R, Wyman CE. Effect of xylanase supplementation of cellulase on digestion of corn stover solids prepared by leading pretreatment technologies. Bioresource Technol. 2009 Sep;100(18):4203-13.
10. Qing Q, Yang B, Wyman CE. Xylooligomers are strong inhibitors of cellulose hydrolysis by enzymes. Bioresource Technol. 2010 Dec;101(24):9624-30.
11. Yang B, Wyman CE. Effect of xylan and lignin removal by batch and flowthrough pretreatment on the enzymatic digestibility of corn stover cellulose. Biotechnol Bioeng. 2004 Apr 5;86(1):88-95.
12. Liu CG, Wyman CE. The effect of flow rate of compressed hot water on xylan, lignin, and total mass removal from corn stover. Ind Eng Chem Res. 2003 Oct 15;42(21):5409-16.
13. McKenzie HL. Tracking hemicellulose and lignin deconstruction during hydrothermal pretreatment of biomass. Riverside: University of California, Riverside; 2012.
14. Kumar R, Wyman CE. Key features of pretreated lignocelluloses biomass solids and their impact on hydrolysis. In: Waldon K, editor. Bioalcohol production: Biochemical conversion of lignocellulosic biomass. Oxford: Woodhead Publishing Ltd.; 2010. p. 73-121.
15. Yang B, Wyman CE. Pretreatment: the key to unlocking low-cost cellulosic ethanol. Biofuel Bioprod Bior. 2008 Jan-Feb;2(1):26-40.

16. Berlin A, Gilkes N, Kurabi A, Bura R, Tu M, Kilburn D, et al. Weak lignin-binding enzymes: a novel approach to improve activity of cellulases for hydrolysis of lignocellulosics. Appl Biochem Biotechnol. 2005 Spring;121-124:163-70.
17. Mansfield SD, Mooney C, Saddler JN. Substrate and enzyme characteristics that limit cellulose hydrolysis. Biotechnol Progr. 1999 Sep-Oct;15(5):804-16.
18. Chang HM, Cowling EB, Brown W, Adler E, Miksche G. Comparative studies on cellulolytic enzyme lignin and milled wood lignin of sweetgum and spruce. Holzforschung. 1975;29(5):153-9.
19. Holtman KM, Chang H-m, Kadla JF. Solution-state nuclear magnetic resonance study of the similarities between milled wood lignin and cellulolytic enzyme lignin. J Agr Food Chem. 2004 2004/02/01;52(4):720-6.
20. Sluiter A, Hames B, Ruiz R, Scarlata C, Sluiter J, Templeton D, et al. Determination of structural carbohydrates and lignin in biomass. Golden, CO, USA: National Renewable Energy Laboratory2008.
21. Hallac BB, Pu Y, Ragauskas AJ. Chemical Transformations of buddleja davidii lignin during ethanol organosolv pretreatment. Energ Fuel. 2010 2010/04/15;24(4):2723-32.
22. Pu YQ, Chen F, Ziebell A, Davison BH, Ragauskas AJ. NMR characterization of c3h and hct down-regulated alfalfa lignin. BioEnergy Research. 2009 Dec;2(4):198-208.
23. Selig M, Weiss N, Ji Y. Enzymatic Saccharification of lignocellulosic biomass. Golden, CO, USA: National Renewable Energy Laboratory2008.
24. Rollin JA, Zhu ZG, Sathitsuksanoh N, Zhang YHP. Increasing cellulose accessibility is more important than removing lignin: a comparison of cellulose solvent-based lignocellulose fractionation and soaking in aqueous ammonia. Biotechnol Bioeng. 2011 Jan;108(1):22-30.
25. Kristensen JB, Thygesen LG, Felby C, Jorgensen H, Elder T. Cell-wall structural changes in wheat straw pretreated for bioethanol production. Biotechnol Biofuels. 2008 Apr 16;1.
26. Pingali SV, Urban VS, Heller WT, McGaughey J, O'Neill H, Foston M, et al. Breakdown of cell wall nanostructure in dilute acid pretreated biomass. Biomacromolecules. 2010 Sep;11(9):2329-35.
27. Xiao LP, Sun ZJ, Shi ZJ, Xu F, Sun RC. Impact of hot compressed water pretreatment on the structural changes of woody biomass for bioethanol production. Bioresources. 2011;6(2):1576-98.
28. Samuel R, Foston M, Jaing N, Cao S, Allison L, Studer M, et al. HSQC (heteronuclear single quantum coherence) 13C-1H correlation spectra of whole biomass in perdeuterated pyridinium chloride-DMSO system: An effective tool for evaluating pretreatment. Fuel. 2011;90(9):2836-42.
29. Kumar R, Wyman CE. Access of cellulase to cellulose and lignin for poplar solids produced by leading pretreatment technologies. Biotechnol Progr. 2009 May-Jun;25(3):807-19.
30. Zhu ZG, Sathitsuksanoh N, Vinzant T, Schell DJ, McMillan JD, Zhang YHP. Comparative study of corn stover pretreated by dilute acid and cellulose solvent-based

lignocellulose fractionation: enzymatic hydrolysis, supramolecular structure, and substrate accessibility. Biotechnol Bioeng. 2009 Jul 1;103(4):715-24.
31. Zhang YHP, Cui JB, Lynd LR, Kuang LR. A transition from cellulose swelling to cellulose dissolution by o-phosphoric acid: Evidence from enzymatic hydrolysis and supramolecular structure. Biomacromolecules. 2006 Feb;7(2):644-8.
32. Igarashi K, Uchihashi T, Koivula A, Wada M, Kimura S, Okamoto T, et al. Traffic jams reduce hydrolytic efficiency of cellulase on cellulose surface. Science. 2011 Sep 2;333(6047):1279-82.
33. Bajpai P. Enzymatic deinking. Adv Appl Microbiol. 1997;45:241-69.
34. Ibarra D, Monte MC, Blanco A, Martinez AT, Martinez MJ. Enzymatic deinking of secondary fibers: cellulases/hemicellulases versus laccase-mediator system. J Ind Microbiol Biot. 2012 Jan;39(1):1-9.
35. Jeffries TW, Klungness JH, Sykes MS, Rutledgecropsey KR. Comparison of enzyme enhanced with conventional deinking of xerographic and laser printed paper. Tappi J. 1994 Apr;77(4):173-9.

Chapter 6

Reduced Methylation of Xylan Side-Chains Lowers Arabidopsis Recalcitrance to Biological Deconstruction in Flowthrough Hydrothermal Pretreatment*

*This whole chapter will be submitted under the following citation:
Li H, Pena MJ, Urbanowicz BR, Kumar R, York WS, Wyman CE. "Reduced methylation of xylan side-chains lowers Arabidopsis recalcitrance to biological deconstruction in flowthrough hydrothermal pretreatment"

6.1 Abstract

A major hemicellulose component in woody biomass is 4-*O*-methyl glucuronoxylan. Recently, a gene was identified and functionally characterized, resulting in synthesis of glucuronoxylans with 75% less methylation in an Arabidopsis mutant (*gxmt1-1*) than in the wild type (WT). Enzymatic hydrolysis of solids produced by flowthrough pretreatment of *gxmt1-1* with just hot water (hydrothermal) at 180^{o}C displayed 25% higher glucose yields than from the WT when pretreated for the same time. Although compositional analysis by traditional wet chemistry showed glucan, xylan + galactan, and lignin contents of *gxmt1-1* and WT to be similar prior to pretreatment at 30.1 and 32.9%, 13.5 and 13.9%, and 13.5 and 13.9%, respectively, 5.0% more xylan + galactan and 10.4% more lignin were removed from the mutant by flowthrough hydrothermal pretreatment compared to the control. The structure of components released during flowthrough pretreatment was also characterized by nuclear magnetic resonance (NMR) spectroscopy. Results showed that less methyl groups in glucuronoxylan side-chains resulted in higher release of lignin and hemicellulose and less recalcitrance to enzymes. This observation provides important insights into how degree of methylation affects interactions of hemicellulose and lignin and cell wall deconstruction.

6.2 Introduction

Attention to utilizing lignocellulosic biomass to replace limited fossil resources for sustainable fuel and chemical production has increased significantly in recent years. Important efforts have been directed at developing fast growing and less recalcitrant energy crops, designing effective and less severe pretreatments, and engineering advanced enzymes and microorganisms to facilitate establishment of a competitive lignocellulosic biomass industry for biological conversion approaches (1-4).

Cellulose, hemicellulose, and lignin are the major components of lignocellulosic biomass, although their contents and structure vary with biomass types (5). Some studies have shown that the content and as well as composition of lignin and hemicellulose affect cell wall deconstruction by enzymes (6-10), while others indicated the interaction of lignin and hemicellulose was also very important (11-13). Thus, understanding the synthesis and breakdown of the cell wall composite matrix will help to overcome biomass recalcitrance as a barrier to low cost biological conversion.

4-O-methyl glucuronoxylan (GX) is the principle hemicellulose in secondary cell walls of most dicots (14). The GX backbone is composed of 1,4-linked β-D-xylosyl residues with glucuronic acid (GlcA) or 4-O-methyl glucuronic acid (4-O-MeGlcA) substitution at the O-2 position (15). Recently, Urbanowicz et al. at the Complex Carbohydrates Research Center (CCRC) identified and functionally characterized an Arabidopsis gene that synthesized glucuronoxylans with less methylation than in the wild type, while producing no other significant carbohydrate structural changes (16). Experimental results showed that the Arabidopsis mutant with less methyl groups in its

glucuronoxylan side chains released more xylose than wild type control during hydrothermal (water-only) pretreatment in batch reactors, most notably at lower severity conditions (16). However, due to batch reactor limitations, detailed investigation of the effects of reduced methylation on xylan and lignin removal during pretreatment and on resulting biomass digestibility was not possible.

Compared to batch reactors, flowthrough pretreatment allows monitoring of the extent and amount of cell wall components released as a function of time, minimizes degradation reactions, and limits re-condensation and deposition of pretreatment products that can obfuscate determining actual reaction sequences (17-20). Thus, flowthrough pretreatment can be an effective tool to track cell wall deconstruction.

In this study, hydrothermal pretreatment in flowthrough reactors was applied to the Arabidopsis mutant (*gxmt1-1*) with 75% less methylation and its wild type (WT) control. Liquid hydrolyzates from pretreatment were collected over a range of time intervals and analyzed for sugars and lignin released by traditional wet chemistry methods and measurement of liquid absorbance at 200 nm with an UV-Vis spectrophotometer, respectively In addition, ^{1}H NMR was employed to characterize the structure of components in the hydrolyzates. Finally, sugar release from enzymatic hydrolysis of untreated *gxmt1-1* and WT samples and their solid residues following pretreatment was measured to determine how changes in methylation affected biological deconstruction. The results provided new insights into how degree of methylation affects interactions of hemicellulose and lignin and cell wall deconstruction.

6.3 Materials and methods

6.3.1 Plant materials

Arabidopsis samples (*Arabidopsis thaliana*) were prepared and provided by Complex Carbohydrates Research Center (CCRC) at the University of Georgia, Athens, GA with details described elsewhere (16). Seeds from the Arabidopsis mutant line (SALK_018081, *gxmt1-1*) were obtained from the Arabidopsis Biological Research Center (www.arabidopsis.org). Both the *gxmt1-1* mutant and wild type control (WT) were grown for 8 weeks in Conviron growth chambers under short-day conditions (12 h photoperiod) at 22°C, 50% relative humidity, and a light intensity of ~180 µmol photons $m^{-2}s^{-1}$. Arabidopsis stems samples were placed on ice immediately upon harvest until they could be transferred to a -80°C freezer. Then, the tissue was ground in liquid nitrogen to a powder with a mortar and pestle. Following that, the powder was suspended in aqueous 80% (v/v) ethanol and then homogenized with a polytron (Kinematica Switzerland). The resulting slurry was filtered through a 50 µm nylon mesh, and the retentate was washed with aqueous 80% (v/v) ethanol. Next, the insoluble residue was suspended in chloroform: methanol (1:1 v/v) solution and stirred for 1 h at room temperature. The suspension was then filtered, and the insoluble residue washed with acetone and air dried. The alcohol insoluble residues (AIR) were shipped to the University of California, Riverside (UCR). The degree of methylation in 4-O-methyl glucuronoxylan side chains of *gxmt1-1* mutant was 75% less than that of WT, as reported elsewhere (16).

6.3.2 Pretreatment in flowthrough reactors

The design of the UCR flowthrough system is described in detail elsewhere (17-20). The flowthrough reactors were constructed of 12.7 by 152 mm stainless steel tube with Swagelok fittings (SS-8-VCR-1, SS-8-VCR-3-8TA, SS-8VCR-6-810, SS-200-R-8, Swagelok, San Diego, CA). For pretreatment, 1 g of dry Arabidopsis biomass was held in the reactor between two 5 micron gaskets (SS-8-VCR-2-5M, Swagelok, San Diego, CA). Deionized (DI) water was pumped through the system at a flow rate of 15 mL/min by a positive displacement pump (Prep100, LabAlliance, State College, PA), with the system pressure controlled by a backpressure regulator (GO, Spartanburg, SC) at 159.6 psi. After inspection for leaks at room temperature, the water preheating coil and reactor were heated by suspending them in a 4kW fluidized sand bath (SBL-2D, Techne, Princeton, NJ). The sand bath was set at 190°C based on results of preliminary runs to maintain temperature in flowthrough reactors at 180 °C as measured by a DigiSense DualLog R Thermocouple Meter (15-176-96, Fisher Scientific, Pittsburgh, PA) equipped with a K-type thermocouple T1 at the reactor outlet. The liquid hydrolyzate exiting the pretreatment reactor was cooled by passing through a coil submerged in a 19 L cold water bath prior to sampling. All pretreatments were performed in duplicate.

The reaction starting time was recorded when the temperature reached 178°C, after which hydrolyzate samples were collected into 125 mL pre-weighed glass flasks with screw caps over 2 min intervals. After 10 min, the reactor and heating coil were transferred to a cold water bath and cooled to 40°C, at which point the water flow was stopped. The hydrolyzates produced during reactor heat up and cool down were also

collected in pre-weighed flasks. The pretreated solids were then vacuum filtered until the moisture reached about 80% and then kept in 50 mL graduate plastic centrifuge tubes (Cat No. 430290, Corning Life Sciences, Tewksbury MA) in a 4°C refrigerator.

6.3.3 Compositional analysis

Biomass samples were dried at 105°C overnight, and the moisture content was determined by an automatic infrared moisture analyzer (Model No. HB43-S, Mettler-Toledo Inc., Columbus, OH). The glucan, xylan, and acid insoluble lignin contents of Arabidopsis *gxmt1-1* mutant and WT samples, both before and after pretreatment, were determined in triplicate according to the National Renewable Energy Laboratory (NREL), Golden, CO LAP "Determination of Structural Carbohydrates and Lignin in Biomass" (21). Sugar concentrations were measured with a Waters Alliance e2695 HPLC outfitted with a 2414 refractive index (RI) detector (Waters Corporation, Milford, MA) and a BioRad Aminex HPX-87H column (Bio-Rad Life Science, Hercules, CA). The same HPLC method was applied to quantify sugar concentrations in liquid samples for all analyses.

6.3.4 Pretreatment liquid hydrolyzate analysis

The total sugar released in liquid hydrolyzate samples collected during flowthrough pretreatment was determined in triplicate using the 4 wt% sulfuric acid post hydrolysis method (22) but scaled down by a factor of 20 (23, 24). The soluble lignin in each hydrolyzate sample was determined by UV absorbance on a SpectraMax M5e UV-

Vis spectrophotometer (Molecular Devices, Sunnyvale, CA) at 200 nm. Prior to UV measurement, the hydrolyzates were centrifuged at 12000 rpm in 2 mL microcentrifuge filter tubes (Cat No. 24137, Grace, Deerfield, IL) for 5 min.

For structural characterizations, liquid hydrolyzate samples collected at different time intervals were first freeze dried overnight in an automatic FreeZone 4.5 Liter Console Freeze Dry System (Labconco, Kansas City, MS). The freeze dried samples (~1 to 2 mg) were dissolved in D2O (0.25 mL, 99.9%; Cambridge Isotope Laboratories, Andover, MA). ^{1}H NMR spectra were recorded at 298°K with a Varian Inova-NMR spectrometer (Agilent Technologies, Santa Clara, CA) operated at 600 MHz for ^{1}H and equipped with a 5-mm NMR cold probe.

6.3.5 Enzymatic hydrolysis

Enzymatic hydrolysis of pretreated Arabidopsis samples was performed according to NREL standard procedures (25), i.e., 1 wt% glucan loading in a 0.05 M sodium citrate buffer (pH 4.8) with 0.2 g/L sodium azide at 50°C and 200 rpm. All hydrolysis experiments were run in triplicate in 25 ml Erlenmeyer flasks with 15 ml total volume in a temperature controlled incubation shaker (Multitron Infors-HT, ATR Biotech, Laurel, MD). Accellerase® 1500 cellulase (Lot No.4901131618, BCA protein content 86 mg/ml) and Accellerase® XY xylanase (Lot No.1681198062, BCA protein content 51 mg/ml) were from DuPont™ Genencor® Science (Palo Alto, CA). A total protein loading of 15 mg per g of glucan plus xylan in the pretreated solids was applied at a cellulase to xylanase 3:1 protein mass ratio. For comparison purposes, 72 hour enzymatic hydrolysis

was also performed on the untreated Arabidopsis *gxmt1-1* mutant and WT, however, at a much higher protein loading of 150 mg per g of glucan plus xylan in raw biomass with a cellulase to xylanase protein mass ratio of 3:1. To analyze sugar release, about 500 µL of the mixture that was undergoing enzymatic hydrolysis was withdrawn into 1.5 ml microcentrifuge tubes at the time points noted in the results and centrifuged at 14,600 rpm for 3.0 min. The solids free liquid supernatants were then pipetted into 500 µL HPLC vials and analyzed on HPLC as previously described. Sugar yields are defined as the amount of sugar released compared to the maximum available sugar in the biomass material being enzymatically digested.

6.4 Results and discussion

6.4.1 Characterization of Arabidopsis solid samples

To characterize compositional differences between the Arabidopsis *gxmt1-1* mutant and the WT both before and during pretreatment, the glucan, xylan+galactan, and acid insoluble lignin (Klason lignin) contents were determined by wet chemistry analysis. As shown in Table 1, the carbohydrate and K-lignin contents in *gxmt1-1* alcohol insoluble residues were almost identical to those of WT, demonstrating that the genetic modification for less methylation substitution in GX side chains did not affect synthesis of other polysaccharides in Arabidopsis cell walls. However, increased methylation of lignin was observed, as shown elsewhere (16). The compositions of Arabidopsis residues after hydrothermal flowthrough pretreatment were compared to those for untreated materials, as also shown in Table 6.1. Applying hydrothermal flowthrough pretreatment

to both Arabidopsis samples revealed that the total amount of solids removed was higher for the gxmt1-1 mutant than WT, as were glucan (~3.9%), xylan + galactan (~5.0%), and K-lignin (~10.4%). The results clearly indicated that the reduced methylation on glucuronoxylan side-chains enhanced hemicellulose and lignin removal during hydrothermal flowthrough pretreatment at conditions often applied to other biomass types (11, 26, 27).

Table 6.1. Chemical compositions of untreated and pretreated Arabidopsis samples resulting from hydrothermal (water-only) flowthrough pretreatment at 180°C at a flow rate of 15 ml/min for 10 min, and component removal by pretreatment (wt %).

	Before pretreatment			After pretreatment			Percentage removal		
	G	X + Gal	KL	G	X + Gal	KL	G	X + Gal	KL
gxmt1-1	30.1	13.5	13.5	56.2	7.1	16.1	6.5	73.7	40.3
WT	32.9	14.7	13.9	58.4	8.4	17.8	2.6	68.7	29.9

Data reported are the mean values of three replicates.
G-glucan; X-xylan; Gal-galactan; KL-K-lignin.
WT- wild type; gxmtl-1 mutant with reduced methylation on glucuronoxylan side-chains.

6.4.2 Characterization of pretreatment liquid hydrolyzates

To further compare differences in hemicellulose and lignin removal between the *gxmt1-1* mutant and the WT, hydrolyzates collected from different time intervals during flowthrough pretreatment were analyzed. Figure 6.1 shows the cumulative xylan + galactan released with pretreatment time, as well as the xylan + galactan release during each time interval. Overall, more xylan + galactan were removed from the cell wall of the Arabidopsis *gxmt1-1* mutant during pretreatment than from the WT. This trend was more noticeable in samples collected in the 0-2 min and 2-4 min intervals, indicating

hemicellulose in *gxmt1-1* with reduced methylation was more easily hydrolyzed at milder conditions.

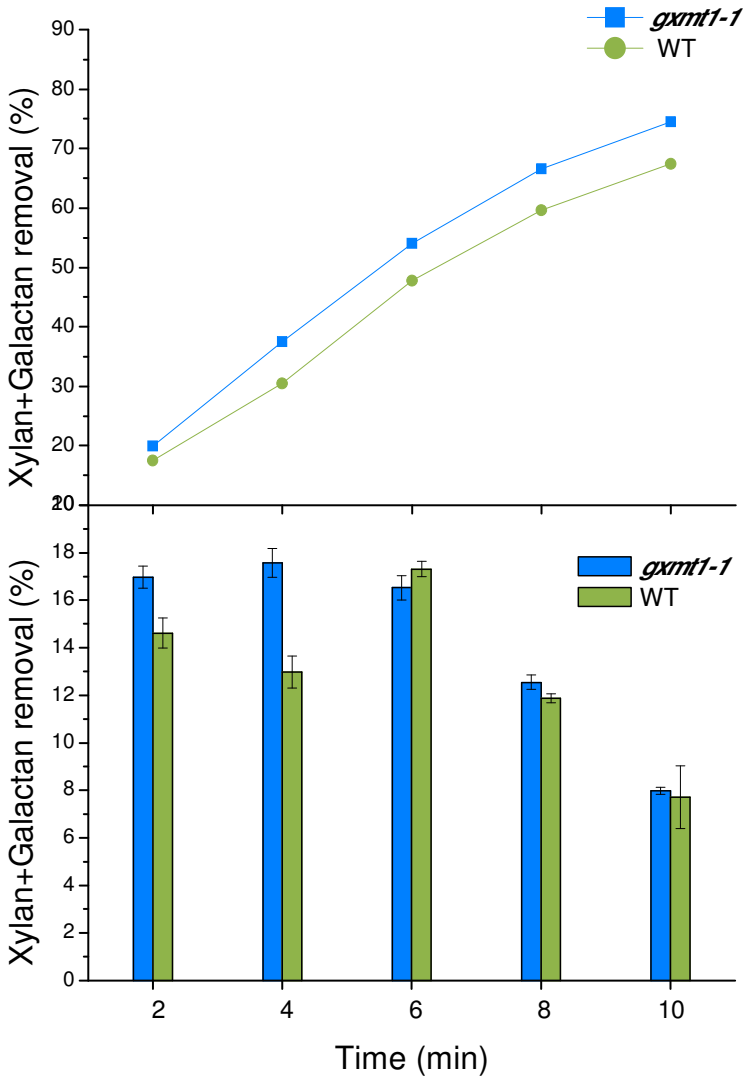

Figure 6.1. Cumulative and incremental xylan plus galactan removal in the liquid hydrolyzate during hydrothermal flowthrough pretreatment at 180°C and 15 ml/min. (a) Cumulative xylan + galactan removal up to each pretreatment time; (b) xylan + galactan removal during each 2 min time interval.

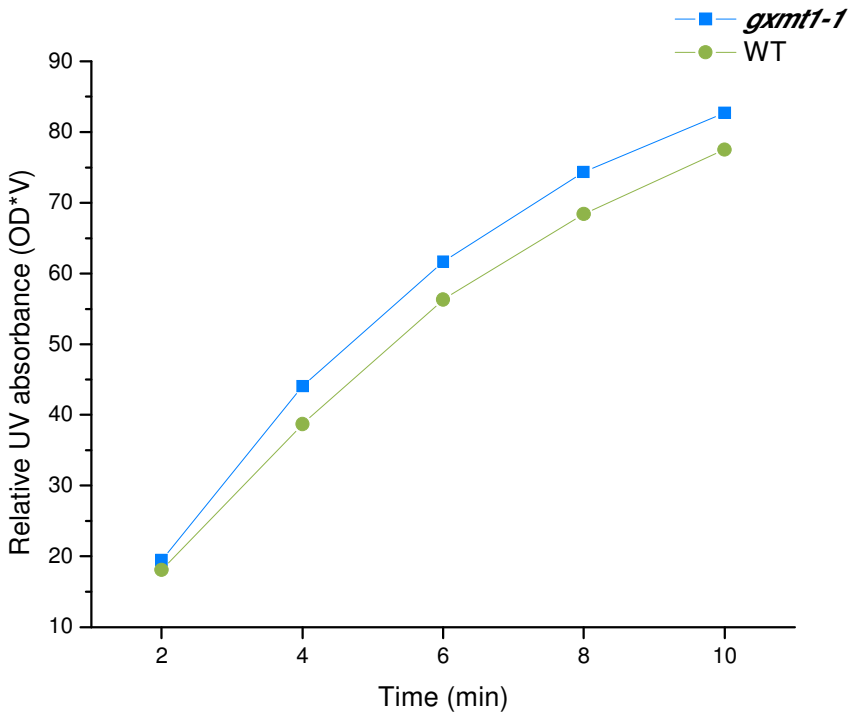

Figure 6.2. Relative UV absorbance (200 nm) of liquid hydrolyzates collected from hydrothermal pretreatment of *gxmt1-1* mutant and wide type (WT) in the flowthrough reactor as a measure of solubilized lignin

The amount of lignin solubilized into the liquid hydrolyzate fraction was estimated by UV absorbance, with the results shown in Figure 6.2. The relative absorbance was calculated as the product of the UV absorbance value and the volume of the hydrolyzate collected during each pretreatment time interval, due to the lack of an absorptivity value at lambda max wavelength (21). Consistent with the lignin removal calculated for the solid residues before and after pretreatment, the results confirmed that the *gxmt1-1* mutant released more lignin than WT. It was reported that the ratio of syringyl lignin (two methyl groups per unit) to guaiacyl lignin (one methyl groups per unit) in pretreated poplar wood was lower than that of untreated material, suggesting

syringyl lignin was more prone to be cleaved than G lignin (28). This observation partially supports the results shown in Figure 6.2, in that about a 20% increase in the overall extent of lignin methylation was found for the *gxmt1-1* mutant, suggesting a greater syringyl lignin content than WT (16). Although the primary mechanism (reduced methylation in GX or increased methylation in lignin) responsible for enhanced lignin removal from the *gxmt1-1* mutant is unclear, these results strongly indicate important interactions between lignin and hemicellulose in both cell wall synthesis and deconstruction during pretreatment.

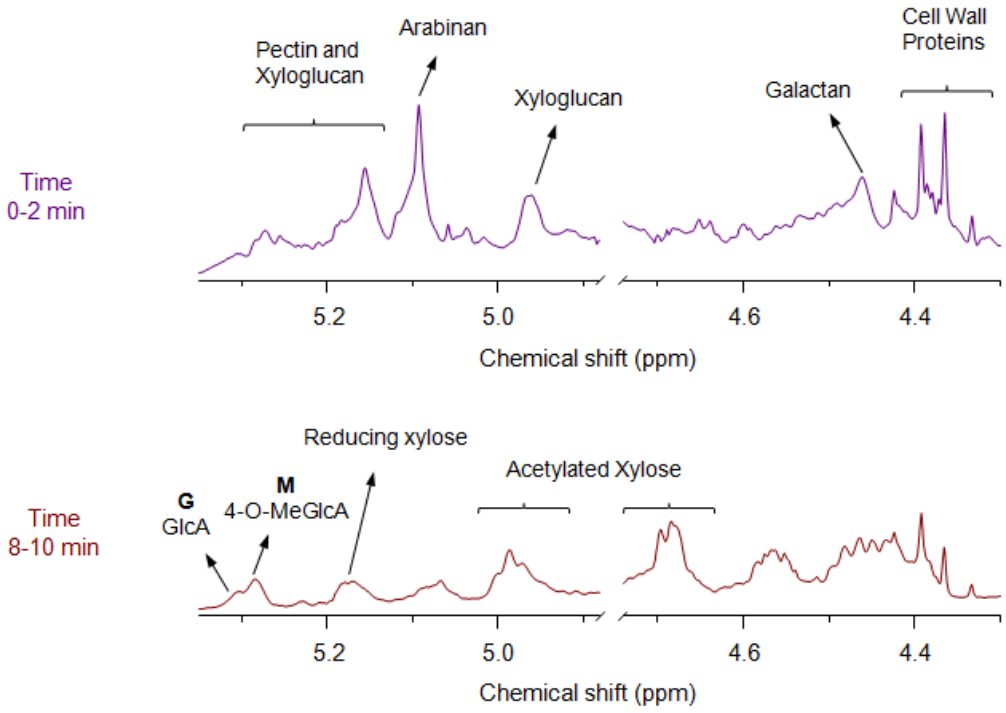

Figure 6.3. ^{1}H NMR spectrum for identification of major components in liquid hydrolyzates collected from hydrothermal flowthrough pretreatment of wild type (WT) Arabidopsis. The top figure is for the liquid sample collected during the time 0 to 2 min interval and the lower figure is for the liquid sample collected in the interval between 8 to 10 min.

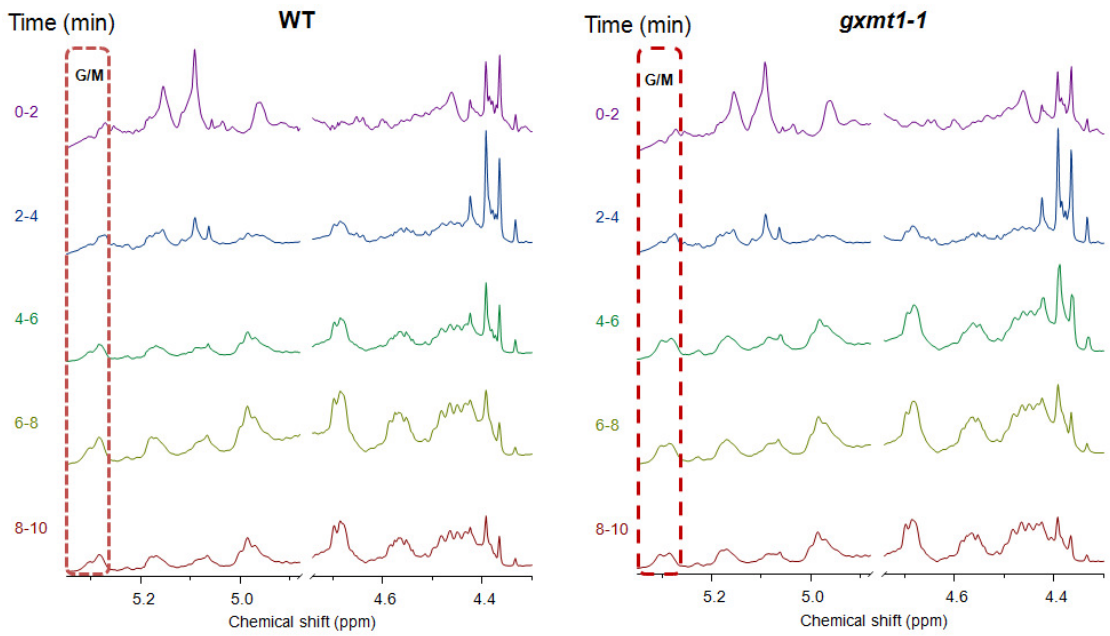

Figure 6.4. ^{1}H NMR spectrum for polysaccharide release patterns in the liquid hydrolyzates produced by hydrothermal flowthrough pretreatment (180°C-15 ml/ min flow rate) of Arabidopsis *gxmt1-1* mutant (right) and wild type (WT; left) samples.

To investigate the structural characteristics of the non-cellulosic cell wall components released during flowthrough pretreatment, the liquid hydrolyzate samples were freeze dried for ^{1}H NMR characterizations. Figure 6.3 displays the major structures identified in this way for the materials solubilized from pretreatment of the WT during early (0-2 min) and late (8-10 min) stages. The results show that xyloglucan, arabinan, galactan, pectin, and cell wall proteins were the first polymers released during pretreatment but that acetylated 4-O-methyl glucuronoxylan became the dominant component in the solubilized hydrolyzate in the later stage. In particular, the signal representing 4-O-MeGlcA was much stronger than that for GlcA, confirming that the GX in the WT was highly methylated. Based on this result, the whole profile ^{1}H NMR spectrum of hydrolyzate fractions from each time interval were compared between the

gxmt1-1 mutant and WT, as shown in Figure 6.4. Overall, similar patterns of polysaccharide solubilization were observed during pretreatment of *gxmt1-1* and WT. However, no significant signal corresponding to methyl groups (5.28 ppm) was observed for the *gxmt1-1* mutant, especially in the latter three fractions compared to WT.

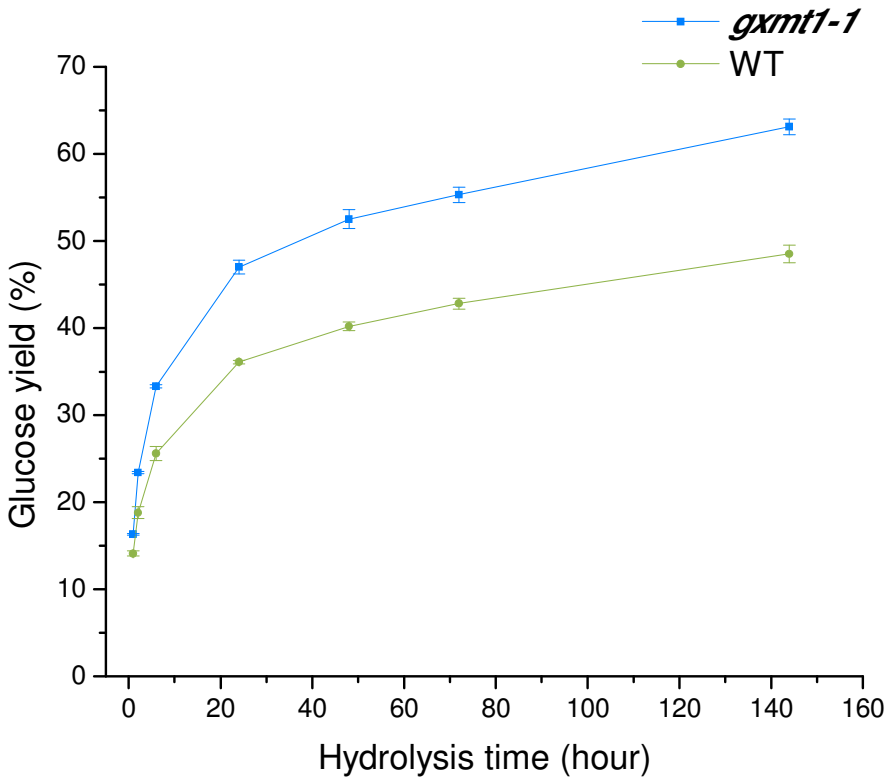

Figure 6.5. Glucose yields vs. time (h) during enzymatic hydrolysis of hydrothermal pretreated (180°C- 15 ml/min for 10 min) Arabidopsis *gxmt1-1* mutant and wild type (WT) samples at a total protein loading of 11.25 mg cellulase + 3.75 mg xylanase / g structural carbohydrates in pretreated materials. Error bars represent standard deviation of three replicates. Enzymatic hydrolysis was performed with 1wt% glucan loading at 50°C, 150 rpm.

6.4.3 Enzymatic hydrolysis

The solids resulting from pretreatment of gxmt1-1 mutant and WT were subjected to enzymatic hydrolysis at relatively low protein loadings of 12.25 mg cellulase + 3.75 mg xylanase per g of structural carbohydrates in pretreated biomass. Sugar concentrations were determined for samples collected at times of 1, 2, 6, 24, 48, 72, and 144 h by HPLC. As shown in Figure 6.5, the pretreated *gxmt1-1* mutant released significantly more glucose than the WT, with about a 25% increase at 144 h. Similarly, results displayed in Figure 6.6 also showed higher xylose + galactose yield for *gxmt1-1* mutant than WT. Such results indicated that the pretreated *gxmt1-1* biomass was more digestible than pretreated WT. To further confirm the effects of reduced methylation on biomass digestibility, untreated Arabidopsis samples were enzymatically hydrolyzed, with the results shown in Figure 6.7. In this case, a relatively high protein loading of 112.5 mg cellulase + 37.5 mg xylanase per g of structural carbohydrates in raw biomass was applied to compare differences in the maximum sugar release potential. For untreated materials, the sugar yields from 72 h enzymatic hydrolysis were comparable for both the mutant and WT and much lower than from pretreated solids despite about a 10 times higher enzyme loading. The *gxmt1-1* mutant showed only 2.2% and 1.9% higher glucose and xylose + galactose yields, respectively, than the WT. These enzymatic hydrolysis results revealed that reduced methylation in the GX side chains had little effect on biomass digestibility of untreated materials but greatly facilitated removal of hemicellulose and lignin and enhanced enzymatic hydrolysis of the pretreated material.

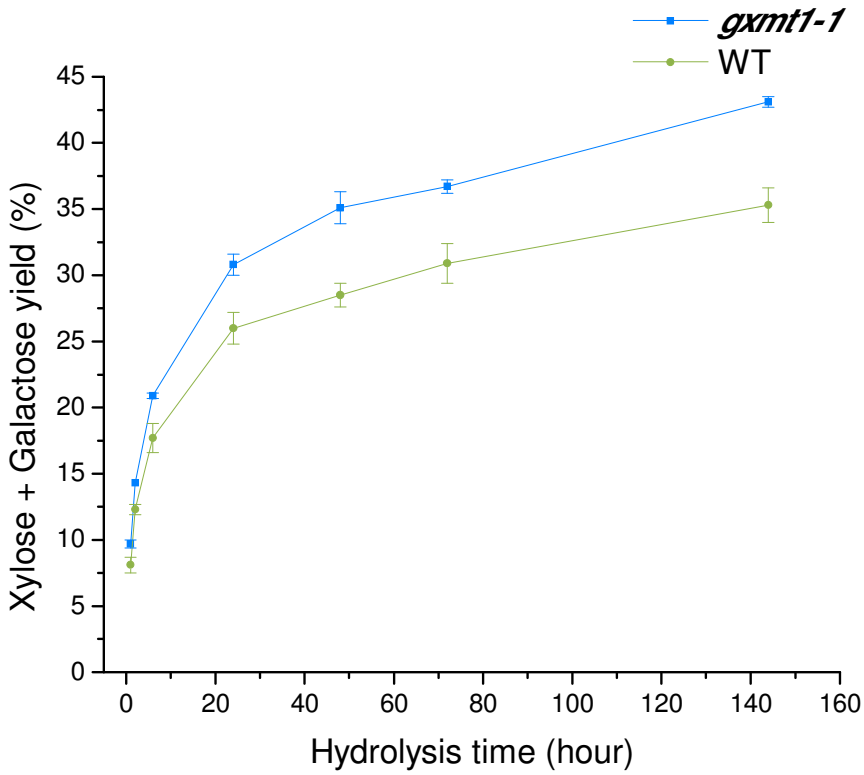

Figure 6.6. Xylose + galactose yields vs. time (h) from enzymatic hydrolysis of hydrothermally pretreated (180C- 15 ml/min for 10 min) Arabidopsis *gxmt1-1* mutant and wild type (WT) samples performed at a total protein loading of 11.25 mg cellulase + 3.75 mg xylanase / g structural carbohydrates in pretreated materials.. Error bars represent the standard deviation of three replicates. Enzymatic hydrolysis was performed with 1wt% glucan loading at 50°C, 150 rpm.

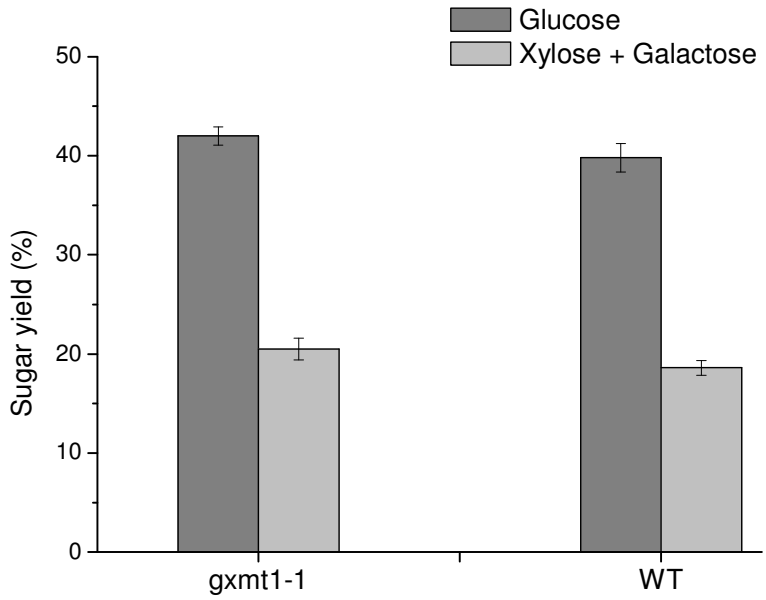

Figure 6.7. Sugar yields from 72 h enzymatic hydrolysis of Arabidopsis *gxmt1-1* mutant and wild type (WT) raw samples for a total protein loading of 112.5 mg cellulase + 37.5 mg xylanase / g structural carbohydrates in untreated materials. Error bars represent standard deviation of three replicates. Enzymatic hydrolysis was performed with 1wt% glucan loading at 50°C, 150 rpm.

6.5 Conclusions

Reduced methylation in the 4-*O*-methyl glucuronoxylan side chains of Arabidopsis enhanced the extent and amount of hemicellulose and lignin removed during hydrothermal pretreatment in flowthrough reactors. NMR characterization showed no significant structural differences in cell wall components solublized in each hydrolyzate fraction between *gxmt1-1* and WT, with exception of the reduced degree of methylation of the *gxmt1-1* mutant. Although reduced methylation did not result in improved digestibility for untreated biomass, enzymatic hydrolysis sugar yields data for pretreated

solids indicated that Arabidopsis cell walls with reduced methylation were disrupted more than WT when pretreated at the same conditions. These results help us better understand the effects of hemicellulose structure on interactions of hemicellulose and lignin, and paths to overcome biomass recalcitrance to cell wall deconstruction.

6.6 Acknowledgements

This research was funded by the BioEnergy Science Center (BESC), a U.S. Department of Energy Bioenergy Research Center supported by the Office of Biological and Environmental Research in the DOE Office of Science. Gratitude is also extended to the Ford Motor Company for funding the Chair in Environmental Engineering at the Center for Environmental Research and Technology of the Bourns College of Engineering at UCR that augments support for many projects such as this.

6.7 References

1. Lynd LR, Cushman JH, Nichols RJ, Wyman CE. Fuel ethanol from cellulosic biomass. Science. 1991 Mar 15;251(4999):1318-23.
2. Wyman CE. Ethanol from lignocellulosic biomass - technology, economics, and opportunities. Bioresource Technol. 1994;50(1):3-16.
3. Ragauskas AJ, Williams CK, Davison BH, Britovsek G, Cairney J, Eckert CA, et al. The path forward for biofuels and biomaterials. Science. 2006 Jan 27;311(5760):484-9.
4. Lynd LR, Cruz CHD. Make way for ethanol. Science. 2010 Nov 26;330(6008):1176-.
5. Abramson M, Shoseyov O, Shani Z. Plant cell wall reconstruction toward improved lignocellulosic production and processability. Plant Sci. 2010 Feb;178(2):61-72.
6. Studer MH, DeMartini JD, Davis MF, Sykes RW, Davison B, Keller M, et al. Lignin content in natural Populus variants affects sugar release. P Natl Acad Sci USA. 2011 Apr 12;108(15):6300-5.
7. Lee CH, Teng Q, Huang WL, Zhong RQ, Ye ZH. Down-regulation of pogt47c expression in poplar results in a reduced glucuronoxylan content and an increased wood digestibility by cellulase. Plant Cell Physiol. 2009 Jun;50(6):1075-89.

8. Grabber JH. How do lignin composition, structure, and cross-linking affect degradability? A review of cell wall model studies. Crop Sci. 2005 May-Jun;45(3):820-31.
9. Chen F, Dixon RA. Lignin modification improves fermentable sugar yields for biofuel production. Nat Biotechnol. 2007 Jul;25(7):759-61.
10. Davison BH, Drescher SR, Tuskan GA, Davis MF, Nghiem NP. Variation of S/G ratio and lignin content in a Populus family influences the release of xylose by dilute acid hydrolysis. Appl Biochem Biotech. 2006 Mar;130(1-3):427-35.
11. DeMartini JD, Pattathil S, Avci U, Szekalski K, Mazumder K, Hahn MG, et al. Application of monoclonal antibodies to investigate plant cell wall deconstruction for biofuels production. Energy & Environmental Science. 2011 Oct;4(10):4332-9.
12. Chundawat SPS, Beckham GT, Himmel ME, Dale BE. Deconstruction of lignocellulosic biomass to fuels and chemicals. Annu Rev Chem Biomol. 2011;2:121-45.
13. Chundawat SPS, Donohoe BS, Sousa LD, Elder T, Agarwal UP, Lu FC, et al. Multi-scale visualization and characterization of lignocellulosic plant cell wall deconstruction during thermochemical pretreatment. Energy & Environmental Science. 2011 Mar;4(3):973-84.
14. York WS, O'Neill MA. Biochemical control of xylan biosynthesis - which end is up? Curr Opin Plant Biol. 2008 Jun;11(3):258-65.
15. Albersheim P, Darvill A, Roberts K, Sederoff R, Staehelin A. Plant cell walls : from chemistry to biology. New York, NY: Garland Science; 2010.
16. Urbanowicz BR, Pena MJ, Ratnaparkhe S, Avci U, Backe J, Steet HF, et al. 4-O-methylation of glucuronic acid in Arabidopsis glucuronoxylan is catalyzed by a domain of unknown function family 579 protein. P Natl Acad Sci USA. 2012 Aug 28;109(35):14253-8.
17. Liu CG, Wyman CE. The effect of flow rate of compressed hot water on xylan, lignin, and total mass removal from corn stover. Ind Eng Chem Res. 2003 Oct 15;42(21):5409-16.
18. Liu CG, Wyman CE. Partial flow of compressed-hot water through corn stover to enhance hemicellulose sugar recovery and enzymatic digestibility of cellulose. Bioresource Technol. 2005 Dec;96(18):1978-85.
19. McKenzie HL. Tracking hemicellulose and lignin deconstruction during hydrothermal pretreatment of biomass. Riverside: University of California, Riverside; 2012.
20. Yang B, Wyman CE. Effect of xylan and lignin removal by batch and flowthrough pretreatment on the enzymatic digestibility of corn stover cellulose. Biotechnol Bioeng. 2004 Apr 5;86(1):88-95.
21. Sluiter A, Hames B, Ruiz R, Scarlata C, Sluiter J, Templeton D, et al. Determination of structural carbohydrates and lignin in biomass. Golden, CO, USA: National Renewable Energy Laboratory2008.
22. Sluiter A, Hames B, Ruiz R, Scarlata C, Sluiter J, Templeton D. Determination of sugars, byproducts, and degradation products in liquid fraction process samples. Golden, CO, USA: National Renewable Energy Laboratory2006.

23. DeMartini JD, Studer MH, Wyman CE. Small-scale and automatable high-throughput compositional analysis of biomass. Biotechnol Bioeng. 2011 Feb;108(2):306-12.
24. Li H, Foston MB, Kumar R, Samuel R, Gao X, Hu F, et al. Chemical composition and characterization of cellulose for Agave as a fast-growing, drought-tolerant biofuels feedstock. RSC Advances. 2012;2(11):4951-8.
25. Selig M, Weiss N, Ji Y. Enzymatic Saccharification of lignocellulosic biomass. Golden, CO, USA: National Renewable Energy Laboratory2008.
26. Kumar R, Mago G, Balan V, Wyman CE. Physical and chemical characterizations of corn stover and poplar solids resulting from leading pretreatment technologies. Bioresource Technol. 2009 Sep;100(17):3948-62.
27. DeMartini JD, Wyman CE. Composition and hydrothermal pretreatment and enzymatic saccharification performance of grasses and legumes from a mixed-species prairie. Biotechnol Biofuels. 2011 Nov 15;4.
28. Cao S, Pu Y, Studer M, Wyman C, Ragauskas AJ. Chemical transformations of *Populus trichocarpa* during dilute acid pretreatment. RSC Advances. 2012.

Chapter 7

Chemical Composition and Characterization of Cellulose for Agave as a Fast Growing, Drought Tolerant Biofuels Feedstock*

*This whole chapter has been published under the following citation:
Li H, Foston MB, Kumar R, Samuel R, Gao X, Hu F, Ragauskas AJ, Wyman CE. "Chemical composition and characterization of cellulose for Agave as a fast growing, drought tolerant biofuels feedstock", *RSC Advances* 2012; 2(11): 4951-4958.

7.1 Abstract

A major issue raised about development of cellulosic biomass derived fuels technologies is the concern about possible competition for land with agricultural crops and impacts on food and feed supply. However, because agave offers high productivity with low water and nutrient demands, it can thrive on semiarid lands not suitable for conventional agriculture, making it a promising lignocellulosic feedstock for biofuels production. Because agave composition will establish the maximum potential fuel yield that is vital to low cost conversion, detailed chemical composition data and cellulose characteristics were measured by standard biomass analysis procedures and solid-state NMR methods, respectively, for four agave samples: A. *americana* leaves, A. *salmiana* leaves, A. *tequilana* leaves, and A. *americana* heart. For the first time, we report substrate characteristics relevant to biochemical conversion for the tested agave species, specifically cell wall compositional data along with the relative proportions of cellulose ultra-structural components. The experimental results also provide an important baseline for further characterization and conversion of different agave species as biofuels feedstocks for semi-arid lands.

7.2 Introduction

Agave, which is well known for tequila production in Mexico, has recently emerged as a potentially attractive lignocellulosic feedstock for conversion to biofuels and chemicals (1). One reason for this new interest is that agave species have high water use efficiency and drought resistance (2). Consequently, agaves can be grown on arid and semi-arid lands not suitable for other lignocellulosic feedstocks, such as poplar, switchgrass, miscanthus, and sugarcane. In addition, although agave species are native to the American continent, they have worldwide potential for production, with agave now grown in semi-arid regions in such diverse locations as Brazil, Australia, Southern and Eastern Africa, and areas across the Mediterranean (3-5). Another vital attribute is the high estimated average annual productivities for agave species of 10-34 Mg ha^{-1} $year^{-1}$(1, 6) compared to about 15 Mg ha^{-1} $year^{-1}$ for switchgrass (7) and 11 Mg ha^{-1} $year^{-1}$ for poplar wood (8, 9). Furthermore, with appropriate cultivation, productivities could be as high as 40 Mg ha^{-1} $year^{-1}$ for A. *salmiana* and A. *mapisaga* (10), although lower values will no doubt result with lower water use. Beyond these features, agave offers such environmental attributes as preventing desertification of dry lands (11, 12) and removing heavy metals from water around mines (4, 13). Such important features as these make agave promising as a means to extend the range of biofuels production to complement that possible with grasses such as switchgrass and woods such as poplar.

Because mass yields from lignocellulosic biomass dominate conversion costs for fuels and any other commodity products, accurate measurements of the chemical composition of biomass are critical to provide a perspective on the maximum fuel yields

and ultimate economic merits. In the case of biological conversion to biofuels or chemicals, cellulose and hemicellulose should comprise a substantial portion of the total dry matter. This information is also essential to assessing how effective pretreatment and enzymatic hydrolysis operations are in deconstructing cellulosic biomass to sugars that can be fermented to fuels (14) or further reacted to furfural, levulinic acid, and other reactive intermediates that may lend themselves to catalytic operations that have recently gained interest for making drop-in fuels (15). In the case of agave, one of the earlier compositional studies applied a multi-step acid hydrolysis method (16) to determine that A. *lechuguilla* contained 20.7% cellulose, 11.3% hemicellulose, and 12.2 % lignin on a dry basis (17). These low values would suggest that agave would suffer from low yields of sugars and any products that could be derived from them. However, several more recent studies from diverse fields reported composition results for a few agave species, as summarized in Table 7.1, that are much more in line with making agave attractive as a biofuels feedstock (3, 18-25). Unfortunately, these results were based on "fiber" or "bagasse" materials prepared by various extraction/isolation procedures that change the chemical composition of the biomass tested, and the corresponding data may not represent the carbohydrate content of raw agave materials. In addition, the analytical methods applied in the literature to determine cellulose and hemicellulose amounts also varied considerably, making it challenging to meaningfully compare compositions of different agave species. Thus, application of consistent and accurate analytical methods was needed to obtain comparable composition information that would support identification of agave species with the best potential for biofuels production and help

select cultivation strategies appropriate to the most promising species. The types of carbohydrates in agave hemicellulose and ultra-structural information about agave cellulose are also important to better understand recalcitrance features of agave and achieve economic agave conversion. Such information, unfortunately, has not been available in previous literature.

Table 7.1. Composition of different agave species and anatomical fractions reported in the literature (wt %)

Species	Anatomical fraction	Cellulose	Hemicellulose	Lignin	Reference
A. *americana*	leaf fiber	68.4	15.7	4.9	Mylasmy & Rajendran, 2010
A. *salmiana*	bagasse	47.3	12.8	10.1	Garcia-Reyes & Rangel-Mendez, 2009
A. *tequilana*	bagasse	43	19	15	Cedeno-Cruz & Alvares-Jacobs, 1999
A. *lechuguilla*	leaf fiber	79.8	3-6	15.3	Vieira et al., 2002
	leaf fiber	46-48	30	11	Marquez et al., 1996
A. *fourcroudes*	leaf fiber	77.6	5-7	13.1	Vieira et al., 2002
A. *sisalana*	-	43	32	15	McDougall et al., 1993

In this study, a series of laboratory analytical procedures (LAPs) for standard biomass analysis defined by the National Renewable Energy Laboratory (NREL) were applied to determine the chemical compositions of the four agave samples. The measured compositions included extractives, water soluble carbohydrates (WSC), structural carbohydrates, acid-insoluble lignin, crude protein, and ash for agave bagasse, as well as the composition of agave juice. In addition, ^{13}C cross-polarization magic angle spinning (CP/MAS) nuclear magnetic resonance (NMR) was employed to determine the ultra-structural features of cellulose extracted from four agave bagasse samples, including

cellulose I_α and I_β, *para*-crystalline cellulose, cellulose associated with accessible and inaccessible fibril surfaces, and the average lateral dimensions of fibril and fibril aggregates. By characterizing such ^{13}C CP/MAS results for isolated agave cellulose, we were able to compare such ultra-structural features of agave to other types of lignocellulosic biomass for the first time. These results should help better understand the potential of agave as a biofuels feedstock suitable for production on semi-arid lands.

7.3 Materials and methods

7.3.1 Chemicals

The following sugars were purchased from Sigma-Aldrich (St. Louis, MO) to serve as standards for determining carbohydrate profiles of agave samples: glucose (Lot No. 089K00601, Sigma), fructose (Lot No. 1253079, Fluka), sucrose (Lot No.1231832, Fluka), and inulin from dahlia tubers (Lot No. 1212695, Fluka). Xylose (Lot No. A0295756, Acros), galactose (Lot No. A0244833, Acros), and arabinose (Lot No.10162224, Alfa Aesar) were purchased from Fisher Scientific (Pittsburgh, PA). Other reagents and chemicals used were of analytical grade and were purchased from Sigma or Fisher Scientific, unless otherwise stated.

7.3.2 Plant materials preparation

Four samples from three agave species were employed for this study: A. *americana* leaves (AAL), A. *salmiana* leaves (ASL), A. *tequilana* leaves (ATL), and A. *americana* heart (AAH). All samples were freshly collected from the San Jose area

(California, USA), wrapped in preservative film, and shipped to the University of California at Riverside (UCR) directly after harvest. Upon receiving the samples, they were frozen at -18℃ to avoid sugar degradation.

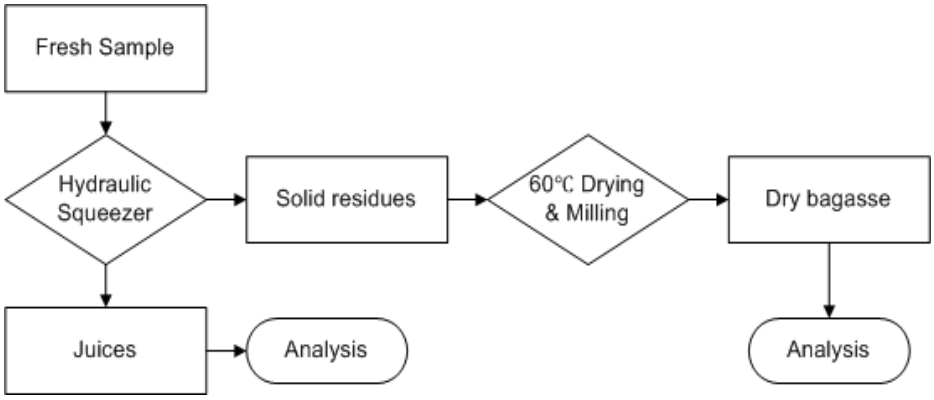

Figure 7.1. Flowchart of major processing steps for preparation of agave samples for analysis.

Figure 7.1 provides a flowchart of the major steps applied to prepare samples for analysis after their arrival at UCR. Agave samples were first thawed at room temperature and cut into small chips using a knife. The juices were then squeezed from the material by placing it in a 9.5 inch long by 3.5 inch diameter metal pipe followed by forcing a tight fitting metal cylinder into the pipe with a hydraulic press (Model No. 14590, Northern Tool + Equipment, Burnsville, MN). The juices were kept in 50 ml polypropylene centrifuge tubes at -18℃ for further analysis. The unwashed agave bagasse solids were then dried at 60℃ in an oven (Thermo Scientific Imperial III Incubator, Fisher Scientific Pittsburgh, PA) for 18-24 hours to reduce the sample moisture to about 5%. This drying method was previously optimized for lowest free sugar degradation of agave materials. Then, a Thomas Wiley® mini mill (Model No. 3383-L20, Thomas Scientific, Swedesboro, NJ) was used to mill the dried agave bagasse through a

40-mesh (425 μm) screen to be sure all tissues were homogeneously milled for further characterization. The moisture content (MC) was measured by an automatic infrared moisture analyzer (Model No. HB43-S, Mettler-Toledo Inc., Columbus, OH).

7.3.3 Juice analysis

Free sugars and inulin contained in the agave juice were directly determined with a Waters Alliance e2695 HPLC with a 2414 refractive index (RI) detector (Waters Corporation, Milford, MA). The components were separated on a BioRad Aminex HPX-87P column (Cat No. 125-0098, Bio-Rad Life Science, Hercules, CA), and chromatograms were recorded and quantified by Empower software (Waters Corporation, Milford, MA). The same HPLC method was applied to quantify sugar concentrations in the liquid samples for all subsequent analysis. For oligomers and total sugar content, a modified NREL post hydrolysis method was used (26) in which the total reaction volume was scaled down by a factor of 20 (27). In addition, hydrolysis was performed at 121^{o}C for 1 hour in 0.5 wt% sulfuric acid instead of the 4wt% acid solution used in the NREL method. Inulin, sucrose, and fructose were used as sugar recovery standards (SRS) to quantify the corresponding fructose degradation, and average sugar recovery yields from 3 samples run in triplicate were used for subsequent calculations. In addition, concentrations of total soluble solids (TSS) in agave juices was also determined by pipetting 10 mL agave juice that had been passed through a 0.2 μm filter into pre-dried and pre-weighed aluminum weighing dishes and drying them at 60℃ for 48 hours in a conventional oven until a constant weight was reached.

7.3.4 Bagasse extractives and Water Soluble Carbohydrates (WSC) analysis

The percentages of water and ethanol extractives were determined in sequence by the Soxhlet method described in the NREL LAP "Determination of Extractives in Biomass" (28). For WSC analysis, 1 g of oven dry unwashed bagasse samples was loaded into 20 mL glass vials. Then, 16 mL of deionized (DI) water and 320 μL of 10 g/L sodium azide solution were pipetted into each vial using Eppendorf pipettes (Eppendorf, Hamburg, Germany). The final slurry contained 0.2 g/L of sodium azide to prevent the growth of organisms. The vials were then sealed and placed in an incubation shaker (Multitron Infors-HT, ATR Biotech, Laurel, MD) for 24 hours at 50℃ and 150 rpm. The amounts of free sugars and total sugar content were measured by the same methods as described in Section 7.3.3.

7.3.5 Bagasse structural carbohydrates and lignin content analysis

The percentage of structural carbohydrates and acid insoluble lignin content were measured for the extractive free agave bagasse prepared in Section 7.3.4 following the NREL LAP "Determination of Structural Carbohydrates and Lignin in Biomass" (29).

7.3.6 Crude protein and ash analysis

The crude protein content was estimated by the equation:

% Protein = % N × Nitrogen factor (NF) (30)

in which the commonly used NF of 6.25 was applied (31). About 5 mg of dry, homogenized sample was weighed into tin capsules (Cat No. 240-064-40, CE Elantech, Lakewood, NJ) and sealed. Then the nitrogen content was measured with a Flash EATM 112 N/Protein plus CHNS/O Analyzer (CE Elantech, Lakewood, NJ) with aspartic acid as a standard (CE Elantech, Lakewood, NJ). The ash content was also measured according to the NREL LAP "Determination of Ash in Biomass" (32) and employed to close mass balances.

7.3.7 Cellulose characterization by ^{13}C CP/MAS NMR

Holocellulose (cellulose + hemicellulose) samples from Agave baggasses were prepared by sodium-chlorite delignification (33). Isolated cellulose was prepared from the holocellulose samples (1.00 g) by hydrolysis for 4 h in HCl (100.0 mL of 2.5 M) at 100ºC. The isolated cellulose samples were then collected by filtration, rinsed with an excess of DI filtered water, and dried in the fume hood. The NMR samples were prepared from isolated cellulose added into 4-mm cylindrical ceramic MAS rotors. Solid-state NMR measurements were performed on a Bruker Avance-400 spectrometer operating at frequencies of 100.55 MHz for ^{13}C in a Bruker double-resonance MAS probe head at spinning speeds of 10 kHz. CP/MAS experiments utilized a 5 μs (90°) proton pulse, 1.5 ms contact pulse, 4 s recycle delay, and 4 K scans. All spectra were recorded on pre-wet samples (30-40% water content), and line-fitting analysis of spectra was performed using NUTS NMR Data Processing software (Acorn NMR Inc., Livermore, CA). Error analysis

was conducted by performing five individual isolations of NMR acquisitions and line-fit data processing on representative biomass samples to assess typical variations.

7.4 Results and discussion

7.4.1 Characterization of agave raw materials

Leaves and heart are the two main portions from an agave plant that could be utilized as biofuels feedstock. The heart, also called agave piña or head, is a pineapple-shape stem base from which the leaves grow. Fresh biomass yields are very close from leaves and heart for some species and close to 50/50 for A. *americana* (34). Generally, leaves contain more fiber resulting in a higher structural carbohydrate content while the heart is rich in non-structural carbohydrates such as inulin and other water-soluble fructose equivalents.

Table 7.2 summarizes mass distribution data of these components as determined according to the methods outlined in section 7.3.2 for the samples received. ATL contained the highest percentage of dry bagasse of the three leaf samples used in this study, and the leaf tissues of *A*. *americana* were much juicier than its heart. AAH contained twice the amount of total soluble solids (TSS) in the juice portion as in the leaf samples. In total, ATL had a higher solids yield than the other two species based on fresh mass, and AAH contributed more dry-biomass than leaves from the same plant. In addition, because agave heart juice has been reported to be weakly acidic in many papers, the pH of both leaf juices and heart juice were measured in this study. As the average of

three measurements, the pH of ATL juice was the lowest (4.58), while the juice pH values of AAL, ASL, and AAH were 5.16, 4.99, and 5.19, respectively.

Table 7.2. Mass distribution of fresh agave samples (wt %)

	Dry bagasse	Juice	TSS[a] in juice	Total solids
AAL	5.0	95.0	5.3	9.6
ASL	4.4	95.6	5.1	8.8
ATL	13.0	87.0	5.2	16.9
AAH	12.4	87.6	10.6	20.0

[a]TSS-% total soluble solids

7.4.2 Sugars in agave juice

As the nutritive storage organ of agave species, agave heart is rich in water-soluble polysaccharides/oligosaccharides, most of which are inulin and its oligomers. In fact, the heart juice is an important sugar source and has been fermented to produce alcoholic beverages for centuries (25, 35). For example, famous tequila is made from *A. tequilana* Weber, while *A. americana* and *A. salmiana* are used to make mezcal and pulque, respectively. Although making beverages has higher value, juice sugars could become an important contributor to the economic conversion of agave into biofuels if agave is grown at a large scale that would outpace beverage markets. However, detailed analysis of sugars in agave heart juice is still limited and the information on leaf juice composition is scarce. Table 3 shows the sugar composition of the four agave juice samples obtained in this study, with the concentrations of inulin, sucrose, glucose, galactose, and fructose directly measured from fresh juice samples. Fructose and glucose were the major monomeric sugar components in all samples, but AAH juice contained

significantly higher inulin and sucrose than the others. To quantify sugar oligomers, the conventional post-hydrolysis acid condition (4 wt% sulfuric acid, 121℃ for 1 hour) could not be directly applied due to the degradation of over 90% of the fructose at these conditions making any sugar recover standard inaccurate for calculating fructose equivalents (36). Thus, various hydrolytic conditions with acid loadings of 0.1 wt% to 2 wt% were applied, as described in section 7.3.3, to completely convert inulin, sucrose and oligomers into monomeric sugars while minimizing fructose degradation. With the modified method, the average fructose equivalent degradation was about 29 %, and was applied to correct for corresponding fructose losses. Glucose, however, was very stable at this condition, with negligible degradation. The percent of oligomers associated with glucose and fructose were calculated by Equation 7.1, assuming there was one glucose residue for every 80 fructose residues in inulin molecules (37). The corresponding results in Table 7.3 show that fructose residues contributed 77.8% to 84.6% of total oligomers, while glucose residues contributed about 14.5% to 17.8% of the total. More than half of the total sugars in AAH juice were oligomers, while monomeric sugars made a major fraction of leaf juices.

$$\%=\frac{C_{\text{after post hydrolysis}}-C_{\text{before post hydrolysis}}-C_{\text{derived from inulin}}-C_{\text{derived from sucrose}}}{C_{\text{oligomers}}} \qquad \text{Equation 7.1}$$

Table 7.3. Sugar composition of agave juices (g/L)

	Inulin	Sucrose	Glucose	Galactose	Fructose	Sugar oligomers	Total
AAL	1.4	1.5	12.7	0.3	6.8	4.2 ± 0.1[a] (*15.4*, 84.6)[b]	26.9
ASL	1.4	0.5	9.1	0.1	8.8	4.6 ± 0.1 (*14.5*, 85.5)[b]	24.5
ATL	1.4	1.3	10.0	0.7	7.3	9.3 ± 0.1 (*15.7*, 80.6)[b]	29.9
AAH	8.4	11.7	7.7	0.6	8.0	44.2 ± 0.4 (*17.8*, 77.8)[b]	80.6

a: Values represent the standard deviation of three replicates.

b: The first values in parenthesis represent the percentage of oligomers associated with glucose; the second values in parenthesis represent the percentage of oligomers associated with fructose.

7.4.3 Composition of agave bagasse

It has been shown that the carbohydrate composition from the same agave species varied according to cultivation regions and climates (3), plant ages, and even the age of leaves when sampled (34). For example, for the same *A. americana* plant, older leaves (12 years old) were found to have about 8% higher cellulose content than younger leaves (4 years old) (34). In this study, the source plants were cultivated in the same area and were all between 4 and 5 years old. To eliminate the effects of leaf age, only the biggest leaves which assumingly were also 4 to 5 years old were collected. The corresponding mass balance of agave bagasse composition is shown in the Table 7.4.

All four agave samples were successively extracted with water and then by ethanol. The water extractives amount shown in the Table 7.4 was calculated by subtracting the amount of WSC, determined by the procedures described in section 7.3.4, from the total water extractive determined by the NREL procedure. In general, the extractives patterns for three leaf bagasse samples were similar, with from 12.6% to 14.2% for water extractives, 1.9% to 3.2% for ethanol extractives, and 4.4% to 7.9% for WSC.

However, AAH contained about 6.6% less water extractives and 11.5% higher free sugars than AAL.

Table 7.4. Mass balance on agave bagasse dry mass composition (%)

	Water extractives[a]	Ethanol extractives[a]	WSC[a]	Structural carbohydrates[b]	K-lignin[b]	Ash[b]	Protein[a]	Total
AAL	12.6	1.9	6.5	45.0 ± 0.3	8.2 ± 0.3	7.4	3.7	85.3
ASL	15.1	2.8	7.9	42.7 ± 1.3	9.8 ± 0.7	6.1	4.9	89.4
ATL	14.2	3.2	4.4	41.7 ± 0.3	11.9 ± 1.2	6.4	5.6	87.5
AAH	6.0	1.3	17.0	39.7 ± 0.9	7.3 ± 0.9	7.2	4.5	83.0

a: Data reported are the mean values of two replicates
b: Data reported are the mean values of three replicates

The breakdown in compositions of structural carbohydrates is shown in Figure 7.2. These carbohydrate profiles of three leaf samples were very similar, containing about 30% glucan, 7% xylan, and even smaller amounts of galactan and arabinan based on the dry weight of raw materials. Davis et al. also reported that structural carbohydrate profiles were similar among species that were grown in the same region, including *A. angustifolia, A. potatorum,* and *A. cantala* (3). Both studies, however, indicated that the production region might have important effects on biomass yields and compositions. Compared to leaf bagasse, AAH had a lower glucan content (20.5%) but about twice as high galactan (8.9%). Overall, all agave bagasse samples tested in this study contained more than 50% of dry weight as carbohydrates including free sugars and structural carbohydrates, but the heart had about 55% or more total structural plus soluble sugars.

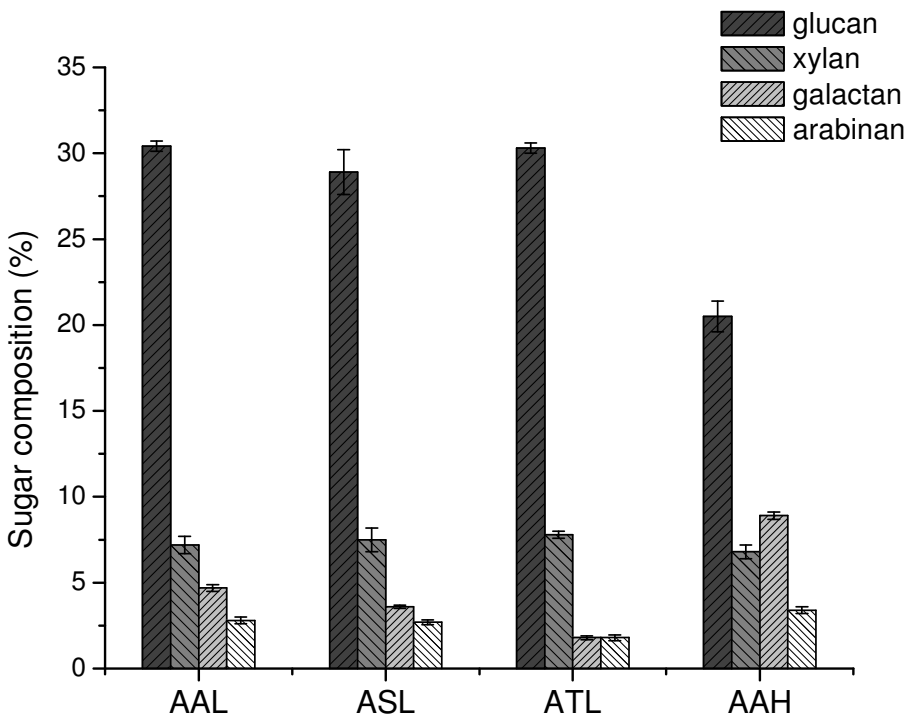

Figure 7.2. Structural carbohydrates composition of agave bagasse.

As a plant that uses the Crassulacean Acid Metabolism (CAM) pathway, agave species have been recognized as low lignin biofuels feedstocks (3). As shown in Table 7.4, the K-lignin contents of the agave bagasse tested were from 7.3% to 11.9%, significantly lower than switchgrass (18.8%) and poplar wood (23.4%) tested by the same method and shown elsewhere (38, 39). The acid insoluble lignin was not measured in this study due to the lack of reference absorptivity constants. Nonetheless, together with ash and protein contents, the mass balance was about 85 to 90% for all agave leaves tested but about 83% for the one heart sample. The remaining unaccounted for mass could be

acid soluble lignin, acetyl and other substituent groups that are often found on the xylan backbone, and pectin, none of which were determined in this study.

7.4.4 Agave cellulose characterization

A 2-peak integration method (40) was used to analyze the cellulose C_4 region resulting from the acquired ^{13}C CP/MAS NMR spectra of isolated cellulose from various agave samples for crystallinity, with , the calculated results and tabulated in Table 7.5. The crystallinity index for the agave leaves (AAL, ASL, ATL) tested in this study varied only slightly from 50 to 54% (±2%). However, the crystallinity index of AAH was significantly lower than AAL, indicating cellulose isolated from the heart contained more amorphous cellulose than its leaf regions. In Figure 7.3 (A) comparing crystallinity data for the agave in this study to values measured by the same methods for other types of cellulosic materials shows that the agave cellulose crystallinity index was similar to that of switchgrass (grass), but was lower than that for poplar (hardwood) and pine (softwood). Several studies suggest that a correlation exists between crystallinity and enzymatic digestibility (40-45), with some data demonstrating that the rate of enzymatic hydrolysis is much faster with amorphous cellulose (40). However, due to the complex interplay of multiple substrate characteristics in native biomass, there has not been a clear consensus on the effect of cellulose ultrastructure on enzymatic digestibility (46). Although recent work indicated that substrate accessibility may be among the most important rate determining factors for enzymatic hydrolysis (47-49), monitoring agave cellulose

ultrastructure should still be valuable in developing a comprehensive representation of the agave cell wall structure and its effects on recalcitrance.

Table 7.5. Non-linear least-squared spectral fit to the results of the C4 region for ^{13}C CPMAS spectra of isolated cellulose

Sample	% Cr ± 2.0	% I_α ± 3.0	% $I_{\alpha+\beta}$ ± 3.6	% Para ± 6.3	% I_β ± 3.6	% Acc ± 2.1	% Inacc ± 1.0	LFD ± 0.5 (nm)	LFAD ± 2.1 (nm)
AAL	54	2.3	7.6	37.7	6.4	6.4	39.6	4.1	34.0
ASL	50	4.6	11.1	24.8	9.5	5.5	44.5	3.8	39.4
ATL	53	5.7	8.1	32.8	6.4	5.0	42.0	4.0	43.3
AAH	46	3.8	6.5	26.0	9.6	8.9	45.1	3.4	24.1

Cr: crystallinity index; I_α: α-cellulose; I_β: β-cellulose; para: Para-crystalline cellulose; Acc: cellulose at accessible surface; Inacc: cellulose at inaccessible surface; LFD: lateral fibril dimension; LFAD: average lateral fibril aggregate dimension

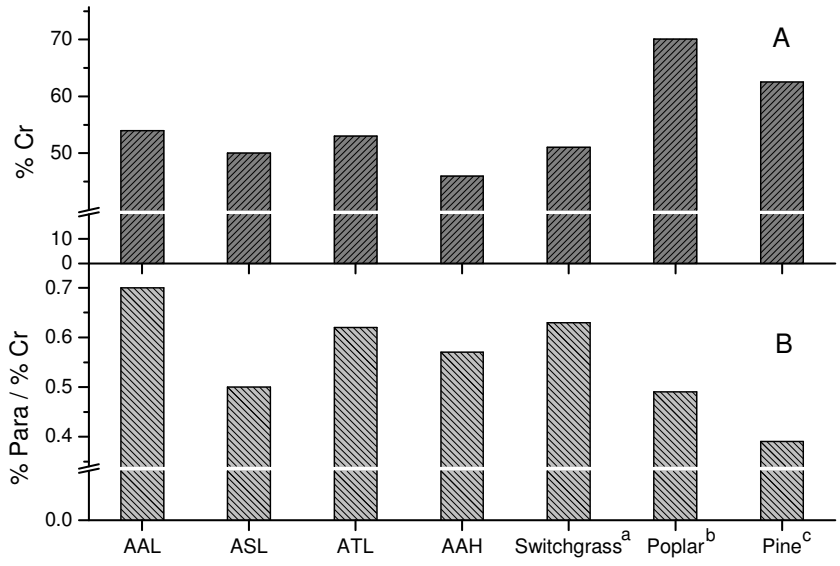

Figure 7.3. Crystalline index (A) and ratio of *para*-crystalline cellulose to crystallinity index (B). a: Alamo switchgrass leaves (50); b: Poplar (51); c: Loblolly pine (52).

A 7-peak non-linear line-fit analysis (53-55) of the cellulose C_4 region was also performed to determine the relative amounts of cellulose crystalline allomorphs and fibril surface for the agave samples employed here, as shown in Table 7.5. This approach was performed by fitting one Gaussian and three Lorentzian line-shapes to the crystalline cellulose C_4 carbon signals from δ 85–92 ppm that are attributed to domains of cellulose I_α, I_β, and *para*-crystalline cellulose (54, 55). I_α and I_β are the two natural forms of crystalline cellulose type I, and *Para*-crystalline cellulose is loosely described as a type of cellulose allomorph between amorphous and crystalline cellulose in chain order and mobility (53). In addition, the non-crystalline cellulose C_4 carbon region δ 80–95 ppm associated with accessible and inaccessible cellulose fibril surfaces was simultaneously fit to three Gaussian line-shapes (54). To further investigate the crystalline allomorphs of agave cellulose, the ratio of *para*-crystalline cellulose to crystallinity index was calculated and compared to results for switchgrass, poplar, and pine samples, as shown in Fig 7.3 (B). All agave samples showed more than a 50% ratio of *para*-crystalline cellulose to crystallinity index, similar to levels for switchgrass but higher than for poplar and pine. These high proportions of *para*-crystalline cellulose suggest that agave could show relatively higher enzymatic digestibility compared to woody materials.

Utilizing a square cross-sectional micro-fibril model, which considers amorphous cellulose as being located only on fibril surfaces, the lateral fibril dimension (LFD) and lateral fibril aggregate dimension (LFAD) can be estimated using the relative intensity of peaks attributed to total fibril surfaces and accessible fibril surfaces (56). The LFD and LFAD of agave cellulose are displayed in Table 7.5.

7.5 Implications of these results

These results reveal several important points about the potential use of agave as a biofuels feedstock. First, as shown in Table 7.6, the range of structural carbohydrate contents based on dry mass of tested raw agave materials from just 21% to 32% is low and only about 30% to at best 55 % of the structural carbohydrate content of energy crops such as switchgrass or poplar. On the other hand, including soluble sugars could increase the total potential sugar content to about 50% of dry mass in the case of agave leaves and nearly 65% for agave heart. Thus, use of soluble sugars from agave will be important to achieve reasonably high mass yields of ethanol or other products through biological or catalytic conversion technologies. However, even if the total sugar content is lower than for some promising energy crops and reduces fuel yields per ton, the sugar yield per land area could be considerably higher when the potentially high productivity of agave is factored in, as shown in Table 7.7. In addition, the low lignin content and crystalline structural features suggest that agave bagasse could be more easily deconstructed into sugars than grasses or hardwoods, and given the large cost contribution of overcoming recalcitrance for biological conversion processes (57), ease of conversion could offset the consequences of lower carbohydrate content. Thus, further research is being completed at our laboratory to determine if agave is more easily converted into sugars in pretreatment and enzymatic hydrolysis. Development of information on the relationship between agave structural features and sugar release could also prove invaluable in defining promising features in native plants or attributes to engineer into new varieties of

switchgrass, poplar, and other plants to make them more amenable to biological conversion.

Table 7.6. Mass distribution of carbohydrates in dry raw agave samples[a] (wt %)

	structural	water soluble	total
AAL	23.5	27.2	50.6
ASL	21.4	27.9	49.3
ATL	32.1	16.5	48.6
AAH	24.6	39.4	64.0

[a]Calculation combined bagasse carbohydrates and juice carbohydrates, and based on total dry weight of raw materials.

Table 7.7. Estimated theoretical maximum ethanol yield

	gallons/ dry ton[a]	gallons/ (hectare · year)[b]
A. americana	96	963-3273
Poplar	115.8	1273
Switchgrass	93.5	1403

[a]Calculation based on 0.51 pounds of ethanol/ pound of sugar and 1 gallon of ethanol/ 6.55 pounds of ethanol, according to the Theoretical Ethanol Yield Calculator of NREL.

[b]Calculation based on average productivity (dry ton ha^{-1} $year^{-1}$) of 10-34 for agave, 11 for poplar and 15 for switchgrass, as introduced in section 7.2.

7.6 Conclusions

For the first time, agave species were characterized by a series of standard biomass analysis procedures to develop detailed information on chemical compositions and cellulose ultra-structural components. The three agave leaf bagasse samples employed had similar total structural plus soluble carbohydrate contents that contributed about 50% to 55% of the mass of dry bagasse. The xylan content was low in agave species relative to grasses and hardwoods, but galactan was a more important component

in agave hemicellulose than for many other plants. Agave heart (AAH) contained lower structural carbohydrates (20.5% of glucan in bagasse) than leaves (AAL) but was rich in inulin, sucrose, and oligosaccharides that were mainly composed of fructose and glucose. Both agave leaves bagasse and heart bagasse had very low lignin contents (7.3%-11.9%). In addition, ^{13}C CP/MAS NMR spectra showed that agave cellulose had a relatively low crystallinity index (around 50%), and *para*-crystalline cellulose contributed over 50% of the total crystalline region. Further research is in progress to determine whether agave offers lower recalcitrance that can offset its lower carbohydrate content and support the use of this plant on semi-arid lands. This research can also suggest features that can be used to identify or improve other plants for conversion to fuels.

7.7 Acknowledgements

This research was funded by the BioEnergy Science Center (BESC), a U.S. Department of Energy Bioenergy Research Center supported by the Office of Biological and Environmental Research in the DOE Office of Science. The authors would especially like to thank Mr. Arturo Velez and Mr. Ramon F. Olmedo from Agave Project of Mexico for providing agave materials. We would also like to thank Professor Eugene A. Nothnagel in the Botany and Plant Science Department and Dr. Jaclyn D. DeMartini in the Chemical and Environmental Engineering Department of the University of California, Riverside for valuable discussions. Gratitude is extended to the Ford Motor Company for funding the Chair in Environmental Engineering at the Center for Environmental Research and Technology of the Bourns College of Engineering at UCR that augments

support for many projects such as this.

7.8 References

1. Somerville C, Youngs H, Taylor C, Davis SC, Long SP. Feedstocks for lignocellulosic biofuels. Science. 2010 Aug 13;329(5993):790-2.
2. Borland AM, Griffiths H, Hartwell J, Smith JA. Exploiting the potential of plants with crassulacean acid metabolism for bioenergy production on marginal lands. J Exp Bot. 2009;60(10):2879-96.
3. Davis SC, Dohleman FG, Long SP. The global potential for agave as a biofuel feedstock. GCB Bioenergy. 2011;3(1):68-78.
4. Garcia-Moya E, Romero-Manzanares A, Nobel PS. Highlights for agave productivity. GCB Bioenergy. 2011;3(1):4-14.
5. Holtum JAM, Chambers DON, Morgan T, Tan DKY. Agave as a biofuel feedstock in Australia. GCB Bioenergy. 2011;3(1):58-67.
6. Nobel PS. Environmental biology of agaves and cacti. Cambridge ; New York: Cambridge University Press; 1988.
7. McLaughlin S, Bouton J, Bransby D, Conger B, Ocumpaugh W, Parrish D, et al., editors. Developing switchgrass as a bioenergy crop. Perspectives on new crops and new uses; 1999; Alexandria, VA: ASHS Press.
8. Sannigrahi P, Ragauskas AJ, Tuskan GA. Poplar as a feedstock for biofuels: A review of compositional characteristics. Biofuel Bioprod Bior. 2010 Mar-Apr;4(2):209-26.
9. Lemus R, Lal R. Bioenergy crops and carbon sequestration. Crit Rev Plant Sci. 2005;24(1):1-21.
10. Nobel PS, Garciamoya E, Quero E. High annual productivity of certain agaves and cacti under cultivation. Plant Cell Environ. 1992 Apr;15(3):329-35.
11. Gentry HS. Agaves of continental North America. Tucson, Ariz.: University of Arizona Press; 1982.
12. Nobel PS. Desert Wisdom/Agaves and Cacti: CO_2, Water, Climate Change. New York: IUniverse; 2010.
13. Romero-Gonzalez J, Parra-Vargas F, Cano-Rodriguez I, Rodriguez E, Rios-Arana J, Fuentes-Hernandez R, et al. Biosorption of Pb(II) by Agave tequilana Weber (Agave Azul) biomass. Rev Mex Ing Quim. 2007 Dec;6(3):295-300.
14. Wyman CE. Biomass ethanol: Technical progress, opportunities, and commercial challenges. Annu Rev Energ Env. 1999;24:189-226.
15. Huber GW, Iborra S, Corma A. Synthesis of transportation fuels from biomass: Chemistry, catalysts, and engineering. Chem Rev. 2006 Sep 13;106(9):4044-98.
16. Waksman SA, Stevens KR. A system of proximate chemical analysis of plant materials. Ind Eng Chem. 1930;2:0167-73.
17. Greene RA. Composition of the fiber and waste of agave lechuguilla. Botanical Gazette. 1932;93(4):484-91.

18. Garcia-Reyes RB, Rangel-Mendez JR. Contribution of agro-waste material main components (hemicelluloses, cellulose, and lignin) to the removal of chromium (III) from aqueous solution. J Chem Technol Biot. 2009 Oct;84(10):1533-8.
19. Iniguez-Covarrubias G, Lange SE, Rowell RM. Utilization of byproducts from the tequila industry: part 1: agave bagasse as a raw material for animal feeding and fiberboard production. Bioresource Technol. 2001 Mar;77(1):25-32.
20. Mancilla-Margalli NA, Lopez MG. Water-soluble carbohydrates and fructan structure patterns from agave and dasylirion species. J Agr Food Chem. 2006 Oct 4;54(20):7832-9.
21. Marquez A, Cazaurang N, Gonzalez I, ColungaGarciaMarin P. Cellulose extraction from agave lechuguilla fibers. Econ Bot. 1996 Oct-Dec;50(4):465-8.
22. McDougall GJ, Morrison IM, Stewart D, Weyers JDB, Hillman JR. Plant fibres: Botany, chemistry and processing for industrial use. J Sci Food Agr. 1993;62(1):1-20.
23. Mylsamy K, Rajendran I. Investigation on physio-chemical and mechanical properties of raw and alkali-treated agave americana fiber. J Reinf Plast Comp. 2010 Oct;29(19):2925-35.
24. Vieira MC, Heinze T, Antonio-Cruz R, Mendoza-Martinez AM. Cellulose derivatives from cellulosic material isolated from agave lechuguilla and fourcroydes. Cellulose. 2002 Jun;9(2):203-12.
25. Cedeno Cruz M, Alvarez-Jacobs J. Production of tequila from agave: historical influences and contemporary processes. In: Jacques K, Lyons TP, Kelsall DR, editors. The Alcohol Textbook. 3rd ed. Bottingham, UK: Nottingham University Press; 1999. p. 225-42.
26. Sluiter A, Hames B, Ruiz R, Scarlata C, Sluiter J, Templeton D. Determination of sugars, byproducts, and degradation products in liquid fraction process samples. Golden, CO, USA: National Renewable Energy Laboratory2006.
27. DeMartini JD, Studer MH, Wyman CE. Small-scale and automatable high-throughput compositional analysis of biomass. Biotechnol Bioeng. 2011 Feb;108(2):306-12.
28. Sluiter A, Ruiz R, Scarlata C, Sluiter J, Templeton D. Determination of extractives in biomass. Golden, CO, USA: National Renewable Energy Laboratory2005.
29. Sluiter A, Hames B, Ruiz R, Scarlata C, Sluiter J, Templeton D, et al. Determination of structural carbohydrates and lignin in biomass. Golden, CO, USA: National Renewable Energy Laboratory2008.
30. Kumar R, Wyman CE. An improved method to directly estimate cellulase adsorption on biomass solids. Enzyme Microb Tech. 2008 Apr 4;42(5):426-33.
31. Hames B, Scarlata C, Sluiter A. Determination of protein content in biomass. Golden, CO, USA: National Renewable Energy Laboratory2008.
32. Sluiter A, Hames B, Ruiz R, Scarlata C, Sluiter J, Templeton D. Determination of ash in biomass. Golden, CO, USA: National Renewable Energy Laboratory2005.
33. Hubbell CA, Ragauskas AJ. Effect of acid-chlorite delignification on cellulose degree of polymerization. Bioresource Technol. 2010 Oct;101(19):7410-5.
34. Boguslavsky A, Barkhuysen F, Timme E, Matsane RN. Establishing of agave *americana* Industry in South Africa. http://ccgconsultinginc.com/Documents/TS%20I-5-

Alexander%20Boguslavsky.pdf; 2007 [cited 2011 10/28]; Available from: http://ccgconsultinginc.com/Documents/TS%20I-5-Alexander%20Boguslavsky.pdf.
35. Sanchezmarroquin A, Hope PH. Agave Juice - Fermentation and chemical composition studies of some species. J Agr Food Chem. 1953;1(3):246-9.
36. Nguyen SK, Sophonputtanaphoca S, Kim E, Penner MH. Hydrolytic methods for the quantification of fructose equivalents in herbaceous biomass. Appl Biochem Biotech. 2009 Aug;158(2):352-61.
37. Ronkart SN, Blecker CS, Fourmanoir H, Fougnies C, Deroanne C, Van Herck J-C, et al. Isolation and identification of inulooligosaccharides resulting from inulin hydrolysis. Analytica Chimica Acta. 2007;604(1):81-7.
38. Shi J, Ebrik MA, Wyman CE. Sugar yields from dilute sulfuric acid and sulfur dioxide pretreatments and subsequent enzymatic hydrolysis of switchgrass. Bioresource Technol. 2011 Oct;102(19):8930-8.
39. Kumar R, Mago G, Balan V, Wyman CE. Physical and chemical characterizations of corn stover and poplar solids resulting from leading pretreatment technologies. Bioresource Technol. 2009 Sep;100(17):3948-62.
40. Pu Y, Ziemer C, Ragauskas AJ. CP/MAS 13C NMR analysis of cellulase treated bleached softwood kraft pulp. Carbohydr Res. 2006 Apr 10;341(5):591-7.
41. Chandra RP, Bura R, Mabee WE, Berlin A, Pan X, Saddler JN. Substrate pretreatment: the key to effective enzymatic hydrolysis of lignocellulosics? Adv Biochem Eng Biotechnol. 2007;108:67-93.
42. Fan LT, Lee YH, Beardmore DH. Mechanism of the enzymatic-hydrolysis of cellulose - effects of major structural features of cellulose on enzymatic-hydrolysis. Biotechnol Bioeng. 1980;22(1):177-99.
43. Jeoh T, Ishizawa CI, Davis MF, Himmel ME, Adney WS, Johnson DK. Cellulase digestibility of pretreated biomass is limited by cellulose accessibility. Biotechnol Bioeng. 2007 Sep 1;98(1):112-22.
44. Mansfield SD, Mooney C, Saddler JN. Substrate and enzyme characteristics that limit cellulose hydrolysis. Biotechnol Progr. 1999 Sep-Oct;15(5):804-16.
45. Sinitsyn A, Gusakov A, Vlasenko E. Effect of structural and physico-chemical features of cellulosic substrates on the efficiency of enzymatic hydrolysis. Appl Biochem Biotech. 1991;30(1):43-59.
46. Foston M, Hubbell CA, Samuel R, Jung S, Fan H, Ding S-Y, et al. Chemical, ultrastructural and supramolecular analysis of tension wood in Populus tremula x alba as a model substrate for reduced recalcitrance. Energy & Environmental Science. 2011;4(12):4962-71.
47. Kumar R. Enzymatic Hydrolysis of cellulosic biomass solids prepared by leading pretreatments and identification of key features governing performance. Hanover, NH, USA: Thayer School of Engineering, Dartmouth College; 2008.
48. Zhang YHP, Lynd LR. Toward an aggregated understanding of enzymatic hydrolysis of cellulose: Noncomplexed cellulase systems. Biotechnol Bioeng. 2004 Dec 30;88(7):797-824.

49. Foston M, Ragauskas AJ. Changes in the structure of the cellulose fiber wall during dilute acid pretreatment in populus studied by ^{1}H and ^{2}H NMR. Energ Fuel. 2010 2010/10/21;24(10):5677-85.
50. Hu ZJ, Foston MB, Ragauskas AJ. Biomass characterization of morphological portions of alamo switchgrass. J Agr Food Chem. 2011 Jul 27;59(14):7765-72.
51. Foston M, Hubbell CA, Davis M, Ragauskas AJ. Variations in cellulosic ultrastructure of poplar. BioEnergy Research. 2009 Dec;2(4):193-7.
52. Sannigrahi P, Ragauskas AJ, Miller SJ. Effects of two-stage dilute acid pretreatment on the structure and composition of lignin and cellulose in loblolly pine. BioEnergy Research. 2008 Dec;1(3-4):205-14.
53. Foston M, Ragauskas AJ. Changes in lignocellulosic supramolecular and ultrastructure during dilute acid pretreatment of populus and switchgrass. Biomass Bioenerg. 2010 Dec;34(12):1885-95.
54. Wickholm K, Larsson PT, Iversen T. Assignment of non-crystalline forms in cellulose I by CP/MAS ^{13}C NMR spectroscopy. Carbohyd Res. 1998;312(3):123-9.
55. Lennholm H, Larsson T, Iversen T. Determination of cellulose Iα and Iβ in lignocellulosic materials. Carbohyd Res. 1994;261(1):119-31.
56. Heux L, Dinand E, Vignon MR. Structural aspects in ultrathin cellulose microfibrils followed by 13C CP-MAS NMR. Carbohyd Polym. 1999;40(2):115-24.
57. Lynd LR, Laser MS, Bransby D, Dale BE, Davison B, Hamilton R, et al. How biotech can transform biofuels. Nat Biotech. [10.1038/nbt0208-169]. 2008;26(2):169-72.

Chapter 8

Agave is a Low Recalcitrant Lignocellulosic Feedstock for Biofuels Production on Semi-arid Lands*

*This whole chapter will be submitted under the following citation:
Li H, Pattathil S, Foston MB, Ding SY, Yarbrough JM, Mittal A, Kumar R, Himmel ME, Ragauskas AJ, Hahn MG, Wyman CE. "Agave is a low recalcitrant lignocellulosic feedstock for biofuels production on semi-arid lands"

8.1 Abstract

Agave has recently gained attention because of its attractive potential to launch sustainable bioenergy production from semi-arid and arid lands. We previously found significantly different chemical composition in agave cell walls, suggesting unique recalcitrance compared to conventional C_4 and C_3 crops. Here we report measurements of sugar release from hot water pretreatment followed by fungal enzyme hydrolysis that show agave to be significantly less recalcitrant to deconstruction than poplar or switchgrass. In fact, agave has 5-8 times higher sugar release on untreated material. Cutting-edge techniques were applied to measure interactions of non-cellulosic wall components, cell wall hydrophilicity, and enzyme accessibility and identify key structural features that determine cell wall resistance to biological deconstruction in comparison with poplar and switchgrass. These results show agave holds great promise for use in biorefineries on dry-lands and the importance of identifying genes controlling agave's low recalcitrance for application to improving cellulosic energy crops.

8.2 Introduction

A very large cellulosic biomass supply will be critical to establish a lignocellulosic industry that can have a serious impact on supplying sustainable fuels and chemicals in the long term (1, 2). However, water scarcity confines future energy crop production to regions with relatively high annual rainfall that would compete with food farms for irrigation (3). Thus, conversion of drought resistant cellulosic feedstocks, such as Agave, to biofuels will be vital to expand energy crop production beyond valuable irrigation soil to semi-arid lands that contribute about 18% of terrestrial surface (1, 3, 4). As a plant uses the Crassulacean Acid Metabolism (CAM) pathway, agave has high biomass productivity with minimal inputs of water and nutrients (5). In addition, agave offers environmental attributes such as preventing desertification and removing heavy metals ions from contaminated mines ground soil (6). These attractive features greatly facilitate agave's potential to be a low-cost global biofuels feedstock (7).

A recent study by our group showed agave cell walls contained relatively low amounts of lignin and a diverse range of non-cellulosic polysaccharides (Table 8.1) compared to conventional plants such as poplar (hardwood) and switchgrass (herbaceous) (8). Because lignin and cell-wall non-cellulosic structural polysaccharides protect cellulose microfibrils from degradation (9), the low amounts of these components in agave suggest low cell wall recalcitrance, in other word, high sugar release. However, although overcoming biomass recalcitrance is the primary roadblock to low cost biofuels that realize large scale benefits (1, 10), little information is available on the susceptibility of structural carbohydrates in agave species to sugar release that would validate its

potential as an energy crop for arid and semi-arid lands. Thus, it is important to validate if these compositional differences do enhance sugar release from agave in pretreatment and enzymatic hydrolysis compared to results from more conventional plants. Furthermore, if these results support our hypothesis that agave offers lower recalcitrance, understanding unique cell wall features that influence sugar release from pretreatment and enzymatic hydrolysis can provide valuable insights into characteristics to introduce into other plants to improve biofuels production.

Table 8.1. Chemical composition of agave, poplar, and switchgrass[1] (%)

	WSC[2]	Glucan	Xylan	Galactan	Arabinan	K-lignin
AAL	6.5	30.4	7.2	4.7	2.8	8.2
ASL	7.9	28.9	7.5	3.6	2.7	9.8
ATL	4.4	30.3	7.8	1.8	1.8	11.9
AAH	17.0	20.5	6.8	8.9	3.4	7.3
Poplar[3]	-	46.3	20.2	-	-	23.4
Switchgrass[3]	-	32.4	21.2	-	-	18.8

[1]Data reported are the mean values of three replicates

[2]Water soluble carbohydrates

[3]WSC, galactan and arabinan contents for poplar and switchgrass were not determined due to the low amount

8.3 Materials and methods

8.3.1 Plant materials

A. americana leaves (AAL), *A. salmiana* leaves (ASL), *A. tequilana* leaves (ATL), and *A. americana* heart (AAH) were freshly collected from the San Jose area (California, USA) and prepared at UCR, as described in detail elsewhere (8). Poplar and switchgrass were grown at Oak Ridge National Laboratory (ORNL) and provided

through the BioEnergy Science Center (BESC). Dry biomass samples were knife milled through a 40-mesh (425 μm) screen before experiments.

8.3.2 Compositional analysis

The composition of agave samples was determined using the National Renewable Energy Laboratory (NREL) standard biomass analysis procedures and was reported elsewhere (8). For poplar and switchgrass, the glucan and xylan contents were determined using unwashed biomass.

8.3.3 Pretreatment and enzymatic hydrolysis

Pretreatment and/or enzymatic hydrolysis were performed in a high throughput pretreatment and enzymatic hydrolysis (HTPH) system (11-13), using a customized 96-well plate reactor. A 4.5 mg of dry biomass was added to each well by an automated solid and liquid dispensing robotics platform (Core Module II, Freeslate Inc., Sunnyvale, CA) followed by 445 μL of deionized (DI) water. The well plates were then clamped together and placed in a custom-built steam chamber for pretreatment, as described in detail elsewhere (11). Following pretreatment, a 30.5 μL of citric acid buffer (1 M, pH 4.8) sodium azide (10 g/L), and diluted enzyme mixture was added to each well and plates were incubated at 50^{o}C in a Multitron shaker (Multitron Infors-HT, ATR Biotech, MD) at 150 rpm for 72 h. Then the well-plates were centrifuged at 2700 rpm for 30 min and hydrolyzate was transferred to HPLC vials for analysis. All enzymatic hydrolysis experiments were performed in quadruplicate. Sugar concentrations were determined by

a Waters Alliance e2695 HPLC with a 2414 refractive index (RI) detector (Waters Corporation, Milford, MA) and a BioRad Aminex HPX-87H column (Bio-Rad Life Science, Hercules, CA).

8.3.3.1 Enzyme loading and formulation

A high protein loading of 150 mg/g structural carbohydrates in raw materials was applied, using DuPont™ Genencor® Science (Palo Alto, CA) enzymes: cellulase (Accellerase® 1500, Lot No.:1681198062), xylanase (Accellerase® XY, Lot No.:4901131618), xylanase (Accellerase® XC, Lot No.:4861066335), and pectinase (Multifect® Pectinase, Lot No.:4861295753). Enzyme formulations are listed in Table 8.2.

Table 8.2. Enzymes, formulations, and protein percentage of fungus enzyme cocktails for biomass hydrolysis

Enzyme	Protein mass, %			
	Accellerase® 1500	Accellerase® XY	Accellerase® XC	Multifect® Pectinase
1500	100	-	-	-
1500+XY	75	25	-	-
1500+XC	75	-	25	-
1500+P	75	-	-	25
1500+XY+P	75	12.5	-	12.5
1500+XC+P	75	-	12.5	12.5
1500+XY+XC	75	12.5	12.5	-

Accellerase®1500: mostly cellulase
Accellerase® XY: xylanase
Accellerase® XC: xylanase with multiple hemicellulase activities
Multifect® pectinase: pectinase and hemicellulase activities

8.3.3.2 Enzymatic hydrolysis of non-pretreated biomass

Citric acid buffer, sodium azide, and diluted enzyme solution was added to each well without taking the plates through pretreatment. The protein loading of 150 mg/g structural carbohydrates in raw materials was used with mass ratio of Accellerase® 1500, Accellerase® XY, Multifect® Pectinase is 6:1:1.

Table 8.3. Conditions of low severity hydrothermal pretreatment

Temperature (℃)	Reaction times for corresponding severities[1] (min)	
	Log Ro=3.0	Log Ro=3.4
105	712.8	-
120	257.4	-
140	66.5	166.8
160	17.1	43.0
180	4.4	11.1

[1]Pretreatment severity is defined as $R_0 = t \cdot e^{\frac{T-100}{14.75}}$, where t is in minutes and T in ^{o}C

8.3.3.3 Low severity hydrothermal pretreatment and enzymatic hydrolysis

A series of relatively mild hydrothermal pretreatment conditions were conducted, as listed in Table 8.3. After pretreatment, the same enzyme protein loading and formulation were applied as in section 8.3.3.2.

8.3.4 Glycome Profiling

Glycome Profiling is an ELISA-based method which uses plant glycan-directed monoclonal antibodies (mAbs) to identify cell wall carbohydrate components isolated from sequential extractions with increasingly harsh chemical reagents (14-16). About 250 mg (dry weight) each of untreated agave, poplar, and switchgrass samples were

sequentially washed with absolute ethanol and acetone to remove extractives. The washed residues were then vacuum-dried overnight and subjected to extraction steps in 10 mg mL^{-1} suspensions based on the starting dry biomass weight used. First, the biomass was suspended in 50 mM ammonium oxalate (pH=5.0) and incubated overnight with constant mixing at room temperature. After incubation, the mixture was centrifuged at 3400 g for 15 min. The resulting supernatant was decanted and saved as the oxalate fraction. Following the same protocol, the pellet was then subjected to additional sequential extractions using in turn 50 mM sodium carbonate (pH 10) containing 0.5% w/v sodium borohydride, and 1 M KOH, 4 M KOH, each containing 1% w/v sodium borohydride. The pellet remaining after the 4 M KOH extraction was then treated with sodium chlorite (100 mM) in order to breakdown lignin polymers into smaller components, as described previously(16). Lastly, the pellet left following the sodium chlorite treatment was subjected to a final extraction with 4 M KOH containing 1% w/v sodium borohydride to isolate material that had previously been secured within the walls by lignin (4 M KOH PC). The resulting residual pellet was not analyzed any further. The 1 M KOH, 4 M KOH, and 4 M KOH PC extracts were neutralized with glacial acetic acid. All extracts were dialyzed against four changes of DI water (with an approximate sample to water ratio of 1:60) for 48 hours at room temperature and subsequently lyophilized. After estimating the total sugar contents of the cell wall extracts using the phenol-sulfuric acid method, the extracts were dissolved in DI water to a concentration of 0.2 mg mL^{-1}. Next, all extracts were diluted to the same sugar concentration of 20 μg mL^{-1} for loading onto ELISA plates. Diluted extract (50 μL) was added to each well and

allowed to evaporate overnight at 37°C until dry. The ELISAs were conducted as described using an array of 155 monoclonal antibodies specific to epitopes from most major groups of plant cell wall polysaccharides (16). Negative controls consisting of water blanks without antigen were included in all assays and their absorbance subtracted from all samples. None of the monoclonal antibodies that were used show background in the ELISA assays. ELISA data are presented as heat maps in which antibodies are grouped based on a hierarchical clustering analysis of their binding specificities against a diverse set of plant glycans. Monoclonal antibodies were obtained from the Complex Carbohydrate Research Center collection (available through CarboSource Services; http://www.carbosource.net).

8.3.5 Simons' stain

A modified Simons' stain assay based on procedures that were developed previously was applied (17). D_O (Pontamine Fast Orange 6RN) and D_B (Pontamine Fast Sky Blue 6BX) dyes were obtained from Pylam Products (Garden City, NY). First, 1% w/v orange dye solution was poured into an Amicon ultrafiltration apparatus and filtered through a 100 K ultrafiltration membrane under 28 psi nitrogen gas pressure (18), until 20% of the original solution was left. 1.0 mL of the retained dye solution in the filter was dried in a 50 ℃ vacuum oven for 5 days, and the weight of the solid residue was then measured to determine the concentration of the filtered solution. The corresponding result was then used to dilute the filtered orange dye solution to the concentration required (10 mg mL^{-1}) for the Simons' staining. 100 mg of biomass samples were

weighed into five 15 mL centrifuge tubes, followed by adding 1.0 mL of phosphate buffered saline solution (pH 6, 0.3 M PO_4, 1.4 mM NaCl). Then, both D_O solution (10 mg mL^{-1}) and D_B solution (10 mg mL^{-1}) were added in increasing volumes (0.25, 0.50, 0.75, 1.0, 1.5 mL) to the five tubes containing biomass sample and buffer, thus creating a 1:1 mixture of D_O and D_B dyes at increasing concentrations. Following that, DI water was added to each tube to make the final volume 10.0 mL. The tubes were incubated at 70 ℃ with shaking at 200 rpm for 6 hours and then centrifuged at 10,000 rpm for 8 min. After that, UV absorbance of supernatant was measured on a Lambda 35 UV-Vis spectrophotometer (PerkinElmer, Waltham, MA) at 455 nm and 624 nm. The concentration of the D_O and D_B dyes (C_O and C_B, respectively) in the supernatant was calculated using the following two equations (based on Lambert-Beer law for a binary mixture) (18):

$$A_{455nm} = \varepsilon_{O/455}LC_O + \varepsilon_{B/455}LC_B \quad (1)$$

$$A_{624nm} = \varepsilon_{O/624}LC_O + \varepsilon_{B/624}LC_B \quad (2)$$

The extinction coefficients ε_O and ε_B were determined by preparing standard calibration curves at 455 and 624 nm. The amount of dye adsorbed by the biomass was then calculated by deducting the dye in the supernatant from the dye that was initially added. Total adsorption is reported as mg of dye per gram of biomass.

8.3.6 Water mobility

Biomass samples were conditioned in a sealed desiccator at 25°C and ~ 100% relative humidity over a 0.01 (w/v) NaN_3 solution for 7 days. The moisture contents in

all samples were found to be 26 ± 3 %. ^{1}H spin-spin (T_2) NMR measurements were carried out on a Bruker DSX-300 spectrometer, operating at frequencies of 300.13 MHz for ^{1}H in a Bruker static probe. The spin-spin relaxation times were determined using a standard 2D Carr-Purcell-Meiboom-Gill (CPMG) sequence with a 5 μs (90°) ^{1}H pulse, 10 μs (180°) ^{1}H pulses, 16 scans, 10 s recycle delay and $\tau = 0.0002$ s. 16 data points were recorded between n = 4 - 1024 echoes (0.00164 – 0.41984 s). Inverse Laplace transforms (ILT) were accomplished by Matlab 7.13 program written by P. T. Callaghan at Victoria University of Wellington (Wellington, New Zealand) to process 1- and 2-dimensional ASCII data measuring either diffusion or relaxation characteristics of heterogeneous proton systems. This program is based on unconstrained regularization, non-negative least squared fit, and singular value decomposition algorithms. The routine was tested using a series of multi-exponential and stretched-exponential functions of varying component weights, widths and characteristic decay times demonstrating fairly good accuracy, resolution and stability in the corresponding distributions produced. To assess the effect of noise, relaxation curves were generated using a multi-exponential function, and each data point was allow to increase or decrease by a maximum of 10% of its only value. The particular variance at each data point was controlled by a random number generator to simulate a randomly noisy relaxation curve. Again the resulting transforms produce reliable peak intensities, positions, and widths. A common technique to extract information for comparison on systems having wide distributions of nuclear relaxers or T_2 decays utilizes an ILT routine (19, 20).

8.3.7 X-ray Diffraction (XRD)

X-ray diffraction (XRD) was performed to evaluate the crystalline structure of biomass samples by using a Rigaku (Tokyo, Japan) Ultima IV diffractometer with CuKα radiation having a wavelength λ(Kα1) = 0.15406 nm generated at 40 kV and 44 mA. The diffraction intensities of air dried samples placed on a quartz substrate were measured in the 2θ range of 8 to 42° using a step size of 0.02° at a rate of 2°/min.

8.4 Results and discussion

Because leaves and heart are the two main portions from a single agave plant that could be utilized as cellulosic feedstocks, we prepared four agave samples from three popular specie (Figure 8.1), *A. americana* leaves (AAL), *A. salmiana* leaves (ASL), *A. tequilana* leaves (ATL), and *A. americana* heart (AAH). Among them, *A. americana* and *A. salmiana* were chosen because they are common in most countries and have high productivity (4, 7). A. *tequilana* was selected because it is widely cultivated in Mexico for Tequila, with large amount of leaves left as waste and the heart bagasse can be utilized as cellulosic feedstock for biofuels production (21). To better understand the agave recalcitrant characteristics, poplar (*Populus trichocarpa*) and switchgrass (*Panicum virgatum*) were included for comparison as two leading energy crop candidates.

Figure 8.1. Pictures of agave species selected for this study.

We first determined how different enzyme activities affected biological deconstruction of biomass to identify enzyme formulations that maximized sugar release from agave species, poplar, and switchgrass. Thus, seven fungal enzyme cocktails were prepared from commercial DuPont™ Genencor® cellulase, xylanase, hemicellulase and pectinase at the same total protein loadings (Table 8.2). The results showed that supplementing with hemicellulase, especially pectinase, was important to achieve high sugar release from AAL, ASL and AAH (Figure 8.2a,b,d), while xylanase supplementation enhanced sugar release most from ATL (Figure 8.2c). Although xylanase is normally employed along with cellulase in hydrolyzing poplar and switchgrass(22), enzyme supplementations did not have as significant impact for these two species as for agave (Figure 8.2e,f). Overall, the enzyme cocktail designated "1500+XY+P" (Table 8.2) provided the highest total sugar release for all samples (Figure 8.2a-f) and was applied as the enzyme formulation for all subsequent experiments.

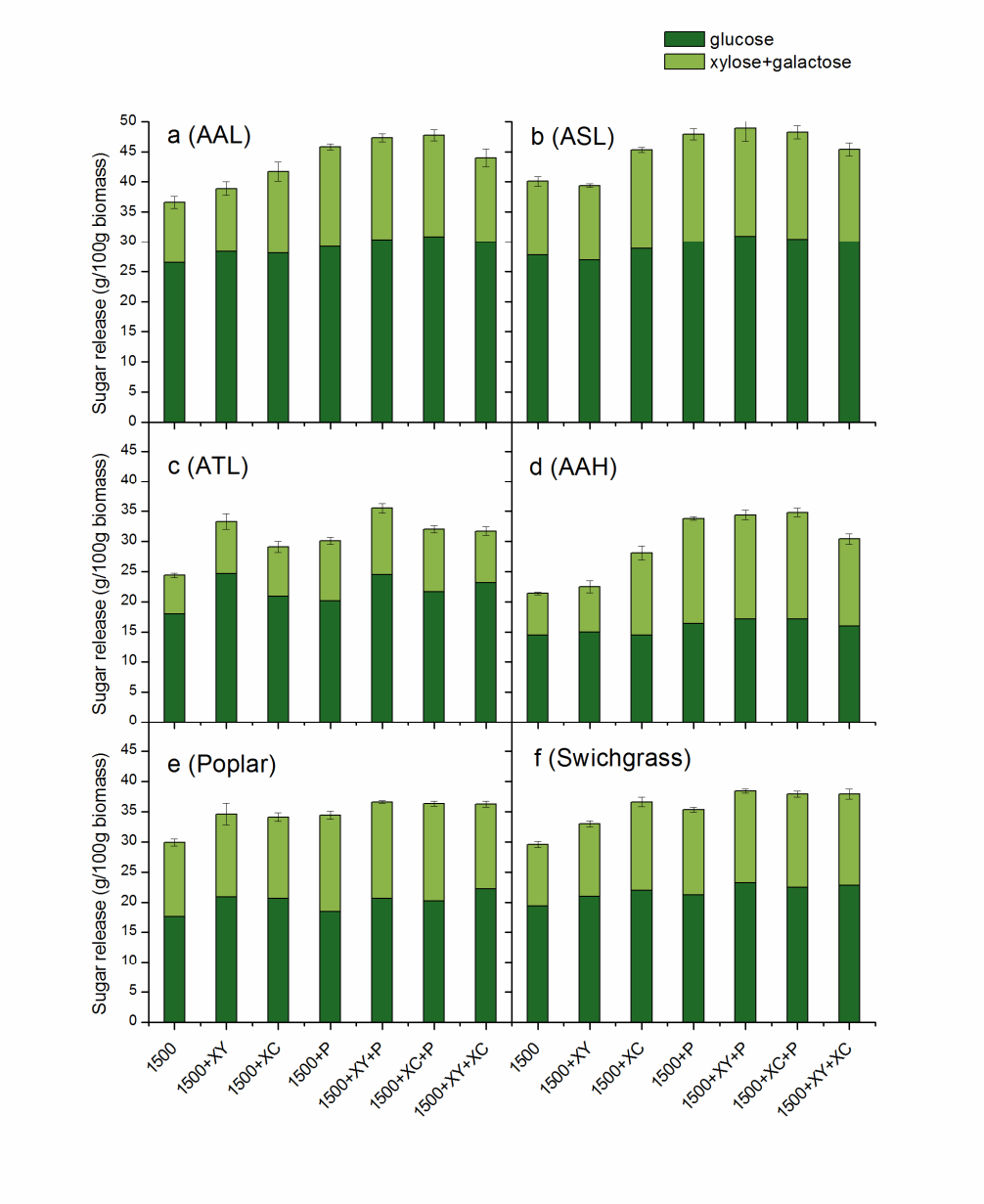

Figure 8.2. Total sugar release from hydrothermal pretreatment (180C- 11.1 min) followed by enzymatic hydrolysis from (a) A. *americana* leaves (AAL), (b) A. *salmiana* leaves (ASL), (c) A. *tequilana* leaves (ATL), (d) A. *americana* heart (AAH), (e) poplar, and (f) switchgrass at different enzyme formulations and a protein loading of 150 mg/g structural carbohydrates in raw biomass. Details on enzymes formulations are shown in Table 8.2. In the figures, 1500 represents Accellerase®1500 cellulase, XY represents Accellerase® XY xylanase, XC represents Accellerase® XC xylanase, and P represents Multifect® pectinase.

The wide variation in enzyme formulations that are most effective in deconstructing different biomass materials suggests significant differences in the complex non-cellulosic polysaccharides in the matrix of agave cell walls. To better understand structural differences that could contribute to cell wall recalcitrance, we employed a glycome profiling technique that employs glycan-directed monoclonal antibodies (mAbs) to monitor the structure and extractability of non-cellulosic wall polysaccharides in agave species and compare the results to those with poplar and switchgrass. Antibodies interacting with groups of Xyloglucans (XG), Xylans, Rhamnogalacturonan I pectins (RG-I), and Arabinogalactan (AG) showed strong absorbance on fractions extracted from agave cell walls, while antibodies interactions were mainly on Xylans for poplar and switchgrass (Figure 8.3). Such results demonstrate that multiple non-cellulosic polysaccharides bonds occur in agave plants, with the result that enzymes like hemicellulases and pectinase will be needed to realize high sugar yields from agave cell walls. In addition, wall components extracted by less harsh chemical reagents (Oxalate, carbonate) accounted for relatively greater proportion of the total extractives from agave materials, while the amount of wall components associated with lignin (Chlorite) and secured within the walls by lignin (4M KOH PC) was significantly lower in agave than poplar and switchgrass (Figure 8.3). Thus, the high extractability and low level of protection for cellulose from non-cellulosic cell wall components in the agave cell walls suggest that agave is less recalcitrant than poplar and switchgrass.

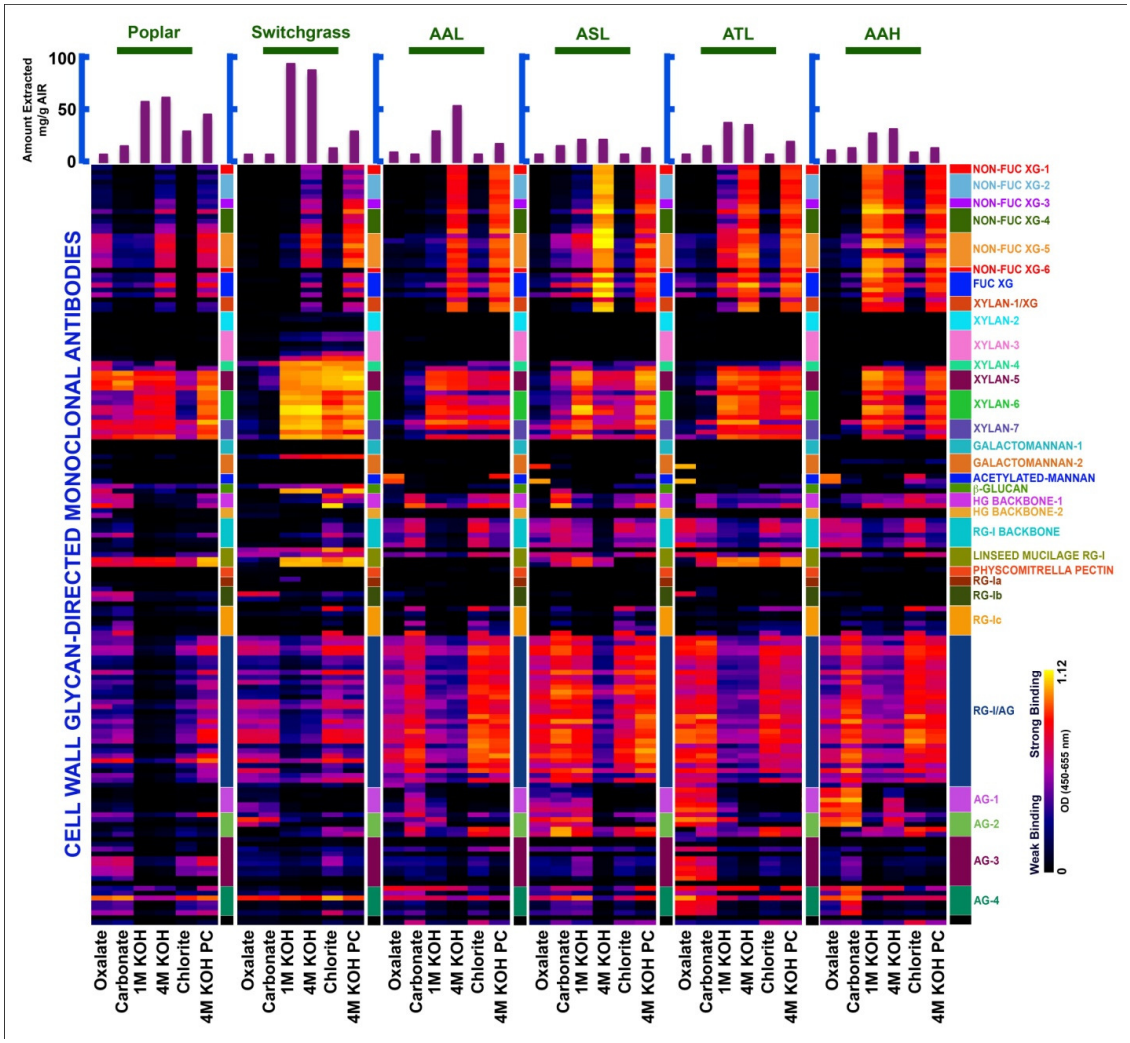

Figure 8.3. Glycome profiling of untreated *Populus trichocarpa* (Poplar), *Panicum virgatum* (Switchgrass), A. *americana* leaves (AAL), A. *salmiana* leaves (ASL), A. *tequilana* leaves (ATL), and A. *americana* heart (AAH) biomass. Sequentially extracted materials released from each biomass sample by various reagents (as labeled at the bottom of each map) were loaded onto the ELISA plates and were screened against an array of plant glycan-directed monoclonal antibodies. The legend panel on the right of the figure displays the nature of the polysaccharides predominantly recognized by these mAbs. Antibody binding is represented as colored heat maps, with black signifying no binding, light yellow representing the strongest binding. The bar graphs at the top indicate the amount of material recovered at each extraction step per gram of alcohol insoluble residue (AIR).

Based on these findings, we enzymatically hydrolyzed raw biomass using the optimized enzyme formulation to quantitatively determine biomass recalcitrance and found that untreated agave biomass achieved dramatically higher sugar yields than poplar or switchgrass after 72 hours of hydrolysis at high enzyme loadings of 150 mg protein/ g structural carbohydrate in raw biomass (Figure 8.4a). In fact, the best AAL and ASL samples released about 80% of total cell wall carbohydrates, compared to only 11-16% of total polysaccharides from poplar or switchgrass cell walls under the same condition. To confirm this significant finding, we applied the same enzymatic hydrolysis conditions to agave samples that had been sequentially extracted with water and ethanol to avoid any potential interference from free sugars in raw biomass and only focus on the deconstruction of structural polysaccharides. Extractives free agave materials showed consistently outstanding sugar release (Figure 8.4b) that were about 7.3-4.3 times higher than from poplar and 5.3-3.1 times higher than from switchgrass. These results successfully confirmed that agave species have very low recalcitrance to biological deconstruction and are significantly less recalcitrant than poplar, switchgrass, and most other cellulosic biomass that have been studied as biofuels feedstocks.

Much less recalcitrant lignocellulosic feedstocks would dramatically reduce the production cost of advanced biofuels through using mild pretreatment conditions and low enzymes doses (23-25). Thus, a series of low severity hydrothermal pretreatments (Table 8.3) were applied to further understand how differences in plant recalcitrance affect sugar release from pretreatment and enzymatic hydrolysis. At the same severity (26), higher temperatures resulted in higher sugar yields than those with longer reaction time (Figure

8.4c-e), indicating that pretreatment temperature is more important to achieve high biomass digestibility than reaction time. However, increasing the harshness of pretreatment conditions had limited impact on sugar yields from agave species, especially AAL, ASL and AAH samples but significantly increased yields from poplar and switchgrass (Figure 8.4c-e). Furthermore, glucose yields from the least recalcitrant AAL and ASL, interestingly, did not reach over 90% of the maximum possible as expected at such mild conditions (Figure 8.4c). These results suggest that agave recalcitrance is not as sensitive to pretreatment as conventional cellulosic feedstocks. Thus, the economic tradeoffs between a slight sugar yield increase must be weighed against additional cost of mild pretreatment. Another interesting difference between agave and poplar and switchgrass is the ratio of glucose yield to "xylose+galactose" yield that were plotted at the pretreatment conditions applied. The decreasing trend of such ratios for poplar and switchgrass indicates that increasingly pretreatment severity was more effective in improving hemicellulose digestibility than that of cellulose (Figure 8.4f), as is normally true because the amorphous hemicellulose is relatively loose and protects crystalline cellulose. In contrast, however, the corresponding ratios for agave materials stayed nearly constant (Figure 8.4f). This interesting result suggests that agave cellulose, as well as easily hydrolyzed hemicellulose (including pectin), was disrupted to a similar extent over the full range of pretreatment conditions. Thus, agave cell walls must have some unique features compared to those for other biomass that result in high cellulose reactivity.

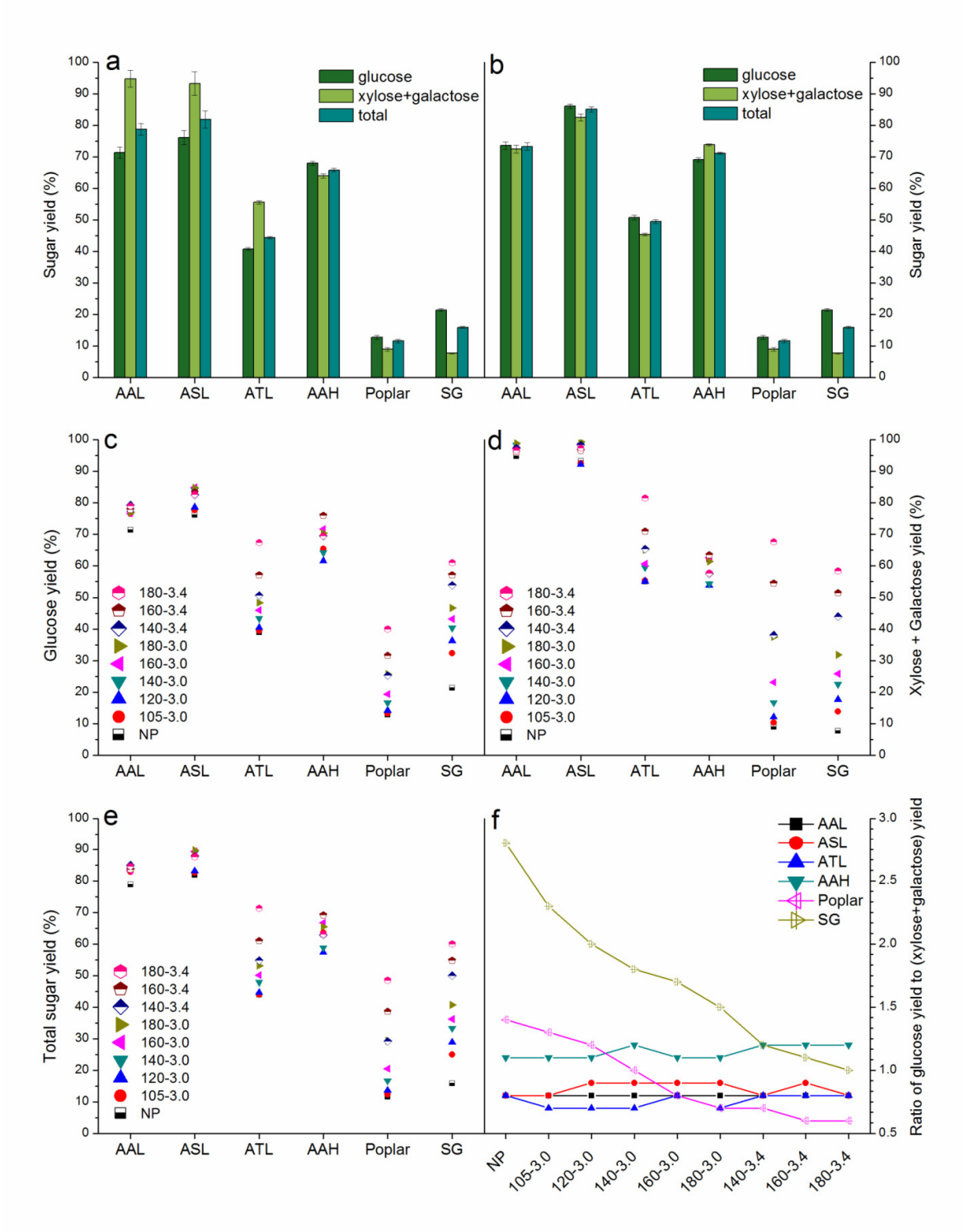
a
b
c
d
e
f
glucose
xylose+galactose
total
Sugar yield (%)
Glucose yield (%)
Xylose + Galactose yield (%)
Total sugar yield (%)
Ratio of glucose yield to (xylose+galactose) yield
AAL
ASL
ATL
AAH
Poplar
SG
180-3.4
160-3.4
140-3.4
180-3.0
160-3.0
140-3.0
120-3.0
105-3.0
NP

Figure 8.4. Sugar yield data from enzymatic hydrolysis of (a) untreated (b) extractives free untreated and (c-f) hydrothermal-pretreated *Populus trichocarpa* (Poplar), *Panicum virgatum* (Switchgrass: SG), A. *americana* leaves (AAL), A. *salmiana* leaves (ASL), A. *tequilana* leaves (ATL), and A. *americana* heart (AAH) biomass. Biomass samples were digested with cellulase supplemented with xylanase and pectinase as described in Section 8.3.3.2 and 8.3.3.3. Hydrothermal pretreatment conditions are described in Table 8.3. Pretreatment conditions, 105-3.0, for example, represents pretreatment at 105°C of severity factor of 3.0; and NP represents no pretreatment. Yields reflect the amount of sugar released out of available sugar in raw biomass.

To gain better insight into agave structural characteristics of agave that could enhance cell wall reactivity, we first applied the Simons' Stain test to provide insights into pore surface area (Figure 8.5a) and the relative accessibility (Figure 8.5b) of the biomass samples. The results showed that agave had more accessible surface area (amount of adsorbed large dye: orange dye) and higher relative accessibility (ratio of adsorbed large to small dye: orange to blue dye) than poplar and switchgrass, especially for samples of AAL and ASL, which are in strong agreement with sugar release results. Because the high enzyme accessibility of raw agave materials enables enzymes to easily hydrolyze cell wall polysaccharides without pretreatment, this finding helps explain why the sugar yield from agave was not as sensitive to pretreatment conditions as poplar and switchgrass. Next, ^{1}H-NMR was applied to monitor water mobility in biomass cell walls by measuring the distribution of spin-spin relaxation times (T_2) of absorbed water within the tested biomass samples. Agave samples showed shorter T_2 than switchgrass or poplar (Figure 8.5c), indicating stronger cell wall interactions with water molecules, in other words, higher hydrophilicity that facilitates mass transfer and cell wall reactivity in water media during pretreatment and enzymatic hydrolysis. Furthermore, X-Ray Diffraction (XRD) was applied to qualitatively compare the ordered structure of the cellulosic materials in this study.

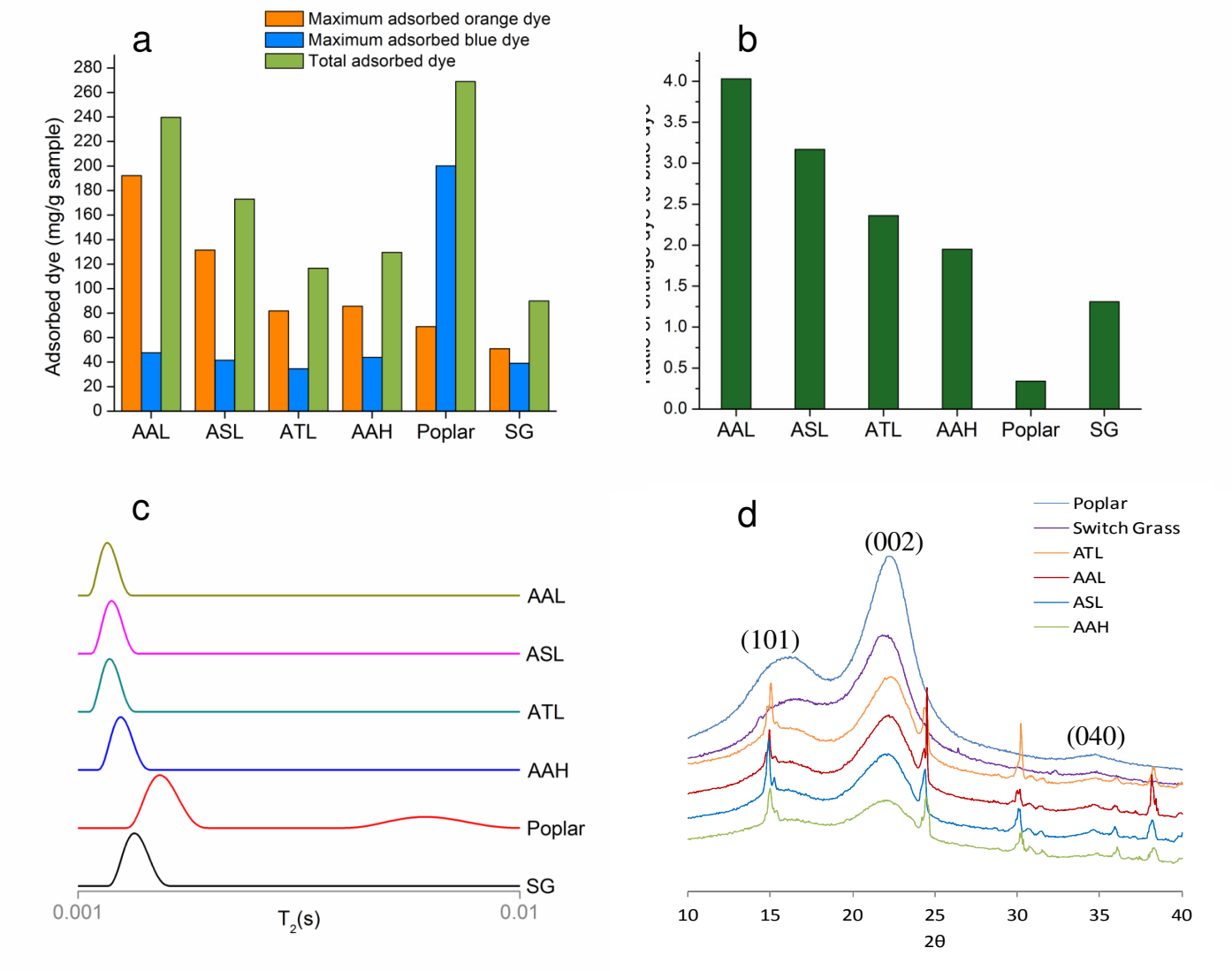

Figure 8.5. Structural characterization of untreated *Populus trichocarpa* (Poplar), *Panicum virgatum* (Switchgrass: SG), A. *americana* leaves (AAL), A. *salmiana* leaves (ASL), A. *tequilana* leaves (ATL), and A. *americana* heart (AAH) biomass. (a) Simons' Stain results for biomass pore surface area represented by the amount of absorbed dye, mg dye/g of sample. (b) Simons' Stain results for relative enzyme accessibility represented by ratio of absorbed large dye to small dye, [mg orange dye/g sample] / [mg blue dye/g sample]. (c) Spin-spin relaxation times (T_2) of absorbed water within biomass samples produced via ILTs of CMPG T_2 experiments. (d) XRD spectrum.

The XRD spectrum of Avicel PH 101 cellulose showed diffraction peaks of cellulose I, corresponding to (101), (002), and (040) lattice planes (Figure 8.6). By comparing such typical peaks of agave samples to those of poplar and switchgrass, it is certain that agave cell walls did not contain as much well defined crystalline structure as cellulose I in most lignocellulosic biomass (Figure 8.5d). In fact, agave heart bagasse, AAH, was even more amorphous than 6-hour ball milled Avicel (Figure 8.6).

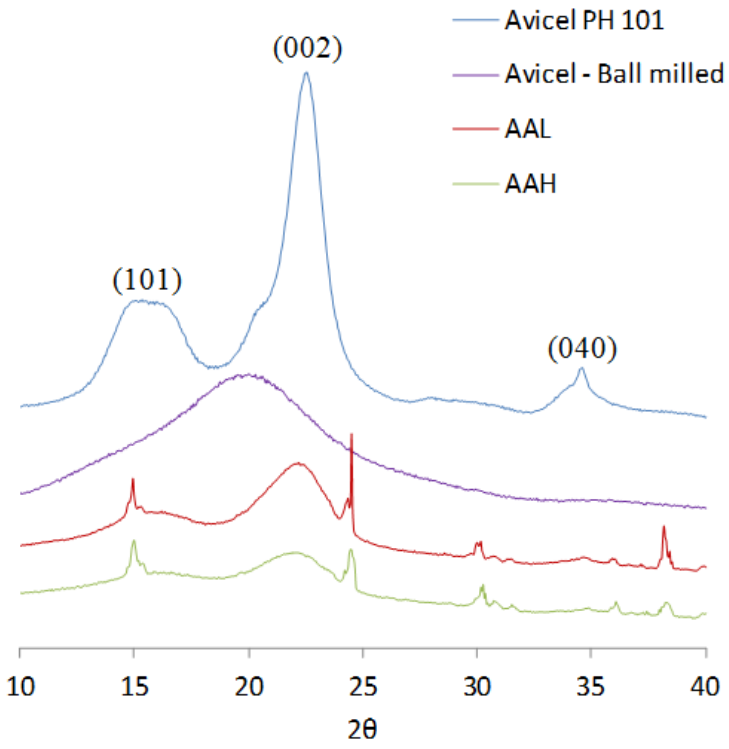

Figure 8.6. X-Ray Diffraction (XRD) spectrum of Avicel PH 101 cellulose, 6-hour ball milled Avicel cellulose, A. *americana* leaves (AAL), and A. *americana* heart (AAH).

These unique structural characteristics of agave species provide strong insights to explain why its sugar release patterns from pretreatment and enzymatic hydrolysis is so different from poplar and switchgrass and why the recalcitrance of agave is so low. In addition, we find it very interesting to postulate how these low recalcitrant features of

agave cell walls could explain the way agave plants survive in arid regions. For example, the green and thick agave leaves serve as both photosynthetic and water storage organs, within which large, thin walled parenchyma and collenchymas cells form succulent water-storing tissues (27). This is consistent with our findings that agave cell walls are relatively highly hydrophilic and less lignified (less secondary cell wall thickening). Another example is that during agave's final season, the agave plant is believed to extract polysaccharides from its vegetative and storage organs to produce its flower stalk, leaving the leaves yellow, thin, and dry. This plant physiology phenomenon suggests that the defensive cell wall structure in woody and grass biomass against biological deconstruction might not be beneficial to agave plants because they need to hydrolyze those polysaccharides to facilitate reproduction. The possible associations of such special plant characteristics with cell wall structural features provide a promising direction to discover, identify, and develop new, advanced low recalcitrant energy crops.

8.5 Conclusions

In summary, we discovered and demonstrated that agave is a low recalcitrant material that could dramatically reduce processing costs and expand production of biofuels to arid and semi-arid lands. Furthermore, we have shown that its low recalcitrance could benefit from several key features, such as a loose non-cellulosic wall component structure, high enzyme accessibility, good hydrophilicity, and less ordered crystalline structure. Determining which agave genes control such traits could provide valuable insights into approaches to greatly facilitate development of low recalcitrant,

highly productive, and drought resistant biomass. Thus, it is possible that the future biorefineries can bypass the lignocellulosic recalcitrance problem, water and food crisis, and desertification threat by producing biomass and biofuels on semi-arid and arid lands.

8.6 Acknowledgements

This research was funded by the BioEnergy Science Center (BESC), a U.S. Department of Energy Bioenergy Research Center supported by the Office of Biological and Environmental Research in the DOE Office of Science. The authors would especially like to thank Mr. Arturo Velez and Mr. Ramon F. Olmedo from Agave Project of Mexico for providing agave materials. We would also like to thank Professor Eugene A. Nothnagel in the Botany and Plant Science Department of the University of California, Riverside for valuable discussions. Gratitude is extended to the Ford Motor Company for funding the Chair in Environmental Engineering at the Center for Environmental Research and Technology of the Bourns College of Engineering at UCR that augments support for many projects such as this.

8.7 References

1. Wyman CE. What is (and is not) vital to advancing cellulosic ethanol. Trends in Biotechnology. 2007 Apr;25(4):153-7.
2. Lynd LR, Laser MS, Brandsby D, Dale BE, Davison B, Hamilton R, et al. How biotech can transform biofuels. Nat Biotechnol. 2008 Feb;26(2):169-72.
3. Energy USDo. U.S. billion-ton update: biomass supply for a bioenergy and bioproducts industry. Oak Ridge, TN: Oak Ridge National Laboratory2011.
4. Somerville C, Youngs H, Taylor C, Davis SC, Long SP. Feedstocks for lignocellulosic biofuels. Science. 2010 Aug 13;329(5993):790-2.
5. Garcia-Moya E, Romero-Manzanares A, Nobel PS. Highlights for agave productivity. GCB Bioenergy. 2011;3(1):4-14.

6. Nobel PS. Desert wisdom/agaves and cacti: co_2, water, climate change. New York: IUniverse; 2010.
7. Davis SC, Dohleman FG, Long SP. The global potential for Agave as a biofuel feedstock. GCB Bioenergy. 2011;3(1):68-78.
8. Li H, Foston MB, Kumar R, Samuel R, Gao X, Hu F, et al. Chemical composition and characterization of cellulose for Agave as a fast-growing, drought-tolerant biofuels feedstock. RSC Advances. 2012;2(11):4951-8.
9. Albersheim P, Darvill A, Roberts K, Sederoff R, Staehelin A. Plant cell walls : from chemistry to biology. New York, NY: Garland Science; 2010.
10. Lynd LR, Wyman CE, Gerngross TU. Biocommodity engineering. Biotechnol Prog. 1999 Oct 1;15(5):777-93.
11. Studer MH, DeMartini JD, Brethauer S, McKenzie HL, Wyman CE. Engineering of a high-throughput screening system to identify cellulosic biomass, pretreatments, and enzyme formulations that enhance sugar release. Biotechnol Bioeng. 2010 Feb 1;105(2):231-8.
12. Studer MH, Brethauer S, Demartini JD, McKenzie HL, Wyman CE. Co-hydrolysis of hydrothermal and dilute acid pretreated populus slurries to support development of a high-throughput pretreatment system. Biotechnol Biofuels. 2011;4(1):19.
13. DeMartini JD, Wyman CE. Composition and hydrothermal pretreatment and enzymatic saccharification performance of grasses and legumes from a mixed-species prairie. Biotechnol Biofuels. 2011 Nov 15;4.
14. Pattathil S, Avci U, Baldwin D, Swennes AG, McGill JA, Popper Z, et al. A Comprehensive toolkit of plant cell wall glycan-directed monoclonal antibodies. Plant Physiol. 2010 Jun;153(2):514-25.
15. DeMartini JD, Pattathil S, Avci U, Szekalski K, Mazumder K, Hahn MG, et al. Application of monoclonal antibodies to investigate plant cell wall deconstruction for biofuels production. Energy & Environmental Science. 2011 Oct;4(10):4332-9.
16. Pattathil S, Avci U, Miller JS, Hahn MG. Immunological approaches to plant cell wall and biomass characterization: glycome profiling. Methods Mol Biol. 2012;908:61-72.
17. Chandra R, Ewanick S, Hsieh C, Saddler JN. The characterization of pretreated lignocellulosic substrates prior to enzymatic hydrolysis, Part 1: a modified simons' staining technique. Biotechnol Progr. 2008 Sep-Oct;24(5):1178-85.
18. Esteghlalian AR, Bilodeau M, Mansfield SD, Saddler JN. Do enzymatic hydrolyzability and Simons' stain reflect the changes in the accessibility of lignocellulosic substrates to cellulase enzymes? Biotechnol Progr. 2001 Nov-Dec;17(6):1049-54.
19. Elder T, Labbe N, Harper D, Rials T. Time domain-nuclear magnetic resonance study of chars from southern hardwoods. Biomass Bioenerg. 2006 Oct;30(10):855-62.
20. Felby C, Thygesen LG, Kristensen JB, Jorgensen H, Elder T. Cellulose-water interactions during enzymatic hydrolysis as studied by time domain NMR. Cellulose. 2008 Oct;15(5):703-10.

21. NÚÑEz HM, RodrÍGuez LF, Khanna M. Agave for tequila and biofuels: an economic assessment and potential opportunities. GCB Bioenergy. 2011;3(1):43-57.
22. Selig M, Weiss N, Ji Y. Enzymatic Saccharification of lignocellulosic biomass. Golden, CO, USA: National Renewable Energy Laboratory2008.
23. Lynd LR, Laser MS, Bransby D, Dale BE, Davison B, Hamilton R, et al. How biotech can transform biofuels. Nature Biotechnology. 2008 Feb;26(2):169-72.
24. Fu C, Mielenz JR, Xiao X, Ge Y, Hamilton CY, Rodriguez M, et al. Genetic manipulation of lignin reduces recalcitrance and improves ethanol production from switchgrass. Proceedings of the National Academy of Sciences. 2011;108(9):3803-8.
25. Pu Y, Kosa M, Kalluri U, Tuskan G, Ragauskas A. Challenges of the utilization of wood polymers: how can they be overcome? Applied Microbiology and Biotechnology. 2011;91(6):1525-36.
26. Chum HL, Johnson DK, Black SK, Overend RP. Pretreatment catalyst effects and the combined severity parameter. Appl Biochem Biotech. 1990 Spr-Sum;24-5:1-14.
27. Graham LE, Graham JM, Wilcox LM. Plant biology. 2nd Edition ed. San Francisco, CA: Benjamin Cummings (Pearson); 2006.

Chapter 9

Conclusions

9.1 Summary of key developments and findings

The main motivation for this thesis was to facilitate fundamental understanding of the roles of plant cell wall structural polymers, especially interactions of lignin and hemicellulose, in defining biomass recalcitrance during cell wall deconstruction in pretreatment and enzymatic hydrolysis. With studies such as this, future pretreatment can use much milder conditions to avoid side-reactions while maintain high sugar yields; future enzymatic hydrolysis can be more effective by minimizing inhibitory factors while use lower enzyme doses; and future energy crops can be designed to have high water use efficiency and more digestible cell wall structure to improve biological deconstruction.

In light of this, an integrated chromatographic method was first developed to quantify xylooligosaccharides with different chain lengths. In this study, high purity liner 1,4-β-xylooligosaccharide fractions with DP values from 2 to 14 were isolated by GPC and characterized by HPAEC-PAD, wet chemistry method, and MALDI-TOF-MS. The corresponding response of different DP xylooligosaccharides on PAD detector was found dropping significantly with DP. This result demonstrates the calculation method to estimate xylooligosaccharide concentration using HPAEC-PAD technique was not accurate in previous literatures, because it assumed equal PAD response for xylooligosaccharide with different DP. Instead, a series of response factors were developed that can be used to quantify xylooligosaccharides of DP from 2 to 14 without standards. This provided an approach to profile xylooligosaccharides during pretreatment using less expensive chromatographic methods, which was previously not possible.

Another method development study in this thesis was accomplished in Chapter 4. Pretreatment with 1 wt% sodium hydroxide at 120℃ of 10 wt% solids loadings of poplar and switchgrass was successfully combined with enzymatic co-hydrolysis in the HTPH system. The one step buffering and neutralizing method developed with a pH 4.5 citrate buffer for a dilute acid HTPH system (1) effectively neutralized and adjusted the pH of sodium hydroxide pretreatment slurries to a range of 4.69-4.89 prior to whole slurry enzymatic co-hydrolysis. Sugar yields showed different trends for poplar and switchgrass with increasing pretreatment times, demonstrating the method was capable of clearly discerning differences in the susceptibility of different feedstocks to alkali pretreatment.

In addition to methods development, the major parts of this thesis facilitated understanding how the changes/differences of plant cell wall structural polymers affect biomass deconstruction in pretreatment and enzymatic hydrolysis. Chapter 5 observed that lignin migrated out of the poplar wood cell wall and deposited on the Avicel cellulose surface during hydrothermal pretreatment. As a result, enzymatic hydrolysis was retarded initially by the lignin droplets deposited on the surface of Avicel cellulose, but such inhibition decreased with increased hydrolysis time and was virtually eliminated at high cellulose conversion. This chapter demonstrated that nonspecific binding of enzymes to lignin droplets was not the primary mechanism for inhibition. Instead, surface blockage of cellulose by lignin droplets was proposed to be responsible for the inhibition pattern of enzymatic hydrolysis of LDA and iLDA. By comparing experimental results from this study to those from previous studies, the key mechanisms

responsible for inhibition of cellulose hydrolysis by lignin, nonspecific binding or surface blockage or both, are believed to depend on the chemical nature and particle size of lignin polymer molecules.

After figuring out the inhibitory mechanism of deposited lignin droplets on enzymatic hydrolysis, fundamental research regarding to hemicellulose structure was also conducted. In Chapter 6, reduced methylation in 4-*O*-methyl glucuronoxylan side chains of Arabidopsis was found to enhance the extent and amount of hemicellulose and lignin removal during hydrothermal pretreatment in flowthrough reactors. Results also showed that although reduced methylation didn't result into improved digestibility for untreated biomass, Arabidopsis cell walls with reduced methylation was disrupted more than WT when pretreated at the same conditions. The results provided better understanding towards the effects of hemicellulose structure on interactions of hemicellulose and lignin, as well as overcoming the biomass recalcitrance in cell wall deconstruction.

The last two experimental chapters focus on developing Agave as a promising biofuels feedstock on semi-arid lands. In Chapter 7, agave species were characterized for the first time by a series of standard biomass analysis procedures to develop detailed information on chemical compositions and cellulose ultra-structural components. The three agave leaf bagasse samples employed had similar total structural plus soluble carbohydrate contents that contributed about 50% to 55% of the mass of dry bagasse. The xylan content was low in agave species relative to grasses and hardwoods, but galactan was a more important component in agave hemicellulose than for many other plants. In addition, agave had very low lignin contents (7.3%-11.9%). Based on these findings,

Chapter 8 further discovered and demonstrated that agave is a low recalcitrant material that could dramatically reduce processing costs and expand production of biofuels to arid and semi-arid lands. Furthermore, several key features of agave were identified to contribute its low recalcitrance, such as a loose non-cellulosic wall component structure, high enzyme accessibility, good hydrophilicity, and less ordered crystalline structure. Results in this chapter showed that determining which agave genes control such traits could provide valuable insights into approaches to greatly facilitate development of low recalcitrant, highly productive, and drought resistant biomass. Thus, it is possible that the future biorefineries can bypass the lignocellulosic recalcitrance problem, water and food crisis, and desertification threat by producing biomass and biofuels on semi-arid and arid lands.

9.2 Closing remarks and suggestions for future work

Most of previous studies tried to isolate the role of lignin or hemicellulose from other cell wall components in defining biomass recalcitrance, and they contributed significant insights towards understanding of recalcitrant features of lignin or hemicellulose. However, because plant cell walls are such a complex and synergetic ensemble, findings and observations from isolated research do not always correlate well with each other and sometimes even conflict. The most important learnings from this thesis include the following three aspects:

1. The inhibitory mechanism of lignin on cellulose enzymatic hydrolysis depends on the structure, morphology, and size of lignin polymers. Small lignin droplets formed

during pretreatment inhibited enzymes from digested cellulose mainly by physical blockage of the cellulose surface, with the inhibition pattern decreasing with hydrolysis time. On the other hand, larger lignin complexes isolated from pretreated biomass solids tended to non-specifically bind to enzymes, with the inhibition pattern increasing with hydrolysis time (2).

2. The reduced methylation of 4-*O*-methyl glucuronoxylan side chains in an *Arabidopsis* mutant resulted in increased methylation of lignin. The combined effects enhanced hemicellulose and lignin removal during hydrothermal pretreatment in flowthrough reactors, and the resulting pretreated solid was more digestible than the wild type control. Because lignin and hemicellulose closely interact through covalent and non-covalent bonds (3), genetic modification of one is highly likely to alter the structure of the other. Furthermore, glucuronoxylan biosynthesis and lignin biosynthesis are biochemically intertwined because both involve methylation reactions in which *S*-adenosyl-L-methionine is the methyl donor. Genetically altering methylation in one pathway might alter substrate availability for methylation in the other. Thus, characterization of structural changes in both and considering them in combination will facilitate consistent understanding of their role in affecting recalcitrance of biomass to pretreatment and enzymatic hydrolysis.

3. The learnings about agave cell wall architecture in this thesis suggest that cell wall enzymatic accessibility is the essential parameter that can represent effects from several recalcitrant characteristics, such as lignin content and composition, hemicellulose extractability, and cellulose ultra structure. In addition, the results from agave indicate

that the high digestibility of primary cell wall might be correlated with its high water retention ability. Obvious structural characteristics of primary cell wall were identified in agave biomass (4-5 years old, big plants) and determined to be important contributors to the low recalcitrance of agave. Two implications to explain the lower recalcitrance of agave cell walls were gained from the ways that agave plants live and reproduce in semi-arid and arid environments. The one is that agave uses its leaves as a water storage organ, which requires more parenchyma cells (only primary walls, high hydrophilcity) to hold the water within leaves. The other is that agave plant tend to hydrolyze and extract most of the polysaccharides accumulated in its leaves and heart for reproduction at the end of their life cycle, which suggests that agave might never built the highly recalcitrant structure against cell wall deconstruction as most other lignocellulosic biomass.

This thesis has provided important insights towards interactions of lignin and hemicellulose as important to the recalcitrance of biomass to deconstruction. However, it is still very difficult to track all structural variables for hemicellulose, lignin, and the bonds among them when efforts are made to compare different biomass types or different pretreatment conditions. Thus, a combined parameter, which could represent the overall changes of the interactions of hemicellulose and lignin, would be very helpful to more fully understand the process. Based on the results of this thesis, cell wall accessibility measured by the Simons' Stain method (4,5), cell wall hydrophilcity determined by NMR (6,7), or water retention value (8) have great potential to reach this goal. Examining the enzymatic digestibility of cell walls of more lignocellulosic feedstocks with varying compositions and cell wall structures and correlating the results to cell wall accessibility

and hydrophilcity could shed new insights into the interactions among lignin, hemicellulose, and cellulose. In addition, advancing the understanding of plants that use the Crassulacean Acid Metabolism (CAM) pathway as highly productive, drought resistant biofuels feedstocks appears to be a very promising route to improve the current C_4 and C_3 lignocellulosic energy crops by genetic tools and extend biorefineries to semi-arid and arid lands.

9.3 References

1. Gao X, Kumar R, DeMartini JD, Li H, Wyman CE. Application of high throughput pretreatment and co-hydrolysis system to thermochemical pretreatment. Part1: Dilute acid. Biotechnol Bioeng. 2012:n/a-n/a.
2. Kumar R, Wyman CE. Access of cellulase to cellulose and lignin for poplar solids produced by leading pretreatment technologies. Biotechnol Progr. 2009 May-Jun;25(3):807-19.
3. Albersheim P, Darvill A, Roberts K, Sederoff R, Staehelin A. Plant cell walls : from chemistry to biology. New York, NY: Garland Science; 2010.
4. Chandra R, Ewanick S, Hsieh C, Saddler JN. The characterization of pretreated lignocellulosic substrates prior to enzymatic hydrolysis, Part 1: a modified simons' staining technique. Biotechnol Progr. 2008 Sep-Oct;24(5):1178-85.
5. Esteghlalian AR, Bilodeau M, Mansfield SD, Saddler JN. Do enzymatic hydrolyzability and Simons' stain reflect the changes in the accessibility of lignocellulosic substrates to cellulase enzymes? Biotechnol Progr. 2001 Nov-Dec;17(6):1049-54.
6. Elder T, Labbe N, Harper D, Rials T. Time domain-nuclear magnetic resonance study of chars from southern hardwoods. Biomass Bioenerg. 2006 Oct;30(10):855-62.
7. Felby C, Thygesen LG, Kristensen JB, Jorgensen H, Elder T. Cellulose-water interactions during enzymatic hydrolysis as studied by time domain NMR. Cellulose. 2008 Oct;15(5):703-10.
8. Scandinavian Pulp, Paper and Board. Water retention value. 2000; SCAN-C 62:00.